ANALYSIS OF TWENTY-FIVE YEARS OF HEAVY RAINFALL EVENTS IN THE TEXAS HILL COUNTRY

A Thesis

presented to

the Faculty of the Graduate School

at the University of Missouri-Columbia

In Partial Fulfillment

of the Requirements for the Degree

Master of Science

---

by

AMY ELISA SCHNETZLER

Dr. Patrick Market, Thesis Supervisor

August 2008

The undersigned, appointed by the dean of the Graduate School, have examined the thesis entitled

ANALYSIS OF TWENTY-FIVE YEARS OF HEAVY

RAINFALL EVENTS IN THE TEXAS HILL COUNTRY

presented by Amy E Schnetzler,

a candidate for the degree of master of Soils, Environmental, and Atmospheric Sciences,

and hereby certify that, in their opinion, it is worthy of acceptance.

Associate Professor Patrick Market

Assistant Professor Neil Fox

Associate Professor Allen Thompson

Associate Professor Anthony Lupo

I am dedicating this work to my loving parents. You both have been a rock for me throughout my undergraduate and graduate years. Not once did your faith in my ability to succeed ever falter. Your continuous support has always been a great comfort to me and has enabled me to overcome numerous obstacles along the way.

Many thanks are also in order to my two sisters, to both sets of my grandparents, my aunts, uncles, cousins, and roommates for words of encouragement during many stressful times.

With much love,

Amy

ACKNOWLEDGEMENTS

I would like to thank Dr. Patrick Market and Jon Zeitler for their valuable contribution of knowledge and assistance on this project. Dr. Market served as my thesis supervisor and as a member of my defense committee. I also would to thank Dr. Neil Fox, Dr. Allen Thompson, and Dr. Anthony Lupo for providing valuable insight and serving as members of my defense committee.

Many thanks are due to Dr. Christopher Melick, Dr. Brian Pettegrew, and George Limpert for providing assistance in the Weather Analysis and Visualization Lab throughout the project.

Last, but not least, I would like to think COMET for providing funding for this research. Note that this work was performed as part of a Subaward with the University Corporation for Atmospheric Research (UCAR) under Cooperative Agreement No. NA17WD2383 with the National Oceanic and Atmospheric Administration (NOAA), U.S. Department of Commerce (DoC). The statements, findings, conclusions, and recommendations are those of the author and do not necessarily reflect the views of NOAA, DoC or UCAR.

TABLE OF CONTENTS

LIST OF ILLUSTRATIONS

Figure Page

LIST OF TABLES

Table Page

ABSTRACT

Forecasting heavy rain events and the area of greatest threat has been a long standing challenge in operational meteorology. This is especially true in certain regions where the physical geography lends itself to the creation of such events. With its thin soil layers, low latitude, and proximity to the Gulf of Mexico, the Texas Hill County is one such region.

Twenty-five years of daily (24-hour) rainfall data were examined for the Texas Hill Country using observations from 86 cooperative climate stations in the region; the period examined for this study was 1982-2006. Days with measurable precipitation were treated as a gamma distribution in order to determine the top 2%, 1%, and 0.5% to define events as unusual, rare, and extreme, respectively. Quantifying rainfall as a distribution provides forecasters with supplementary information on precipitation thresholds that can lead to significant flash flooding or major flooding. This approach was applied to each station as well as to the aggregate data for all 86 stations, resulting in an analysis of 130,986 observations of 24-hour precipitation.

Soundings were then constructed for each using the 3-hourly North American Regional Reanalysis (NARR) gridded datasets. From these individual soundings mean values were created, and composite

soundings were then made for each rainfall threshold for the Mesohigh, Frontal and Synoptic classifications. Convective stability parameters were also tested for each of the classes of heavy rain events. From these exercises, it was learned that high values of precipitable water and wind shear are key ingredients for heavy rainfall to occur.

Chapter 1: Introduction

Operational forecasters face many challenges in each region. A common challenge across the United States is forecasting quantitative precipitation, especially for heavy amounts (> 50.8 mm (2 inches) in 24 hours) and in locales where topography and/or urbanization concentrate runoff. The Texas Hill Country and surrounding plains is one such place, where topography, increasing urbanization, and extreme rainfall combine to produce one of the most flash flood and fatality prone areas in the country (Ashley and Ashley 2008).

Texas is unique in that the air masses that affect the region have both maritime and continental influences. In most tropically-based events it is generally easier to predict heavy precipitation due to the moisture source and the dynamics of the system. Non-tropically influenced events are not as easy to forecast and are less frequent. Non-tropical events (e.g., initiated by synoptic features such as stalled fronts/boundaries) are the focus of the study.

To address this forecasting problem, Grice and Maddox (1982) performed an in-depth study of such events that produced large amounts of rainfall over localized areas in the Texas Hill Country. They were able to identify and define three distinct synoptic classifications that were associated with key plan-view features. Their findings were beneficial, but there has been no systematic follow up study in the past 25 years.

To update and expand upon previous findings, the approach of the present project is to analyze vertical profiles to determine which convective instability parameters are key identifiers for the three classification types. Finding mean sounding composites for each classification can act as a guide for the operational meteorologist in Texas.

1.1 Goals of the Study

One objective for this study is to better quantify the rainfall distribution for the Texas Hill Country. The second objective is to improve forecast skill for heavy rainfall events through sounding analysis. A combination of the objectives

implies capability to better anticipate flash flood events. Anticipation is important, since providing longer watch and warning lead times is a significant factor in evacuation decisions, saving lives, and reducing property losses.

1.2 Statement of Thesis

Although Grice and Maddox (1982) focused on south Texas and the Texas Hill Country, they were unable to identify a unique event type separate from those identified by Maddox et al. (1979), namely the synoptic, frontal, and mesohigh. The work in this thesis corroborates that basic premise. Within those three basic event types, it is thus important to look carefully at the sounding profiles that attend a heavy rain event.

Sounding analysis is thus the backbone of this study. In that vein, it is hypothesized that events with higher rainfall totals will be borne of environments that possess

1) higher precipitable water contents, and

2) lower wind shear values of direction and speed.

These ideas will be investigated by examining mean composite soundings for each of the event types.

Chapter 2: Literature Review

Even though this study is primarily focused on the meteorological aspects of heavy rainfall amounts over a 24-hour period, the operational application is of a more hydrological nature. Rainfall, that occurs in large quantities, often cause flash flooding and large-scale floods to occur. One factor that can lead to flooding is heavy rainfall rapidly falling within an artificial or natural drainage basin. The characteristics of the basin (such as slope of the land, soil profile, etc.) determine the likelihood of flooding (Collier and Fox, 2003). A variety of weather scenarios can produce rainfall in large quantities.

Typing and quantifying heavy rain events are of primary interest in this study. Two sections focus on typing 1) all heavy rain events across the United States and 2) heavy rainfall over the south Texas region. Statistical applications in meteorology are then explored to properly quantify rainfall.

2.1 Climate-Scale Heavy Rain Studies

Basic studies of rainfall intensity and duration have guided the inquiry into heavy rainfall and flash flooding for decades. Events such as the record rainfall in Holt, Missouri, in 1947 (Locatelli and Hobbs 1995), which deposited ~ 305 mm (12 inches) in 42 minutes prompted deeper investigation of rainfall intensity and duration for the purposes of flood and flash flood forecasting, preparedness, and disaster mitigation.

As an example, Jennings (1963) focused on rainfall during specific time thresholds, including intensity, seasonal distribution, and depth duration. Maximum rainfall amounts were recorded for 5, 10, 15, 30, and 60 minutes, as well as, 2, 3, 6, 12, and 24 hours for 296 stations across the contiguous United States. The sample is indeed small but does provide some insight on typical seasonal variations across the United States. Maximum values were used from published and unpublished tabulations and summaries that were issued by the Weather Bureau stations with at least five years of records. A majority of the observations were generated by automated stations. Jennings (1963) states that accurate measurements of

intense rainfall suffer limitations from the tipping bucket and may result in values up to 5% too low.

Stations that had at least 20 years of data were used in the seasonal distribution. The largest increase in the percentages that were recorded occurred in durations greater than 3 hours. It was found that July and August had the highest percentage occurrences for the 6-hr duration. September had the highest percentage occurrence for durations of 12-and 24-hours, and nearly 50% of the events occurred in July-September. Overall, a slight tendency towards a more uniform seasonal distribution could be seen as the length of the duration increased. Summer was the leading season for all rainfall durations, with autumn close behind.

Geographic variations were noticeably skewed towards eastern United States for both seasonal and daily distributions. For daily distributions, time was broken into quarters. The third quarter, 1200 to 1800 local standard time, was the most reoccurring time period; but, was exceeded by the fourth quarter when the storm duration was greater than 60 minutes. The number of storms rapidly dropped off as the storm duration

increased. Most of the maximum values that were recorded for longer than 60 minutes were associated with thunderstorms.

Studying large-scale patterns, key ingredients, and even durations provide a more qualitative than quantitative approach for studying heavy rainfall events. Quantification can arise through viewing rainfall as a distribution. Panofsky and Brier (1968) discussed multiple statistical distributions and how they are calculated. The distributions listed focused on displaying meteorological parameters and the best way to represent data sets.

Probability is the likelihood that a situation, event, or condition will occur. Graphically, the probability is shown as the area below the curve between values of the variant. A basic equation that will yield such a curve is given below.

$$P = \int_{x_1}^{x_2} p \, dx \qquad (2.1)$$

P is defined as the probability density between the two variables x_1 and x_2. The normal distribution is most frequently used because it fits a rather vast range of data. This "best-fitting" curve is defined as a distribution that has the same area,

the mean and σ-value as the sample. This curve can be used to make an estimate of the probabilities of unusual conditions that may occur. However, some variates cannot be fit with a normal distribution, or even other popular distributions such as binomial or Poisson; daily rainfall is one such dataset.

All types of frequency distributions can be transformed into frequency distributions of a given form by an appropriate transformation or functional relationship. A gamma distribution is such a transformation that has been used effectively with rainfall data (e.g. Collier and Hardaker (1997) and Guinan (2005)). It is very useful in fitting and transforming various distributions that only yield positive values (such as daily rainfall, for which there is a lower bound at 0). Using the following equation (Panofsky and Brier 1968), daily values of rainfall can be represented by a gamma distribution.

$$f(X) = \frac{1}{\beta^{\gamma}\,\Gamma(\gamma)}\, X^{\gamma-1} e^{-X/\beta}; \quad (\beta > 0, \gamma > 0) \qquad (2.2)$$

β is a scale factor that changes to represent the mean of the exponential distribution and determines the practical range. The term γ is a shape factor that represents the number of variables

and determines the profile of the distribution. Γ(γ) is the gamma function of the parameter γ, and is also equal to (γ -1)!.

$$A = \ln \overline{X} - \frac{1}{N} \sum \ln X \tag{2.3}$$

$$\hat{\gamma} = \frac{1 + \sqrt{1 + \frac{4}{3} A}}{4A} \tag{2.4}$$

$$\hat{\beta} = \frac{\overline{X}}{\hat{\gamma}} \tag{2.5}$$

The variable N is the sample size, while the variable A determines the shape of the distribution. The parameters, $\hat{\beta}$ and $\hat{\gamma}$, are optimal estimations. If the value of A increases then the values of $\hat{\gamma}$ decrease. The value of $\hat{\beta}$ was larger when the values of $\hat{\gamma}$ was lower. Transformations can now be calculated for any distribution if the above parameters are known.

Similar in fashion to the previous procedure was a study by Huff and Angel (1982) in finding distributions of rainfall data in time and space. A distribution was found by using data from

a blended network of daily reports. Recurrence intervals for time periods of 2 months to 100 years were found for the intense rainfall. Even though the data were placed in log-log, log-normal, semi-log, as well as L-moments and maximum likelihood fitting, no distribution provided a satisfactory fit. Unsatisfactory estimates of rainfall were found for the 2 month to 2 year reoccurrence interval. A log-log graphical analysis was the final selection.

Utilizing isohyetal and areal averages, errors from poor exposure as well as improperly maintained equipment were minimized (Huff and Angel 1992). These averages were vulnerable to large bias and in errors from sampling for smaller-scale features in water-control design processes. The patterns were sketches based off station data that indicate distinct weather patterns. These sketches help overcome unrealistic precipitation differences approximating homogeneous precipitation climates. By following the three criteria provided in the study: 1) frequency relations for each precipitation station, 2) climatological knowledge of the station, and 3) effects of physiographic features), isopatterns were produced that strongly

approximated the accurate distance of heavy rainfall. Map series derived from the isopatterns showed features associated with approximating the accurate distance of heavy rainfall.

Huff and Angel (1992) found an areal mean frequency distribution by dividing a state into regions of nearly homogeneous climates in regards to heavy rainstorms. This process does not abolish sampling errors; however, it does moderate their outcome in regions of comparable precipitation climates. It should also improve approximations of true distributions of heavy rainstorms around the region, although it might disguise small-scale effects.

Time distributions were defined as a cumulative percentage of storm rainfall and its duration to allow valid comparisons to be made between each storm and make things easier for analyzing the data. Areal groupings yield very small changes within the time distribution as the sampling data increases. This results in rainfall distributions being grouped in quarters by the timing of the heaviest rainfall.

2.2 Synoptic-Scale Heavy Rain Studies

2.2.1 Contiguous United States

Classification of storm types arose in the Maddox et al. (1979) study of the synoptic and meso-α aspects of more than 150 flash flood events across the nation. Using the Storm Data reports issued by NOAA for the years 1933-1977, a flood climatology was compiled. This climatology supplied essential information to identify a sample of intense precipitation events. The flash floods were broken down into four sub-categories: synoptic, frontal, mesohigh and western, and can be seen in Fig. 2.1 as a monthly distribution.

General characteristics were then identified for these sub-categories. Synoptic events were associated with rather strong tropospheric wind fields and significant, large-scale weather systems. Frontal events were linked with quasi-stationary frontal zones (usually orientated west-to-east) that occurred with weak large-scale patterns. Mesohigh events were connected with quasi-stationary, cool-air outflow boundaries that

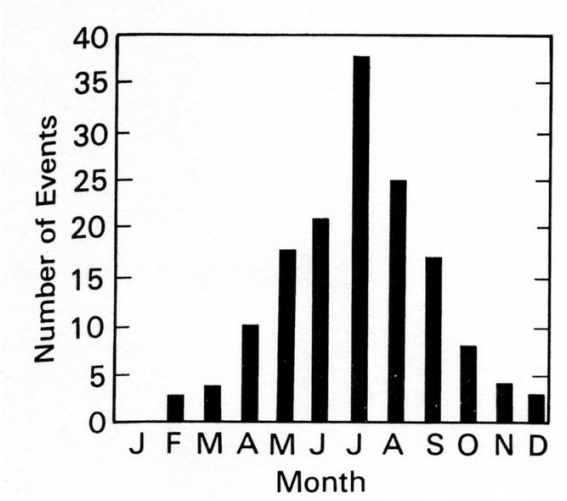

Figure 2.1 The monthly occurrences for the flash flood events. Reproduced from Maddox et al. (1979).

were produced by previous thunderstorm activity. Western events used a geographical criterion.

Common features of all types of flood events included: heavy rain from convective storms, very high surface dew points, large amounts of moisture through a deep tropospheric layer, and weak-to-moderate wind shear through the depth of the cloud. Diurnally, mesohigh and frontal events were more nocturnal in their nature while western events primarily occurred in the afternoon. Some of the larger-scale synoptic systems experienced the heaviest periods of rainfall at night.

Approximately 20% of the flash floods were classified as synoptic events that developed from an intense cyclone or frontal system that frequently occurred in the spring and fall months. Figure 2.2 shows October as the month receiving the most synoptic events. One key feature was that the winds aloft were parallel to the frontal zone. The typical scenario for this type of events can be observed in Fig 2.3. Figure 2.4 displays temperature, wind speed, and wind direction averages for the standard synoptic levels including standard deviations.

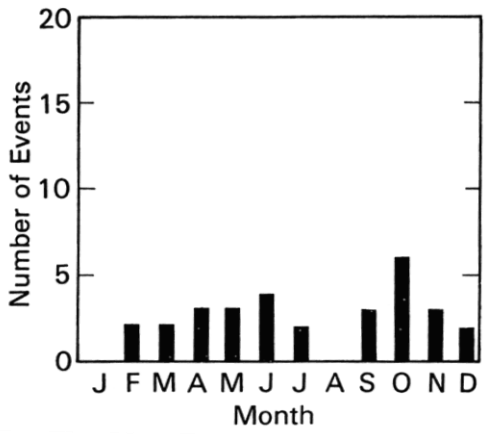

Figure 2.2 Monthly distribution of the synoptic-type events. Reproduced from Maddox et al. (1979).

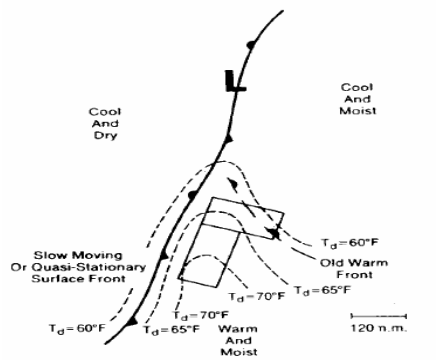

a)

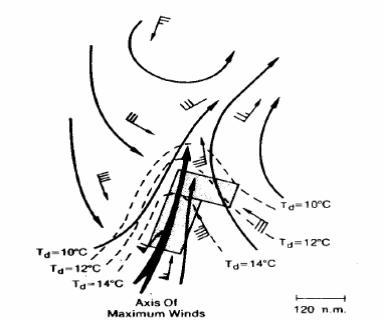

b)

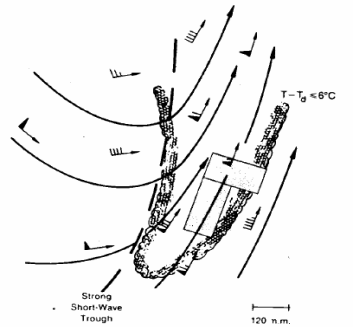

c)

Figure 2.3 Plan view of a) surface, b) 850-mb, and c) 500-mb for synoptic-type flash flood events. Reproduced from Maddox et al. (1979).

Level	T	T_d	Wind Direction	Wind Speed
Surface				
1009 mb / 6 — Mean / Std. Dev.	74(°F) / 7	67(°F) / 4	165° / 33	13 (kt) / 3
		$T - T_d$		
850 mb	15(°C) / 3	2(°C) / 1	195 / 28	32 / 11
700 mb	5 / 2	3 / 3	215 / 29	36 / 11
500 mb	−11 / 3	8 / 9	220 / 29	47 / 14
300 mb	−38 / 3	10 / 7	230 / 30	57 / 21
200 mb	−57 / 3	—	235 / 32	66 / 21

Figure 2.4 Scanned reproduction of a Table from the Maddox et al. (1979) article showing averaged temperatures, dewpoint temperatures, wind direction and wind speeds and their standard deviations for synoptic-type events.

Nearly 25 % of the sample was comprised of frontal events. The monthly distribution for frontal flash flood events is given in Fig. 2.5. Unlike synoptic events that favor autumn, frontal events occurred more frequently in late summer with a significant peak in July.

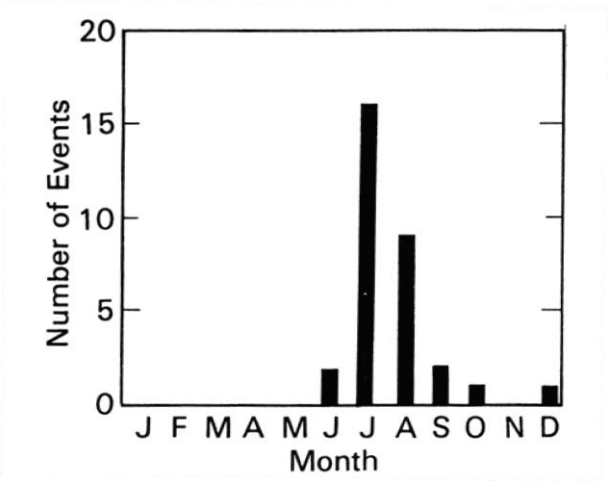

Figure 2.5 Monthly distribution of frontal-type flash floods. Reproduced from Maddox et al. (1979).

Two important features of this type of flooding event were the presence of 1) a nearly stationary frontal boundary that focused heavy precipitation upon a particular area (the cool side of the surface front), and 2) significant veering of the winds aloft (Fig. 2.6).

These storms typically formed and remained on the warm side of a front and were nocturnal in nature. A meso-α-scale short-wave trough was present just upstream during the majority of the events, which primarily took place from March to September. Figure 2.7 displays temperature, wind speed, and

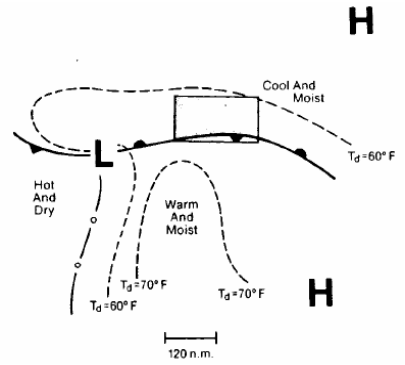

a)

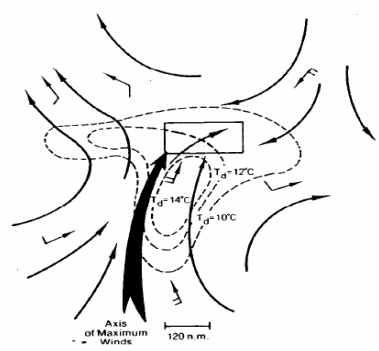

b)

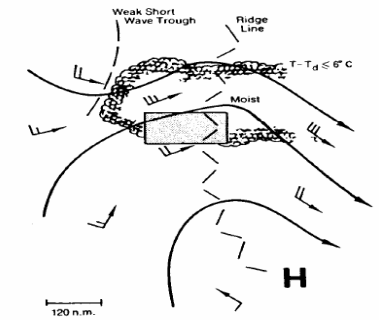

c)

Figure 2.6 Plan view of a) surface, b) 850-mb, and c) 500-mb for frontal-type flash flood events. Reproduced from Maddox et al. (1979).

Level	T	T_d	Wind Direction	Wind Speed
Surface				
1013 mb / 4 — Mean / Std. Dev.	70(°F) / 6	65(°F) / 5	100° / 36	9 (kt) / 2
		$T - T_d$		
850 mb	17(°C) / 3	4(°C) / 2	200 / 26	20 / 8
700 mb	7 / 2	3 / 3	235 / 30	20 / 10
500 mb	−10 / 3	6 / 7	250 / 34	28 / 12
300 mb	−36 / 3	15 / 11	260 / 29	40 / 16
200 mb	−56 / 3	—	270 / 22	47 / 21

Figure 2.7 Scanned reproduction of a Table from the Maddox et al. (1979) article showing averaged temperatures, dewpoint temperatures, wind direction and wind speeds and their standard deviations for frontal-type events.

wind direction averages for the standard levels aloft including standard deviations for the frontal events.

Floods associated with mesohighs were the most dominant of the four types of events (34%). A monthly distribution of mesohigh flash flood events are given in Fig. 2.8. A distinct

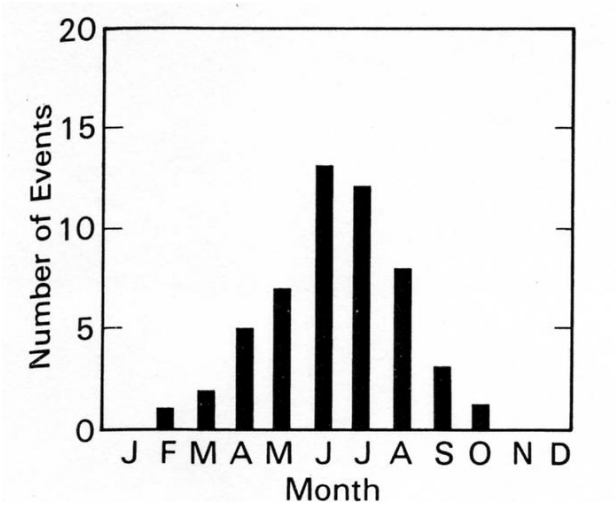

Figure 2.8 Monthly distribution of mesohigh-type flash flood events. Reproduced from Maddox et al. (1979).

association with the summer season can be seen. June was the peak month with July as a very close second.

Thunderstorm outflow boundaries, produced by convective activity, that remain nearly stationary are a key feature of mesohigh events (Fig. 2.9). The area of heaviest rainfall occurs south/southwest of the mesohigh on the cool side of the boundary.

A meso-α short wave trough at 500 mb was associated with more than half of these types of events as well as having a

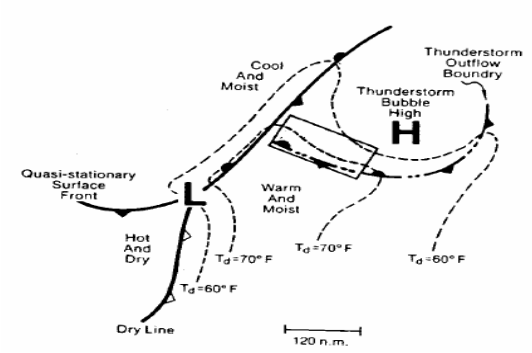

a)

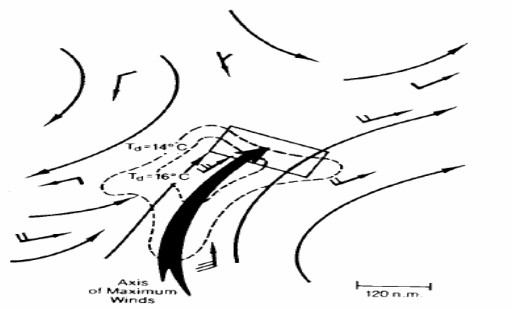

b)

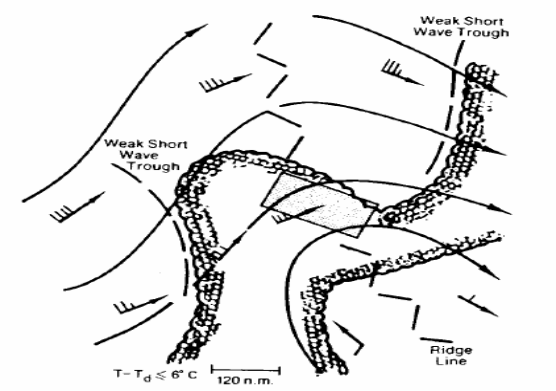

c)

Figure 2.9 Plan view of a) surface, b) 850-mb, and c) 500-mb for mesohigh-type flash flood events. Reproduced from Maddox et al. (1979).

Level		T	T_d	Wind Direction	Wind Speed
Surface					
1014 mb	Mean	71(°F)	66(°F)	090°	9 (kt)
4	Std. Dev.	4	4	41	3
			$T - T_d$		
850 mb		18(°C)	3(°C)	205	22
		3	2	33	8
700 mb		7	4	230	21
		2	3	32	10
500 mb		−10	6	240	27
		3	6	27	11
300 mb		−36	10	255	37
		4	8	32	16
200 mb		−57	—	260	41
		3		40	20

Figure 2.10 Scanned reproduction of a Table from the Maddox et al. (1979) article showing averaged temperatures, dewpoint temperatures, wind direction and wind speeds and their standard deviations for mesohigh-type events.

nocturnal nature. Mesohighs were most prevalent in the summer months. Figure 2.10 provides the mean temperature, wind speed, wind direction each of the standard levels aloft, including standard deviations.

Western events comprised 21% of the floods and occurred under relatively weak large-scale patterns that were not defined at the surface. Figure 2.11 gives the monthly distribution of these type of flash flood events. May, July, and August had the

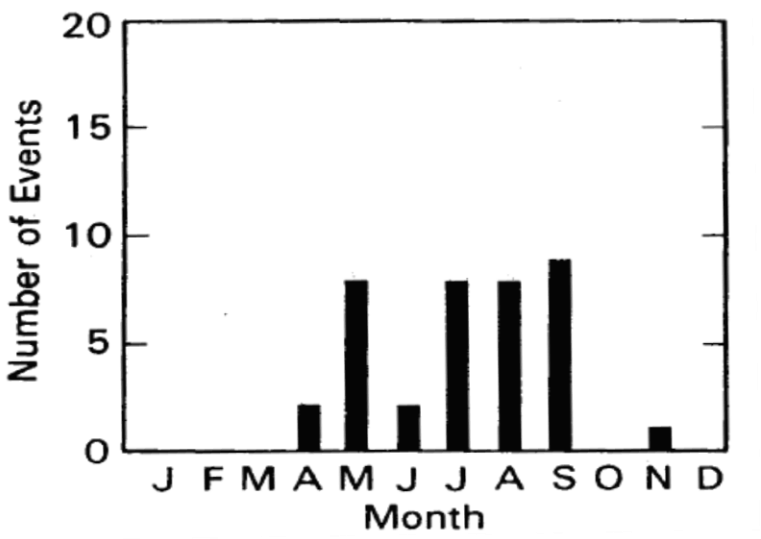

Figure 2.11 Monthly distribution of western-type flash flood events taken. Reproduced from Maddox et al. (1979).

same number of events occurring; however, September had the most.

It is likely that the localized heavy rainfall resulted from an old frontal boundary, a thunderstorm outflow boundary, or from an orographic feature that would have interacted with the larger scale features. July and August are the two months where western events occur the most and are likely to be linked with the monsoon in southwest United States. Figure 2.12 displays the mean temperature, wind speed, and wind direction for each of the standard levels aloft including standard deviations. One

Level		T	T_d	Wind Direction	Wind Speed
Surface					
1012 mb / 4	Mean / Std. Dev.	86(°F) / 6	56(°F) / 6	120° / 57	9 (kt) / 4
			$T - T_d$		
700 mb		10(°C) / 2	6(°C) / 4	190 / 73	11 / 7
500 mb		−9 / 2	4 / 3	210 / 79	16 / 11
300 mb		−34 / 3	10 / 7	220 / 62	27 / 19
200 mb		−55 / 2	—	235 / 65	34 / 20

Figure 2.12 Scanned reproduction of a Table from the Maddox et al. (1979) article showing averaged temperatures, dewpoint temperatures, wind direction and wind speeds and their standard deviations for western-type events.

major point of Maddox et al. (1979) was that most of the flash flood storms regularly occurred very close to the large-scale ridge position and, as a rule, generally benign surface pressure patterns.

Another study carried the idea of looking at key features that must work together to produce heavy rain. Doswell et al. (1996) advanced forecasting flash floods using a basic ingredients approach. An event's likelihood in producing a flash flood are affected significantly by such factors as antecedent

precipitation, the areal extent of the drainage basin, topography of the basin, and urban influences within the basin. Since rainfall is usually an ordinary occurrence, raising public awareness about heavy rainfall and flash flooding is a challenge.

A few ingredients that lead to flash floods include: heavy precipitation, high precipitation rate, and deep, moist convection. Where the rainfall rate is the highest for the longest duration describes heavy precipitation. The higher the rainfall rate, the greater the chance is for a flash flood. Each heavy rainfall event is different so having set thresholds is not necessary, but roughly speaking a moderately high rate begins at 25 mm (~ 1 inch) h^{-1} and a moderately long duration is 1 hour or longer.

Flash flooding scenarios can be associated with high precipitation rates. Lifting moist air to condensation forms precipitation. To achieve a high precipitation rate, rising air should contain substantial water vapor content and a rapid ascent rate. Precipitation efficiency is the coefficient of proportionality relating rainfall rate to input water flux which is represented in the equation below.

$$R = Ewq \tag{2.6}$$

The variable R represents the instantaneous rainfall rate at a specific location, w is the ascent rate, and q is the mixing ratio of the rising air. Precipitation efficiency, E, is defined as the ratio of the mass of water falling as precipitation, m_p, to the influx of water vapor mass into the cloud, m_i, such that $E= m_p / m_i$. All quantities represent a time average over the history of a precipitation-producing weather system.

The entrainment rate is a factor caused by bringing unsaturated environmental air into a cloud, which typically encourages evaporation. Decreasing the relative humidity causes an increase in the evaporation rate, which leads to a fall in the precipitation efficiency (Doswell et al. 1996). The potential for having a high R exists if one of the three factors (E, w, and q) for high rainfall rates has a large value while the other ingredients have medium-ranged values. This is true for Texas Hill Country events described by Grice and Maddox (1982) where warm, southerly flow pumped in large amounts of moisture and the ascent and mixing ratios values were less.

Flash floods are generally caused by quasi-stationary convective systems and produce their heaviest amounts of rain over the same area. The length of time that a high precipitation rate occurs over a given location depends on the speed of the moving system, the size of the system, and the internal variations of the rainfall intensity. Long durations come from either the slow movement of the systems, large areal extent along the motion vector, or both.

From Doswell et al. (1996), cell movement can be dominated by simple advection. Outflows most active in generating new convection are located downstream of the present storm location when viewed in a middle troposphere wind shear perspective. Strong boundary flow can take place by having ambient flow that is weak, but the boundary that is rapidly moving, or strong ambient flow with a slowly moving boundary. Outflows are typically located downstream of wind in the middle and upper troposphere. Boundaries are reinforced by new cells and can last several hours if an inflow of moist, unstable air is persistent.

Many types of storms can produce flash floods. The six types are multicell, supercell, squall lines (radar), mesoscale convective systems (MCS), squall lines (satellite), and nonconvective precipitation systems. Some MCSs that have a circular nature may appear as linear on radar; therefore squall lines will be examined by both satellite and radar. Such linear MCSs, viewed by the satellite, clearly arrange their convection nearly linearly. A stratiform precipitation region behind the MCS can cause moderate rainfall to continue after the short period of intense rain. These MCSs can appear as squall lines on satellite and these are generally associated with synoptic features (Doswell et al. 1996).

In summary, moist air must ascend rapidly in order to generate heavy rainfall. Additionally, slow storm movement contributes to a longer duration. By using these specific concepts in an ingredients–based approach, forecasters can focus their time to specific features to improve forecasting accuracy.

A recent addition to the ingredients list for heavy rainfall forecasting is the normalized CAPE (NCAPE), which is defined by

Blanchard (1998) as the total CAPE divided by the entire depth of the free convection layer (FCL),

$$NCAPE = \frac{CAPE}{Z_{LFC} - Z_{EL}} \qquad (2.7)$$

where CAPE is given in J kg^{-1}. The depth of the FCL is the difference between the height of the LFC and the height of the EL and is measured in meters. After CAPE has been scaled to its depth, it represents an average acceleration through the depth of the FCL. To achieve acceleration with respect to pressure, the denominator can be replaced with the pressure value at the LFC and the EL. The units of NCAPE are J kg^{-1} mb^{-1}.

CAPE in the past has been used as a measure of instability which is not entirely accurate. NCAPE provides a better measure of instability because it takes into account the changes in the depth of the FCL caused by CAPE.

2.2.2 Heavy Rain Studies for Texas and the Texas Hill Country

Understanding the mechanisms that produce heavy rain is crucial in predicting the location and quantity of rainfall. Texas is unique to this topic due to its location near the Gulf of Mexico and its maritime and dry continental air mass influences. The study conducted by Grice and Maddox (1982) focused on heavy rain events in south Texas and the Texas Hill Country. An event was defined as one receiving equal to or greater than ~127 mm (5 inches) within 24 hours for the area excluding the Hill country, and equal to or greater than ~102 mm (4 inches) in 24 hours within the Hill Country. Thirty-three events met these criteria; and, of those events, 31 were associated with a mesohigh or a front. The data came from the standard levels of 850-mb, 700-mb, 500-mb, 300-mb, 200-mb twice daily maps, as well as, the 3 hour surface maps.

Meteorological conditions that occurred just prior to the heavy rainfall were determined using subjective interpolations in time and space. It was thought that orographic lifting over the western side of the region would play an important role in the frontal type events.

In terms of climatology, mesohigh heavy rain events had a distinct climax during the transition between spring and summer (15 April – 15 June). A combined monthly distribution for both frontal and mesohigh events can be seen in Fig. 2.13. This was the time when the subtropical high becoming established over the Gulf of Mexico and Texas, and the ridge axis was often located over deep south Texas.

Short waves that travel across the central Plains can cause weak cold fronts to move into south Texas. When the sub-tropical high over the Atlantic strengthening, influxes of tropical moisture push into south Texas and intermingle with weak surface fronts and short waves. The Texas Hill Country is further south than most of the U.S. Plains, and thus cold fronts tend to be significantly modified and weaker when they arrive. This arrangement creates very slow movement or possible stalling over the Texas Hill Country, and hence exacerbates heavy rain and flash flooding.

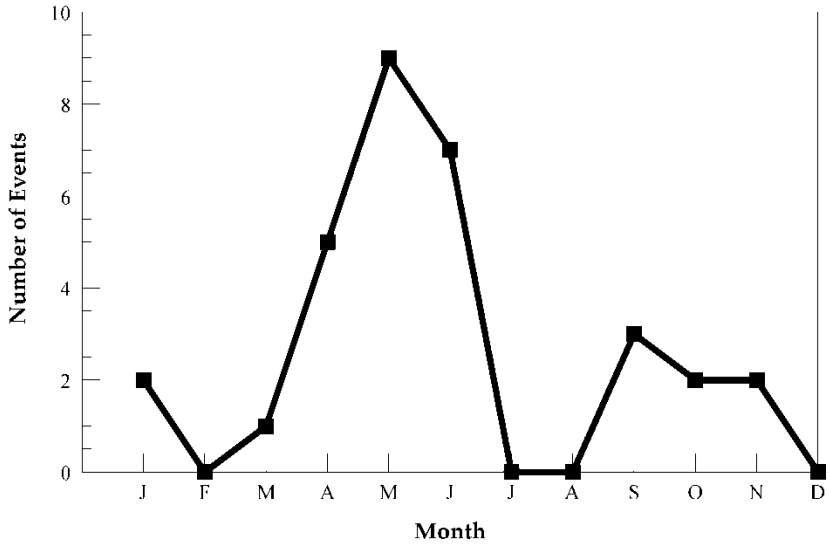

Figure 2.13 Combined monthly distribution of Mesohigh and Frontal events that occurred in South Texas. Reproduced from Grice and Maddox (1982).

The following characteristics were shared by both mesohigh type and frontal type events. The first of these characteristics was that the 850-mb wind and moisture fields are essential constituents for heavy rainfall, but the strength of the moisture ridge and the direction of the greatest winds near the front or boundary are most crucial. Second was the occurrence of low-level convergence near the surface. The 850 mb and 700

mb experience warm air advection. Lastly, the polar or sub-tropical jet was positioned near areas of the greatest rainfall. Wind profiles, along with a few stability parameters are shown in Fig. 2.14 for frontal and mesohigh events.

Mesohigh and frontal events differed mainly by two characteristics. The first was the fact that heavy rain generated by fronts was generally associated with a split-flow pattern in the mid to upper levels and the flow was mostly zonal for mesohigh events. The other difference was that mesohigh heavy rain events organized in front of a weak, moving shortwave and the frontal events occurred with a large, almost stationary middle and upper-level trough located over the western portion of the United States and parts of northern Mexico.

A flash flood event in Austin, Texas, was the focus of a study conducted by Maddox and Grice (1986). An event that occurred on 24 May 1981 caused a flash flood with localized heavy rainfall ~203 mm (8.00 inches) in 2 hours over western regions of Austin. The set-up of this event entailed two MCSs the previous night over the Southern Plains. Antecedent rainfall totaled between 75 to 125 mm (3.00 – 5.00 inches).

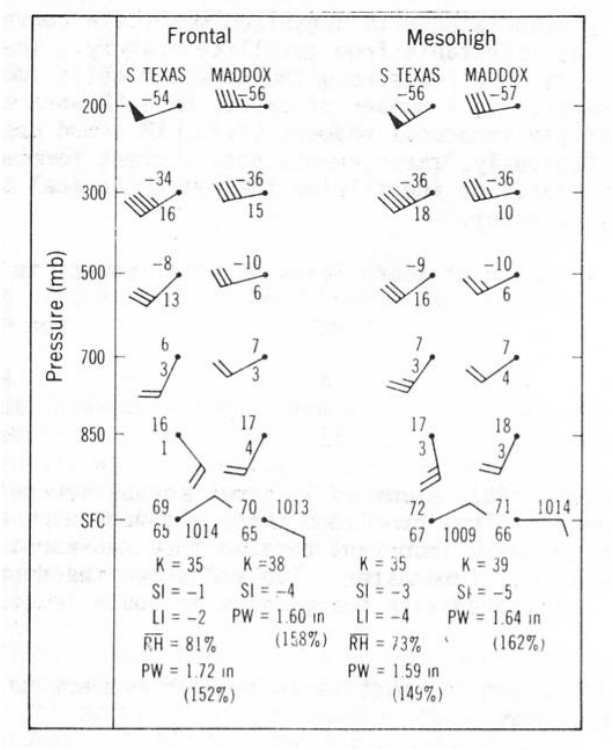

Figure 2.14 Shown is the vertical profile of the winds for frontal and mesohigh heavy rainfall events for south Texas. A selected few stability parameters are given for both types of events. Reproduced from Grice and Maddox (1982).

Looking at large-scale features on the 500 mb 12-hr Limited-area Fine-mesh Model (LFM) forecast and verifying LFM analysis for 0000 UTC 25 May 1981, a cut-off low could be seen propagating across the Northern Plains at the same time as a series of weakly defined short-waves moved across the southern United States (Fig 2.15). The 850 mb map for 0000 UTC (Fig. 2.16) had warm air advection present over central Texas, a

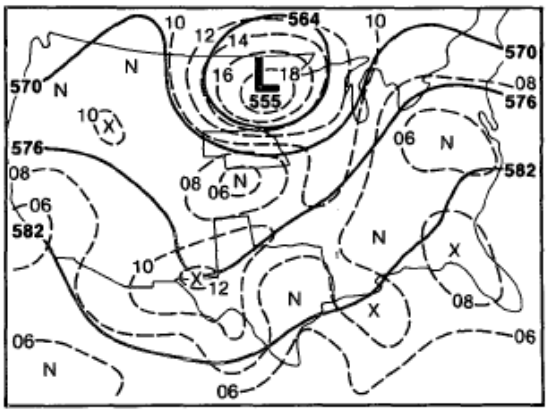

a)

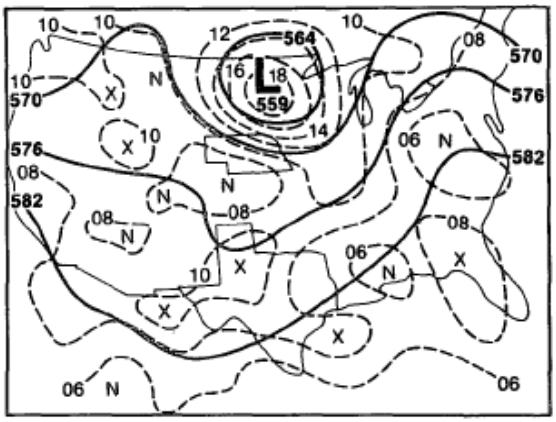

b)

Figure 2.15 a) The National Weather Service Limited-Fine Mesh (LFM) 12-hr model forecast of 500-mb and vorticity valid for 0000 UTC 25 May 1981, b) LFM verification analysis for 0000 UTC. Reproduced from Maddox and Grice (1986).

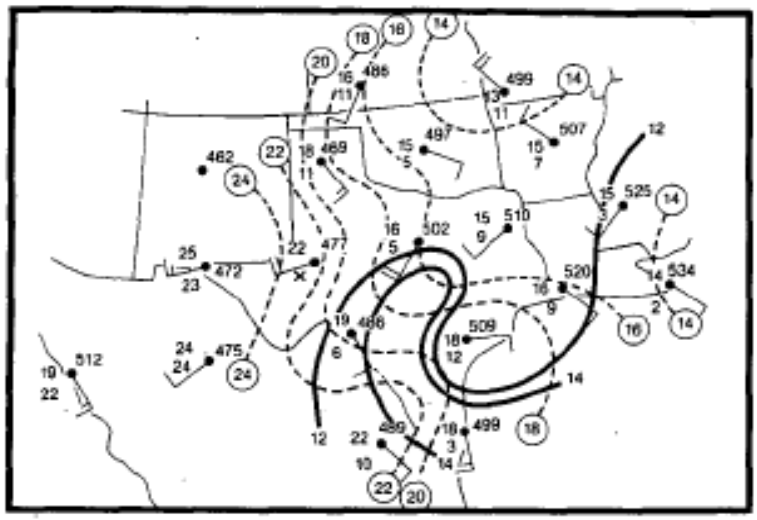

Figure 2.16 The 850-mb analysis for 0000 UTC 25 May 1981 taken from Grice and Maddox (1986). Temperature is shown as dashed contours with 2°C intervals, winds are in knots, heights are in meters minus 1 km, and solid contours show where the dew points exceeded 12° and 14°C.

tongue of high moisture content with dewpoint temperatures greater than 12°C that curled into central Texas, temperatures that increased from the south and west, height gradients were slight and winds were not strong.

Figure 2.17 shows that diffluent flow was present at 200 mb in front of a well-defined short-wave trough located over

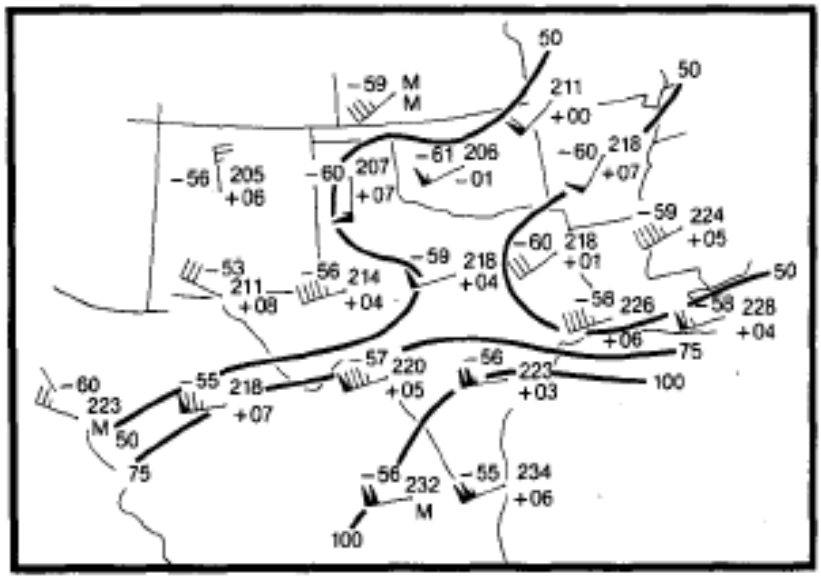

Figure 2.17 The 200-mb analysis for 0000 UTC 25 May 1981 from Maddox and Grice (1986). Selected isotachs are shown as solid contours, heights are dam minus 10 km, winds are in knots, and temperature in °C.

West Texas. The sub-tropical jet flowed over extreme southern Texas, including Austin and parts of Mexico. Large portions of Texas were influenced by large-scale features favorable to rising vertical motion and a warm, moist air mass that could be potentially unstable. This large-scale setting was not unusual for the end of spring in the Southern Plains.

On the smaller-scale, MCSs were present over Texas and formed east of the dryline and continued through the morning

hours. Moisture and instability in the air mass over south Texas helped fuel the system which could then lead to stabilized conditions.

The progression of an arc cloud, shown in Fig. 2.18, over Texas proved that stable conditions were temporarily present and left behind a vast area of subsidence. The morning sounding detected conditions within a deep, moist mesoscale downdraft and would have been considered as outflow from a local thunderstorm if the arc cloud had not been present.

Two of the mesoscale frontal zones stalled near Austin. The southernmost MCS yielded widespread rain that accumulated 76.2 – 127 mm (3.00 – 5.00 inches) leaving soil rather moist.

More thunderstorms with multicell characteristics developed over the same region. One cell was moving rather slowly in a north-northeast direction over Austin. The storm abruptly shifted at 0357 UTC to a north-south orientation as strong westerly outflow winds produced by a line of thunderstorms to the west blew into the Austin region. This resulted in ~203 mm (8.00 inches) of rainfall in 90 minutes.

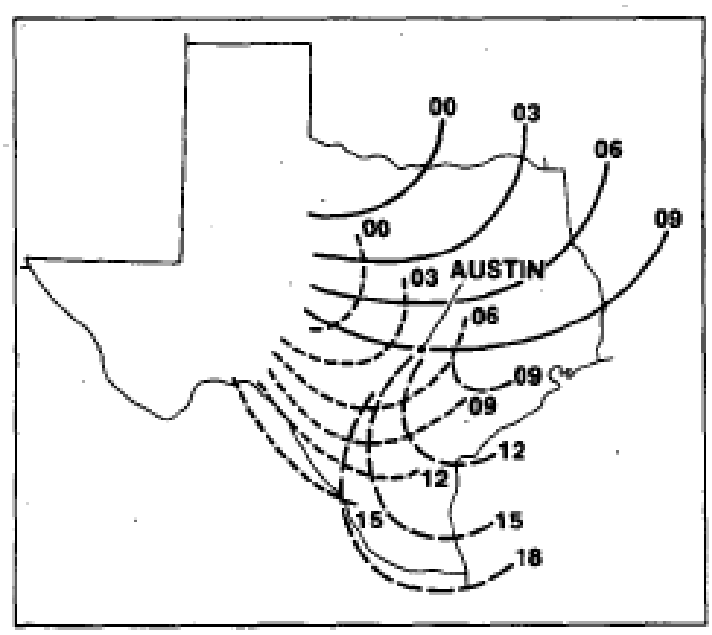

Figure 2.18 Mesoscale Outflow boundary progressions across Texas valid at all time periods for 24 May 1981. Reproduced from Maddox and Grice (1986).

A composite sounding for Austin, Texas, was generated using the three nearest upper-air soundings and satellite data at 0000 UTC. The air mass had destabilized throughout the afternoon according to the lifted indices from the lowest 100 mb to 500 mb and then to 300 mb. Weak vertical wind shear and small dewpoint depressions were present throughout the majority of the troposphere which could support very efficient rainstorms. The thermodynamic environment destabilized rapidly over central Texas. A strong, mesoscale-enhanced sea

breeze may have developed due to the cool mesohigh acting together with surface heating of the Coastal Plains. Thorough understanding of small, mesoscale, and large-scale processes that cause localized heavy rainfall is crucial in improving flash flood detection and warnings.

The following study shares the same approach of looking for dominant features in the patterns aloft. Blaha and Thoren (1997) focused on the subtropical storm system that occurred on 21-22 June 1997, produced 229 - 508 mm (9.00 – 20.0 inches) of rain over the Texas Hill Country, and 127 -279 mm (5.00 – 11.0 inches) throughout areas of south central Texas. They found the heavy rain event was associated with an open wave at 300 mb that overlaid a relatively cold pocket of air at 500 mb. This open wave developed into a closed low aloft as it began to stall in the weak westerlies. An 850-mb ridge was centered over the eastern side of the Gulf of Mexico. The upper-air ridge increased its strength as the low moved downstream. This caused the low aloft to drift southeast becoming quasi-stationary over the Hill Country. A strong low-level jet formed on the

eastern side of Texas allowing deep, warm, moist air to flow into south central and central portions of Texas.

The event began on 20 June 1997 with scattered thunderstorms developing near the dryline in west and southwest Texas. It later organized into a line and pushed eastward during the early hours of 21 June. As the morning progressed, the storms intensified on the outflow of a MCS that had already passed through. Continuous development of storms was the result of upper-air forcing and a mesohigh that had developed just north of the spirals around the low. Drier air aloft enhanced convective instability and strengthened the storms and the outflow boundaries near them. With increased daytime heating, the storms shifted south and west and had a more tropical nature. The intense rain band slowly moved northward, affecting the northern edge of the Hill Country while it dissipated.

The previous studies discussed focused primarily on 1-2 day events. Many cases have occurred that had longer durations. Nielsen-Gammon et al. (2005) analyzed events lasting up to 7 days. The purpose of the study was to explore

the meteorological causes and the predictability of the South-Central Texas Floods. Large-scale weather patterns associated with extreme rain in Texas were determined by using composite analyses.

The data used were from 1948 to 2003 using 6-hourly three-dimensional gridded analyses. An extreme rainfall event was defined as an event that produced at least 500 mm (~20 inches) total precipitation (a quantity nearly 5 times greater than Grice and Maddox 1982) from a time period up to seven days. Eighteen events were identified that met the criteria. The focus was on weather patterns of summer and early fall. Three sub-groups were defined due to the substantial changes in flow patterns over the five-month span. The groups are EARLY, LATE, and NONTROP.

The first group, EARLY, had 5 events that took place during June, July and early August which were associated with tropical cyclones. The second group, LATE, was also associated with tropical cyclones, but had 4 events that took place in September. The third group, NONTROP, had 9 events that were

not associated with tropical cyclones which primarily occurred in September and October.

The composites were generated at 0000 UTC of the date of the onset of the heaviest precipitation. A reference composite, one year exactly after each event, was used to compare the patterns. The following key elements from the composite are needed for heavy rain to occur.

Strong southeast winds carry larger amounts of moisture to lower levels of the atmosphere over Texas from the tropical Atlantic and Gulf of Mexico. The winds decelerate near Texas, which lead to a deeper layer of moisture across the Gulf than from due east. For events associated with tropical cyclones, ascent occurs from dynamic processes and upslope winds. The jet stream, located further north at the time of the tropical events, allowed the systems to move very slowly which focused ascent over Texas. Moist, southerly flow in the low-to-mid-levels aided instability generation and high precipitation efficiency. All of the sub-categories have strong low-level southeasterly flow.

The studies previously discussed show that heavy precipitating events can have a large range of values when

defining an event as extreme. This shows that the need to properly quantify rainfall into thresholds is great.

2.3 Summary

A deeper understanding has been gained from heavy rainfall studies in general, and those localized over the Texas Hill Country and surrounding plains of South Central Texas. The studies provide valuable insight on pinpointing features responsible for intense precipitation. The primary focus for this research will follow the methods described by Collier and Hardaker (1997) and Guinan (2005) for assessing the rainfall distribution, and Grice and Maddox (1982) for typing of the events. Since the root of this study deals with actual rainfall totals, the best statistical distribution to use was the gamma distribution.

Chapter 3: Data and Methodology

Two primary sources of data drive this study. First, the daily precipitation data allowed for the building of a robust gamma distribution for rainfall in the region and the identification of significant rain events in the region during that period. Second, the NARR dataset allowed for creation of soundings to represent the environment with each of the significant rain events.

3.1 Data

3.1.1 Rainfall

Within each county of the study area (Fig. 3.1a), there was at least one site where daily temperature and precipitation amounts are recorded and sent to the local National Weather Service office. The local office for the San Antonio/Austin area and receives 86 of these daily reports from stations with serially complete records spanning the study period of 1982-2006. Each observing station reported approximately 9131 daily reports of temperature and precipitation with a total dataset of approximately 785,266 reports. Measurable precipitation was

attained by eliminating reports of zero or trace values. The final dataset used had 130,986 reports.

Each observing station was plotted on the county warning area (CWA) of the San Antonio/Austin Forecast Office to provide a better view of the distribution across the Texas Hill Country (Fig. 3.1b). Every county was represented, but more stations are present in the eastern counties due to population density.

3.1.2 NARR

The data used for the sounding analysis portion of this study were from the North American Regional Reanalysis (NARR). The NARR archive extends back to 1978 and is 3-hourly. The NARR is on a 32 km grid, which means that finding a sounding for any point (using latitude and longitude) implies interpolation beyond the analysis scheme from the surrounding grid points.

The observing site with the greatest rainfall total was the first chosen to create a sounding representative of the state of the

a)

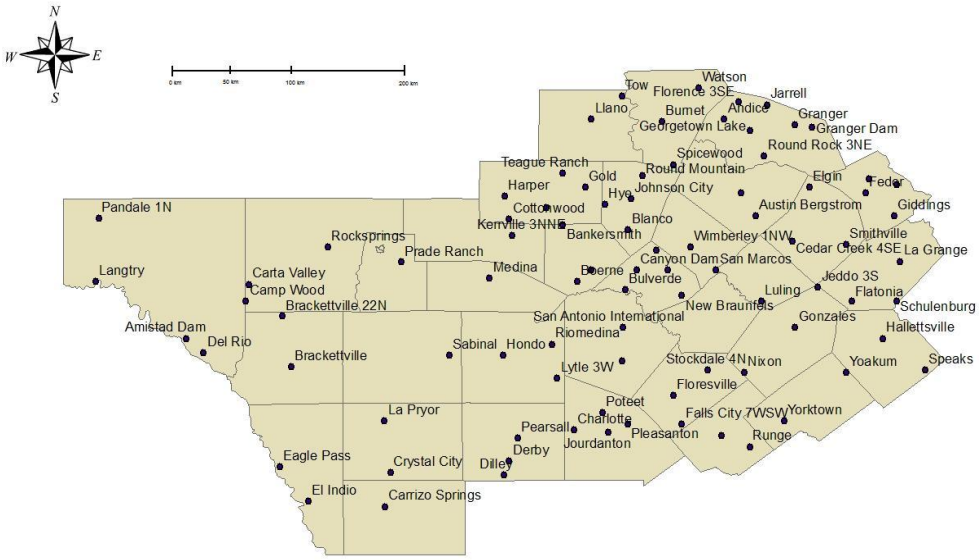

b)

Figure 3.1 *a) A map of the state of Texas. The red box encompasses the Hill Country. b)The San Antonio/Austin county warning area. The 86 reporting stations can be seen on this map with each county having at least one reporting station.*

atmosphere. If another colored dot lay outside a 200-km radius of the first site, then the new site with the next greatest rainfall total was also selected for the same event. This distance was greater than 5Δx and was chosen to avoid having two soundings influenced from the same grid point. Selecting the sites this way allowed the soundings to be less influenced by one grid point. Most of the events had at least two sites chosen.

3.2 Calculating gamma and event thresholds

Data taken from the stations were daily precipitation totals beginning with January 1, 1982 and ending with December 31, 2006. All entries were imported into statistical software to remove all instances of missing data and values of zero, or trace precipitation. Only measurable precipitation was desired. The new filtered data set were then imported into the gamma equation provided within the statistical software to calculate the α and β values for each observing site (Table 4.1). Aggregate values (α = 0.4678 and β = 1.0082) for the entire dataset. The

values vary greatly across the Texas Hill Country so the aggregate values provide a more uniform distribution.

3.3 Spatial Distribution

These values were then used in the gamma distribution equation in Excel to determine the top aggregate 0.5%, 1.0%, and 2% limits. The 2% values set the threshold for unusual events, 1% values represented rare events, and the 0.5% values set the threshold for extreme cases. The gamma distribution equation, from the statistical software, used the α and β values previously calculated, the percent value at which the calculation is to be performed, and the logical statement of true. By doing this rainfall thresholds (inches) were computed. As before, the 2% aggregate values set the threshold for unusual events, 1% aggregate values represented rare events, and the 0.5% aggregate values set the threshold for extreme cases.

Cases that had five or more stations receiving at least the lowest threshold of rainfall in a 24-hour time period were considered events for this study. Some events experienced

rainfall durations longer than 24 hours and the break-down of these events were: 1-day events (76), 2-day events (15), 3-day events (1), 4-day events (1), 5-day events (0), and 6-day events (1). Because the interest of this study was heavy rainfall in durations of 24 hours, only the 1 day events were selected.

Using the 1-day events, a spatial distribution was constructed using the CWA map of the Hill country. Tri-colored dots marked sites that reported rainfall totals above the thresholds mentioned in section 3.1. Unusual events were colored yellow, rare events were colored orange, and red represented extreme events; these maps, such as Fig. 3.2, provide a visualization of the magnitude of these events and guided us in sounding selection as discussed in section 3.1.2.

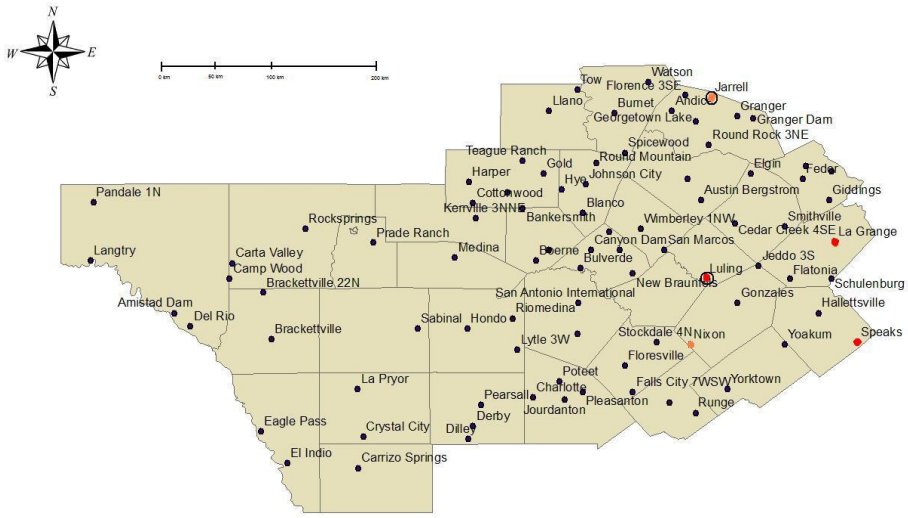

Figure 3.2 *Luling had the greatest rainfall totals for this event. Jarrell was located more than 32 km away from Luling so it was chosen as the second sounding location for the event.*

3.4 First Approximation of Event Typing

The daily weather maps issued at 1200 UTC were found in online archive files (Dept. of Commerce 2008) from the NOAA Central Library. The day before and the day of each event were used as they define the start and end of the time period for the daily precipitation reports of the 86 observing sites discussed in section 3.1.1. The surface maps aided in the judgment of which type of event occurred based on front location and orientation and key features described in Grice and Maddox (1982). Mesohigh events were cross checked using actual hourly data.

3.5 Sounding Analysis of Typed Events

NARR 3-hourly grids were downloaded for each event beginning with 1200 UTC the previous day and ending with the 1200 UTC of the day of the reported event. Model characteristics, such as the 32 km grid spacing and the time interval of 3 hours, may limit the study. Each file was converted over to the General Meteorology Package (GEMPAK) to view in the GEMPAK Analysis and Rendering Program (GARP) (UCAR 2008). A text file of the vertical profile was saved along with a postscript file of the sounding for each of the 3-hourly files at the location of the heavy rain report.

The second round of soundings was a smaller subset of the first. NARR allows a snapshot of the atmosphere every three hours using latitudes and longitudes. These time segments illustrate the system progression for each event. From each of the heavy rain sites, the 3-hourly soundings with the highest CAPE were selected. The rationale for this choice was that this was the time period when the atmosphere was most unstable and so most likely to be immediately before the time when the majority of the precipitation fell.

The new soundings were divided by the Maddox et al. (1979) classifications and by the three rainfall thresholds. This division created nine groups of composite soundings. From the soundings a lengthy list of stability parameters was taken and entered into a spreadsheet. A mean and a standard deviation were found for each parameter. A separate spreadsheet was made for the nine groups using the text files from the soundings. These files included the height in meters, temperature and dewpoint in °C, wind direction in degrees, wind speed in knots, and omega values in μb s^{-1}. Means and standard deviations were found for each atmospheric level; however, and the median value was found for the wind direction. By taking the mean of wind directions in degrees the results were usually around 180° or southerly flow. The median provides a more realistic average of the wind direction.

Using the Mann-Whitney statistical tests, the stability parameters were compared. A confidence level of 95% is typically desired to show that the data from different samples are significantly different. The results among the three thresholds showed that the confidence levels were low that the soundings came from different datasets. The stability

parameters from each group of soundings were thus statistically indistinct from one another, in so far as the Mann-Whitney test is concerned. This implies possible over-classification of event types from Grice and Maddox (1982), and/or implies that the sounding conditions are nearly the same for all heavy rain events, thus it appears that forcing (e.g. cold front, MCS, short wave trough, etc.) is more important for focusing convection to generate heavy rainfall.

3.6 Summary

Thresholds to classify heavy rain events were quantified by fitting the rainfall totals over the past 25 years to a gamma distribution. The thresholds for 24-hr storms were: unusual (2%), rare (1%), and extreme (0.5%). Using the three thresholds, event locations were chosen to create a vertical profile. The most unstable sounding for each event was then created from NARR grids and used to determine mean values of the stability parameters. From these mean values, composite soundings were created for the standard event types (mesohigh, frontal, and synoptic) after Maddox et al. (1979).

Chapter 4: Rainfall Data

4.1 Rainfall Thresholds

For the aggregate gamma distribution of 24-hour rainfall amounts based on 86 stations over 25 years, the parameter values of α=0.4678 and β=1.0082 were obtained. Values for each observing site can be seen in Table 4.1. There were 130,986 24-hour rainfall values were used in determining the distribution. The aggregate data yielded a 24-hour rainfall threshold of 67.1 mm (2.64 inches) for an observation to be in the upper 2%, 82.6 mm (3.25 inches) to be in the upper 1%, and 98.3 mm (3.87 inches) to be in the upper 0.5% of the distribution. The differences between the three thresholds were approximately 15.5 mm (0.61 inches), which were relatively small. Thus, extreme cases were the ones that most closely match the ~102 mm (4 inches) in 24 hr criterion of Grice and Maddox (1982) for a Texas Hill Country heavy rain event, however this value was much less than that of Nielsen-Gammon et al. (2005).

Table 4.1 α and β values for New Braunfels, Texas CWA.

	α	β		α	β
Amistad Dam	0.261	1.038	Jarrell	0.644	0.767
Andice2	0.645	0.743	Jeddo3S	0.487	1.052
Austin-Bergstrom	0.360	1.116	Johnson City	0.415	1.044
Austin-MuellerMabry	0.399	0.962	Jourdanton	0.348	1.109
Bankersmith	0.477	1.092	Karnes City2N	0.618	0.779
Blanco	0.413	0.992	Kerrville3NNE	0.354	1.005
Boerne	0.400	1.218	La Grange	0.639	0.907
Bracketville	0.632	0.853	La Pryor	0.383	1.117
Bracketville22N	0.356	1.241	Langtry	0.492	0.699
Bulverde	0.525	1.167	Lexington	0.524	0.973
Burnet	0.586	0.774	Llano	0.575	0.710
Camp Wood	0.445	1.017	Luling	0.398	1.093
Canyon Dam	0.398	0.961	Lytle3W	0.332	1.016
Carrizo Springs	0.380	0.947	Medina	0.318	1.368
Carta Valley	0.601	1.103	New Braunfels	0.370	1.268
Cedar Creek4SE	0.602	0.841	Nixon	0.423	1.043
Charlotte5NNW	0.424	1.008	Northington Ranch	0.476	1.093
Cottonwood	0.879	0.772	Pandale1N	0.433	0.816
Crystal City	0.409	0.790	Pearsall	0.604	0.886
Del Rio	0.249	1.198	Pleasanton	0.389	1.109
Derby1S	0.554	0.997	Poteet	0.474	1.011
Dilley	0.276	1.404	Prade Ranch	0.538	1.088
Dime Box	0.636	0.881	Riomedina	0.624	1.126
Eagle Pass	0.326	1.083	Rocksprings	0.419	1.007
El Indio	0.528	0.902	Round Mountain1NW	0.798	0.862
Elgin	0.667	0.838	Round Rock	0.617	0.919
Falls City7WSW	0.827	0.823	Runge	0.407	1.026
Fedor	0.878	0.911	Sabinal	0.456	0.890
Fischer's Store	0.668	0.933	San Antonio-KSAT	0.322	1.203
Flatonia	0.446	0.998	San Antonio-Stinson	0.397	1.030
Florence3SE	0.871	0.835	San Marcos	0.374	1.117
Floresville	0.520	1.029	Schulenburg	0.694	0.848
Fredericksburg	0.373	1.023	Smithville	0.587	0.971
Georgetown Lake	0.479	0.894	Speaks2	0.606	1.100
Giddings5E	0.573	0.908	Spicewood	0.552	0.905
Gold	0.600	0.930	Springbranch2SE	0.562	1.009
Gonzales	0.388	1.097	Stockdale4N	0.398	0.996
Granger Dam	0.418	0.949	Teague Ranch	0.500	0.934
Granger	0.531	0.972	Tow	0.731	0.701
Hallettsville	0.404	1.091	Watson	0.557	0.793
Harper	0.499	0.920	Wimberly1NW	0.483	1.138
Hondo	0.499	0.920	Yoakum	0.368	1.202
Hye	0.582	0.995	Yorktown	0.537	0.958

Most cases were either extreme (0.5%) or unusual (2%) events over the 25 year period. There were 23 instances that were unusual events, 28 instances of rare events, and 69 instances of extreme events.

Over the course of 25 years, 127 days were found on which at least five stations in the region had a 24-hour rainfall total that would be in the top 2% (or higher). Of these, only four were the direct result of a tropical cyclone.

Grice and Maddox (1982) used 102 mm (4 inches) as a threshold for determining heavy rainfall events within the Hill Country and 127 mm (5 inches) outside of the Hill Country. The threshold calculated by the gamma distribution for extreme events was comparatively close to the arbitrary value that Grice and Maddox (1982) chose. By having all three thresholds less than the value previously chosen, more events are considered than Grice and Maddox (1982).

Figure 4.1 is color-coded for the values of greatest rainfall totals and shows a bulls eye of higher values of rainfall over the eastern plains, including, Giddings, etc. The average greatest rainfall amount was 7.71 inches with a standard deviation of

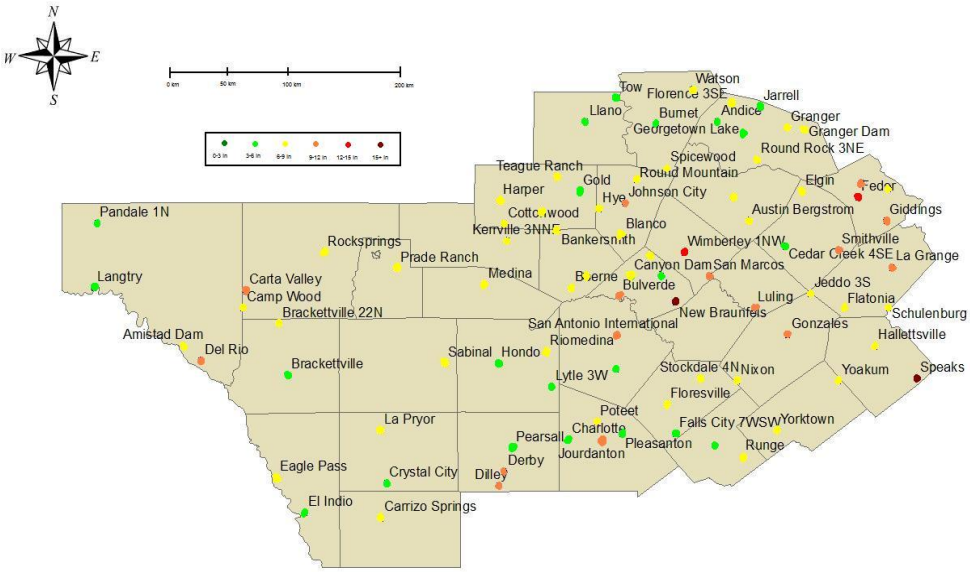

Figure 4.1 *Distribution of the greatest reported rainfall amount from each observing station. Dark green dots had rainfall totals from 0 to 3 inches, green dots had 3 to 6 inches, yellow dots had rainfall totals from 6 to 9 inches, orange dots had 9 to 12 inches, red dots had rainfall totals 12 to 15 inches, and burgundy had rainfall totals in excess of 15 inches.*

2.46 inches. The range was from 4.08 inches at Pandale to 18.35 inches at New Braunfels. The lowest in the range of rainfall totals was 0.25 mm (0.01 inches) and the greatest measurement was ~466 mm (18.35 inches).which fell in New Braunfels in 1998. Table 4.2 displays a list of the highest rainfall measured in the 25-year period for each location.

Table 4.2 Highest reported 24-hour rainfall amounts in the period (1982-2006) for each observing site in the Texas Hill Country.

	mm	in	Date		mm	in	Date
Amistad Dam	180.3	7.1	8/24/1998	Jarrell	148.6	5.85	10/18/1998
Andice2	140.5	5.53	10/18/1998	Jeddo3S	218.4	8.6	11/23/2004
Austin-Bergstrom	220.5	8.68	11/15/2001	Johnson City	232.2	9.14	6/29/1995
Austin-MuellerMarby	191.8	7.55	11/15/2001	Jourdanton	228.6	9	7/16/1990
Bankersmith	176.5	6.95	7/3/2002	Karnes City2N	121.9	4.8	10/19/1998
Blanco	171.5	6.75	9/6/1986	Kerryville3NNE	152.9	6.02	6/22/1997
Boerne	226.8	8.93	6/22/1997	La Grange	231.4	9.11	10/17/1994
Brackettville	147.3	5.8	9/16/1994	La Pryor	211.3	8.32	7/6/2003
Brackettville22N	195.6	7.7	10/28/1996	Langtry	106.4	4.19	9/18/1988
Bulverde	292.1	11.5	10/17/1998	Lexington	257.3	10.13	10/17/1994
Burnet	143.5	5.65	6/30/2002	Llano	134.4	5.29	3/19/1999
Camp Wood	212.6	8.37	11/15/2001	Luling	267.5	10.53	10/18/1998
Canyon Dam	133.4	5.25	10/2/2004	Lytle3W	131.1	5.16	10/23/2000
Carrizo Springs	223.0	8.78	7/16/1990	Medina	223.5	8.8	6/4/1987
Carta Valley	273.1	10.75	8/24/1998	New Braunfels	466.1	18.35	10/18/1998
Cedar Creek 4SE	142.2	5.6	12/21/1991	Nixon	195.6	7.7	5/23/1993
Charlotte5NNW	139.7	5.5	7/1/2002	Northington Ranch	193.3	7.61	6/22/1997
Cottonwood	160.0	6.3	6/22/1997	Pandale1N	103.6	4.08	10/20/1983
Crystal City	112.8	4.44	7/17/1990	Pleasanton	135.4	5.33	6/26/1993
Del Rio	301.5	11.87	8/23/1998	Poteet	166.6	6.56	10/8/1994
Derby1S	263.4	10.37	9/9/2002	Prade Ranch	184.4	7.26	6/10/2004
Dilley	266.7	10.5	7/1/2002	Rio Medina	189.5	7.46	10/28/1996
Dime Box	198.1	7.8	10/16/1994	Rocksprings	172.5	6.79	10/18/1998
Eagle Pass	217.9	8.58	7/22/1992	Round Mountain1NW	211.3	8.32	10/24/2000
El Indio	142.2	5.6	4/5/2004	Round Rock3NE	158.0	6.22	5/11/1983
Elgin	154.9	6.1	11/16/2001	Runge	162.1	6.38	11/16/2001
Falls City7WSW	134.6	5.3	6/26/1999	Sabinal	168.1	6.62	8/30/2001
Fedor	330.2	13	10/17/1994	San Antonio-KSAT	286.0	11.26	8/27/2001
Fischers Store	215.9	8.5	10/17/1998	San Antonio-Stinson	116.8	4.6	10/17/1998
Flatonia	218.4	8.6	10/18/1998	San Marcos	230.4	9.07	10/9/2002
Florence3SE	182.9	7.2	10/17/1998	Schulenburg	165.6	6.52	11/24/1985
Floresville	224.0	8.82	11/19/1992	Smithville	242.1	9.53	10/17/1994
Fredericksburg	169.4	6.67	10/19/1985	Speaks2	386.1	15.2	10/18/1998
Georgetown Lake	139.7	5.5	4/4/1997	Spicewood	211.1	8.31	10/18/1998
Giddings5E	156.5	6.16	10/17/1994	Springbranch2SE	211.3	8.32	11/16/2001
Gold	134.1	5.28	7/4/2002	Stockdale4N	200.9	7.91	10/17/1998
Gonzales	300.5	11.83	10/18/1998	Teague	172.7	6.8	11/19/1992
Granger	158.0	6.22	5/13/2004	Teague Ranch	172.7	6.8	12/20/1991
Granger Dam	199.1	7.84	12/21/1991	Tow	121.9	4.8	12/31/1986
Hallettsville	154.2	6.07	8/31/2001	Watson	166.4	6.55	12/21/1997
Harper	161.3	6.35	10/28/1996	Wimberly1NW	317.5	12.5	10/18/1998
Hondo	128.8	5.07	5/29/1987	Yoakum	224.0	8.82	10/18/1994
Hye	223.5	8.8	6/30/2002	Yorktown	191.5	7.54	6/22/1997

Figure 4.2 provides the monthly distribution for all of the Grice and Maddox (1982) events. Two distinct peaks occur, one near the transition from spring to summer and the other near the transition between fall and winter. The distribution for synoptic events (Fig. 4.2a) shows distinct peaks during the months of May and October. This agrees with Maddox et al. (1979) having the most events occur during the month of October.

Figure 4.2b gives the monthly distribution for mesohigh events. May had the most events with June having the second greatest number. Maddox et al. (1979) found that most events occurred in June and July. The monthly distribution of frontal events is shown Fig. 4.2c. Two significant peaks occur in June and October. The results from Maddox et al. (1979) show July and August having the most events. Overall, the occurrences of the events by month are generally close to the results of previous work.

Table 4.3 lists the number of events separated by the three thresholds for each observing site. Using the same

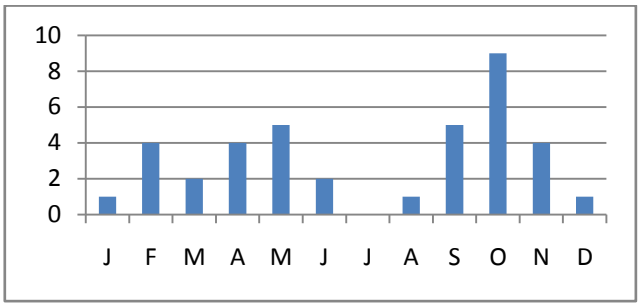

a)

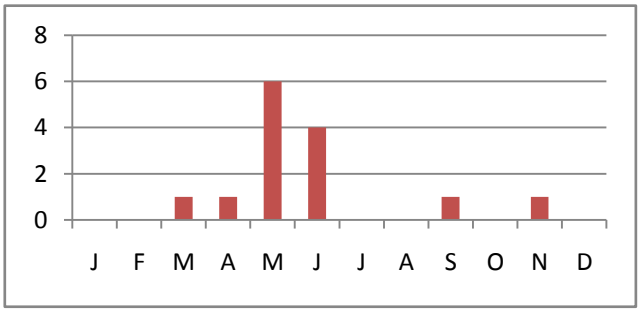

b)

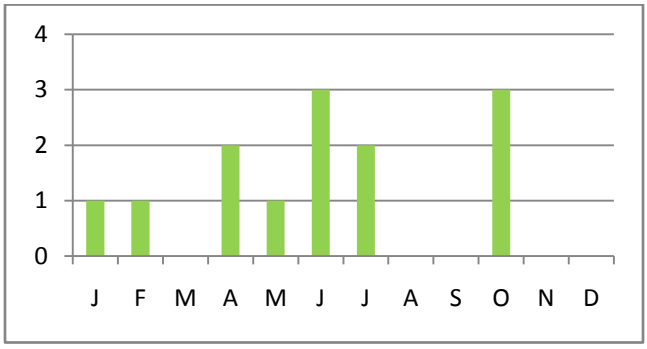

c)

Figure 4.2 *a) The monthly distributionfor synoptic events, b) monthly distribution for mesohigh events, and c) monthly distribution for frontal events in the Texas Hill Country.*

concept of comparing the table to the map of the Hill Country, patterns in the number of events arose for each threshold.

Table 4.3 The breakdown of extreme, rare, and unusual events for each site in the Texas Hill Country for the period 1982-2006.

	2%	1%	0.50%		2%	1%	0.50%
Amistad Dam	17	9	6	Jarrell	27	8	4
Andice2	17	9	6	Jeddo 3S	32	20	12
Austin-Bergstrom	9	5	3	Johnson City	31	19	12
Austin-Mueller Mabry	27	12	8	Jourdanton	30	19	6
Bankersmith	31	19	12	Karnes City 2N	21	10	2
Blanco	34	16	7	Kerrville 3NNE	27	16	10
Boerne	45	27	19	La Grange	29	14	9
Bracketville	11	5	4	La Pryor	22	16	7
Bracketville22N	33	20	10	Langtry	7	2	1
Bulverde	40	25	14	Lexington	30	17	10
Burnet	16	9	4	Llano	15	5	4
Camp Wood	28	17	8	Luling	32	18	12
Canyon Dam	28	17	10	Lytle 3W	29	16	8
Carrizo Springs	12	8	3	Medina	45	27	17
Carta Valley	18	9	6	New Braunfels	24	14	9
Cedar Creek4SE	29	15	7	Nixon	26	15	12
Charlotte5NNW	28	15	9	Northington Ranch	35	23	13
Cottonwood	29	17	8	Pandale 1N	12	7	1
Crystal City	8	4	1	Pearsall	13	9	6
Del Rio	11	5	3	Pleasanton	28	16	3
Derby1S	22	12	7	Poteet	26	17	9
Dilley	17	11	8	Prade Ranch	24	17	12
Dime Box	35	18	10	Riomedina	38	22	15
Eagle Pass	19	8	4	Rocksprings	16	9	5
El Indio	17	7	6	Round Mountain 1NW	34	15	9
Elgin	28	16	12	Round Rock 3NE	36	19	10
Falls City 7WSW	29	14	9	Runge	30	14	11
Fedor	37	17	10	Sabinal	14	7	4
Fischer's Store	37	24	12	San Antonio-KSAT	31	16	9
Flatonia	36	19	7	San Antonio-Stinson	7	2	2
Florence 3SE	29	19	8	San Marcos	35	21	14
Floresville	29	13	8	Schulenburg	38	14	10
Fredericksburg	28	17	9	Smithville	40	19	9
Georgetown Lake	36	15	5	Speaks 2	53	29	16
Gidding 5E	41	19	9	Spicewood	30	16	7
Gold	34	20	11	Springbranch 2SE	31	15	9
Gonzales	30	16	9	Stockdale 4N	27	12	6
Granger Dam	32	19	11	Teague Ranch	25	14	11
Granger	25	10	4	Tow	17	9	5
Hallettsville	46	23	16	Watson	19	10	6
Harper	26	14	9	Wimberly 1NW	34	22	12
Hondo	12	5	5	Yoakum	37	22	12
Hye	37	22	9	Yorktown	40	20	9

Figure 4.3 is color-coded for the number of unusual events for each observing station. The average number of events per location was 12.5 with a standard deviation of 4.88. The range was from 4 events (Austin-Bergstrom, Carrizo Springs, Crystal City, and Pearsall) to 24 events at Speak2 and Schulenberg. It is clear that the western side of the Hill Country had fewer events. The number of events varied between 4 and 13 events for the 25-year period. The eastern side of the Hill Country had significantly more events ranging from 4 to 24. Only a few locations had events in the single digits. The greatest number of events occurred along the eastern boundary.

These locations are closer to the Gulf of Mexico and may have more moisture throughout the column. Southwesterly flow from the Pacific Ocean travels a large distance and loses moisture as it travels towards western Texas. These stations on the western edge will have lower rainfall totals.

Figure 4.4 shows color-coded dots for the number of events for the rare (1%) threshold. The average number of events per station was 6.48 with a standard deviation of 3.25.

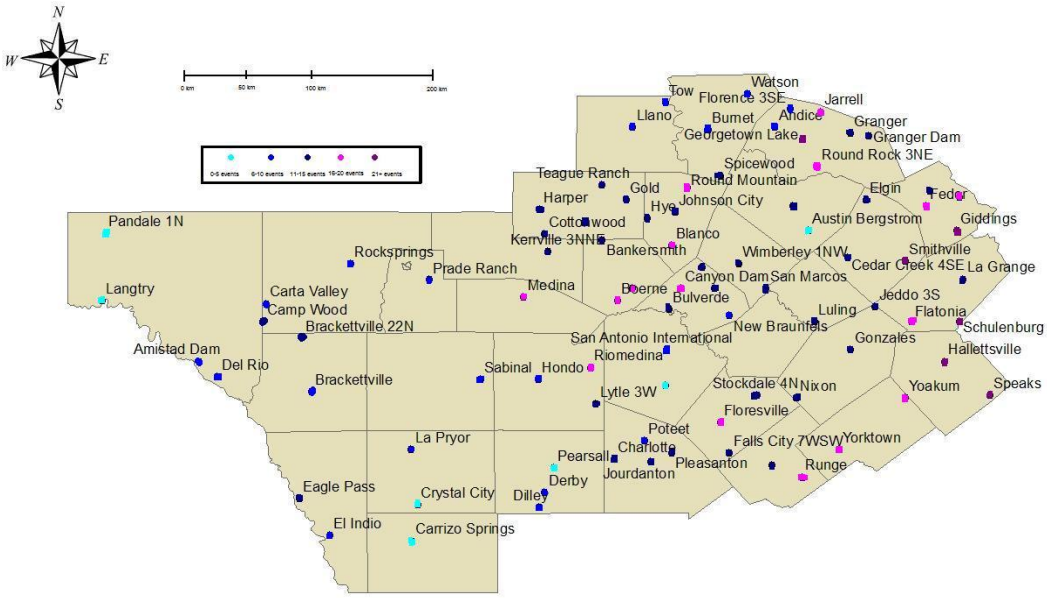

Figure 4.3 *Distribution of number of unusual events from each observing station. Light blue dots had 0 to 5 events, blue dots had 6 to 10 events, navy dots had 11 to 15 events, magenta dots had 16 to 20 events, and purple dots had 21 or more events.*

The range was from 0 events at Llano and San Antonio-Stinson to 13 events at Hye, Jourdanton, Pleasanton, and Speaks2.

The western third of the Hill Country (west of Medina and Dilley) had fewer events just like the unusual threshold. Values ranged from 1 to 10, where further into the Hill Country, the values increased. The eastern two-thirds did have more events. The eastern side ranged from 3 to 13 events. The center portion

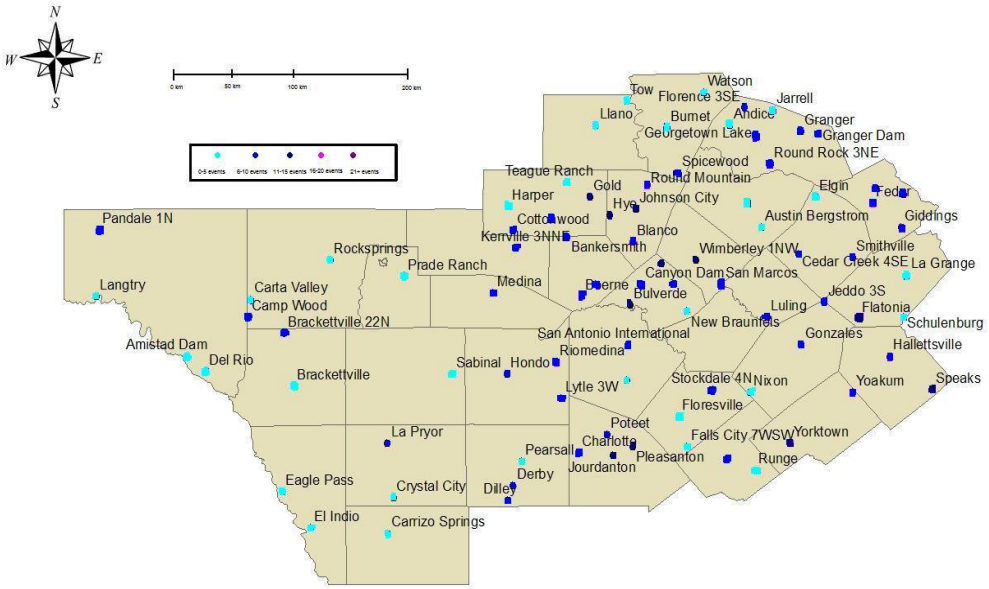

Figure 4.4 *Distribution of number of rare events from each observing station. Light blue dots had 0 to 5 events, blue dots had 6 to 10 events, navy dots had 11 to 15 events, magenta dots had 16 to 20 events, and purple dots had 21 or more events.*

had the highest range of 1 to 13 events; however, most of the values were above 7 events. Medina, Bulverde, Hye, and Wimberley had the most events in the center third.

For extreme (0.5%) events, the average number of events per station was 8.33 with a standard deviation of 3.78. The range was from 1 event at Crystal City, Langtry, and Pandale1N to 19 events at Boerne. Figure 4.5 shows a color-coded map for

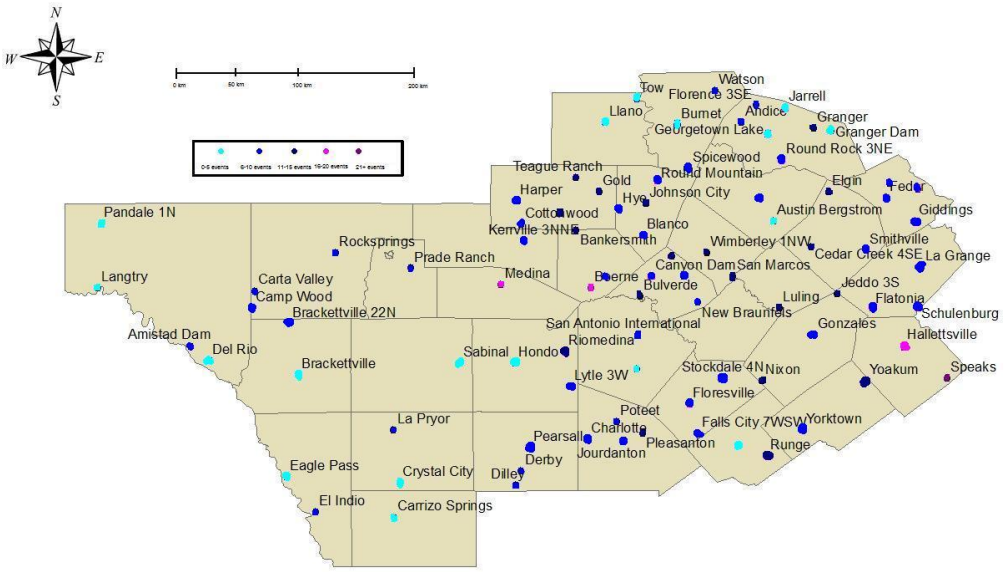

Figure 4.5 *Distribution of number of extreme events from each observing station. Light blue dots had 0 to 5 events, blue dots had 6 to 10 events, navy dots had 11 to 15 events, magenta dots had 16 to 20 events, and purple dots had 21 or more events.*

the number of events for each observing station. The western side had fewer events and with a range of 1 to 12. Most of the sites had values 6 or less. The eastern third varied from 3 to 16. The center section had the highest numbers with values from 2 to 19. The majority of the sites were greater than 8. The highest number of events occurred from Medina to San Marcos and between Riomedina and Bankersmith.

4.2 Summary

Application of the gamma distribution provides a clearer quantification of daily heavy rain thresholds than the empirical choice made by GM82. The limits for the top 2%, 1% and 0.5% were lower than the limits set by Grice and Maddox (1982). The extreme threshold value of ~ 98.0 mm (3.86 inches) was in close agreement of the ~ 102 mm (4 inches) of rainfall within a 24-hour period defined by Grice and Maddox (1982). The difference between the highest and lowest threshold was ~ 31 mm (1.22 inches).

The explanation of having a large number of 'extreme' rainfall events compared to the number of 'unusual' events was that the threshold had relatively low values in comparison to highest reported total. When it rained, it poured to an intensity that resulted in higher occurrences of extreme events.

Chapter 5: Soundings

5.1 NARR 3-Hourly Soundings

Each event had at least one observing site that was chosen to represent that individual case. Soundings were constructed for 1200 UTC and every 3-hrs (1500 UTC, 1800 UTC, etc.) throughout the 24-hr period for the chosen site in each event. With 76 cases, more than 1300 3-hourly soundings were constructed. The purpose of this approach was to determine the three hour time segment that was least stable during the 24-hours that precipitation accumulated. Several assumptions were made: 1) that the precipitation that fell was convective, 2) that the chosen sounding occurred before the heaviest rain fell, and 3) that the NARR grids accurately captured the environment described previously. The sounding that had the largest CAPE was chosen to represent this time period. This procedure greatly reduced the number of soundings to analyze. The CAPE was determined from the most unstable parcel in the lowest 300 mb, which may or may not have been surface-based.

5.2 Assessing Stability from Soundings

The most unstable time period for each event was selected by choosing the time period that had the highest values of CAPE or the lowest values of LI. There were 117 soundings that were the most unstable from the first dataset. From this new dataset, 28 static stability and convection-related parameters were recorded in a spreadsheet. The mean and standard deviations were calculated for each parameter. The median was found only for the wind direction. A comparison was done for each threshold and class. Although statistically significant differences were not found amongst thresholds or between classes (likely due to the small differences between the 0.5% and 2% thresholds), subjective comparisons do reveal some interesting results, which are briefly shown in this section.

5.2.1 Stability Parameters

Instability parameters and sources of lift are important in thunderstorm forecasting (SPC 2008). The lifting condensation level (LCL) provides a good estimation of cloud base height when a parcel undergoes forced ascent. Thunderstorms tend to

initiate and stay maintained when the level of free convection (LFC) heights remain less than 3000 m. The equilibrium level (EL) was generally used to estimate the height of the thunderstorm anvil. Lapse rates of 5.50 – 6.00 °C km^{-1} are "stable" and values near 9.50 °C km^{-1} are "absolutely unstable". The atmosphere is conditionally unstable if the lapse rate lies between the two values. If sufficient moisture is available, lifted parcels can produce positive CAPE and/or negative LI.

A CAPE value less than 1000 J kg^{-1} was considered "weak instability", a value from 1000 to 2500 J kg^{-1} was considered "moderate instability", and a value that was greater than 4000 J kg^{-1} was considered "extreme instability". The Bulk Richardson number (BRN) shear uses the low level wind and density-weighted mean wind difference through mid levels. The parameters above are just a few that were used to analyze the events and predict heavy rainfall. Combinations of these indices and parameter values can lead to impressive events. Figure 5.1 is the most current checklist used for such events.

In the ensuing sections, we examine each of the classes defined by Maddox et al. (1979) in the context of the thresholds

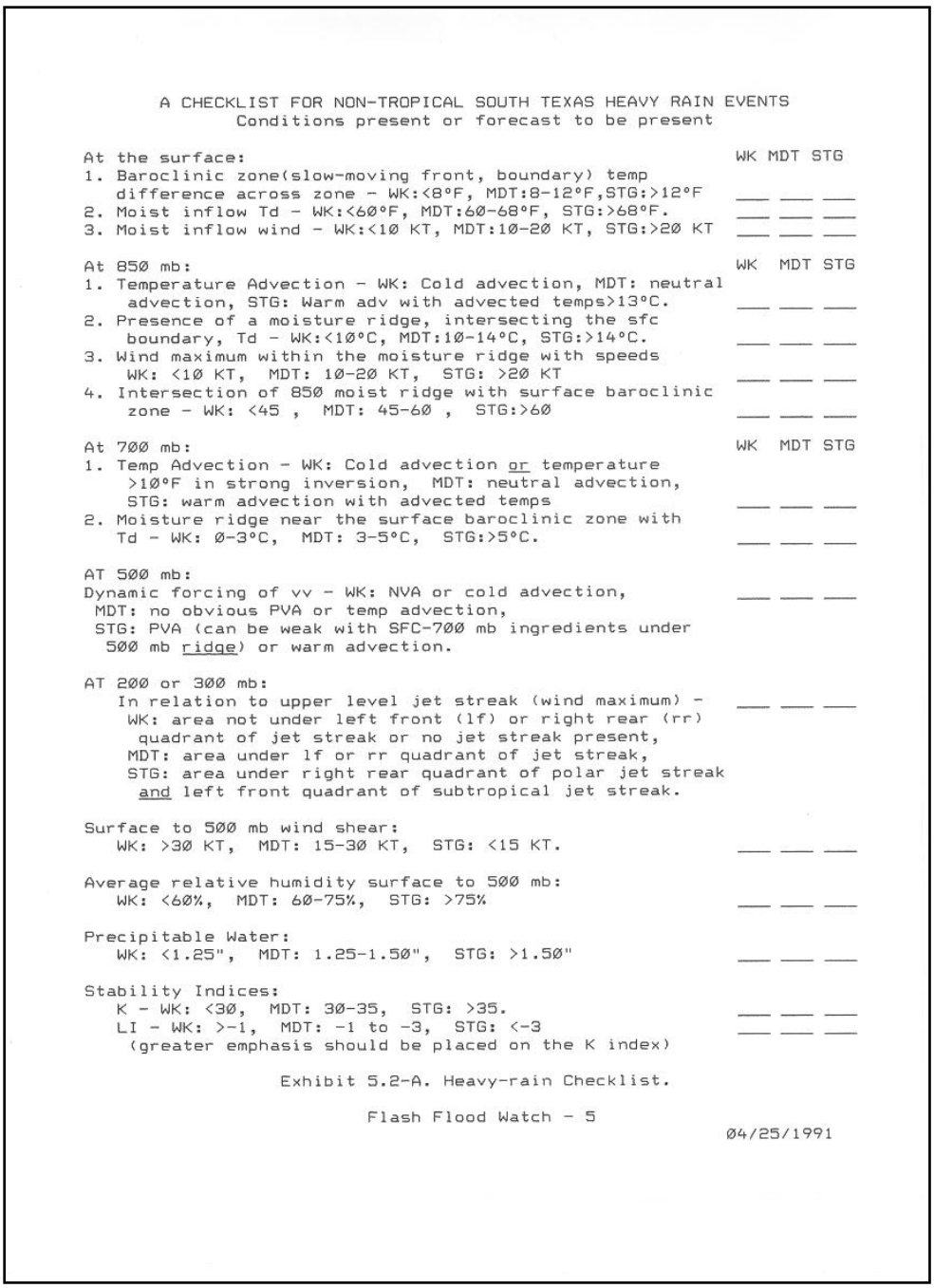

A CHECKLIST FOR NON-TROPICAL SOUTH TEXAS HEAVY RAIN EVENTS
Conditions present or forecast to be present

	WK	MDT	STG
At the surface:			
1. Baroclinic zone(slow-moving front, boundary) temp difference across zone - WK:<8°F, MDT:8-12°F,STG:>12°F	___	___	___
2. Moist inflow Td - WK:<60°F, MDT:60-68°F, STG:>68°F.	___	___	___
3. Moist inflow wind - WK:<10 KT, MDT:10-20 KT, STG:>20 KT	___	___	___
At 850 mb:	WK	MDT	STG
1. Temperature Advection - WK: Cold advection, MDT: neutral advection, STG: Warm adv with advected temps>13°C.	___	___	___
2. Presence of a moisture ridge, intersecting the sfc boundary, Td - WK:<10°C, MDT:10-14°C, STG:>14°C.	___	___	___
3. Wind maximum within the moisture ridge with speeds WK: <10 KT, MDT: 10-20 KT, STG: >20 KT	___	___	___
4. Intersection of 850 moist ridge with surface baroclinic zone - WK: <45 , MDT: 45-60 , STG:>60	___	___	___
At 700 mb:	WK	MDT	STG
1. Temp Advection - WK: Cold advection or temperature >10°F in strong inversion, MDT: neutral advection, STG: warm advection with advected temps	___	___	___
2. Moisture ridge near the surface baroclinic zone with Td - WK: 0-3°C, MDT: 3-5°C, STG:>5°C.	___	___	___
AT 500 mb:			
Dynamic forcing of vv - WK: NVA or cold advection, MDT: no obvious PVA or temp advection, STG: PVA (can be weak with SFC-700 mb ingredients under 500 mb ridge) or warm advection.	___	___	___
AT 200 or 300 mb:			
In relation to upper level jet streak (wind maximum) - WK: area not under left front (lf) or right rear (rr) quadrant of jet streak or no jet streak present, MDT: area under lf or rr quadrant of jet streak, STG: area under right rear quadrant of polar jet streak and left front quadrant of subtropical jet streak.	___	___	___
Surface to 500 mb wind shear: WK: >30 KT, MDT: 15-30 KT, STG: <15 KT.	___	___	___
Average relative humidity surface to 500 mb: WK: <60%, MDT: 60-75%, STG: >75%	___	___	___
Precipitable Water: WK: <1.25", MDT: 1.25-1.50", STG: >1.50"	___	___	___
Stability Indices:			
K - WK: <30, MDT: 30-35, STG: >35.	___	___	___
LI - WK: >-1, MDT: -1 to -3, STG: <-3	___	___	___
(greater emphasis should be placed on the K index)			

Exhibit 5.2-A. Heavy-rain Checklist.

Flash Flood Watch - 5

04/25/1991

Figure 5.1. Reproduction of a checklist for non-tropical heavy rain events in South Texas in use at the New Braunfels, TX, National Weather Service Office.

(2% and 0.5%) determined by the gamma distribution of rainfall events studied in this work. The reader is referred to Section 2.2.1 for a refresher on the details of the mesohigh, frontal, and synoptic classifications.

5.2.1.1 Unusual Mesohigh Events

Unusual (2%) mesohigh heavy rain events are evaluated in this section (Table 5.1). Two soundings contributed to the mean values. Precipitation values ranged from ~ 71.1 – 77.2 mm (2.8-3.04 inches) and had an average of ~74.2 mm (2.92 inches). With these events the indices indicate that the atmosphere was moderately unstable. Indeed, values of CAPE are in excess of 1000 J kg^{-1}, while CINH is not present at all. The normalized CAPE (NCAPE) is not very telling about the vertical distribution of the CAPE with this small sample size. However, the precipitable water values were substantial, while the various metrics for wind shear were all relatively weak. Indeed, the BRN Shear values, expressed as

$$\text{BRN Shear} = 0.5\,(U_{avg})^2 \qquad (5.1)$$

Table 5.1 Statistical analysis of stability parameters for unusual mesohigh events (N=2).

	Min	**Max**	**Mean**	**1 stdev.**
Precipitation (in)	3.87	6.6	4.71	3.96 to 5.46
LPL (mb)	1000	900	954	981 to 926
LCL (mb)	955	804	881	926 to 837
LFC (mb)	933	720	831	910 to 752
EL (mb)	225	145	182	208 to 156
CAPE (J/kg)	1309	4181	2330	1470 to 3190
CINH (J/kg)	-148	0	-28	- 78.1 to 21.7
Precipitable. Water (in)	0.88	1.86	1.44	1.14 to 1.73
FRZ Level (m)	10,244	14,101	12406	11,014 to 14,331
700-500mb LR (°C/km)	5.9	8	7	6.4 to 7.6
850-500mb LR (°C/km)	6	7.9	7	6.4 to 7.5
NCAPE (J/kg-mb)	1.8	5.9	3.6	2.5 to 4.6
LI (°C)	-9	-5	-7	- 9 to - 6
TT	45	56	33	49 to 55
KI	25	41	52	28 to 38
ThetaE Diff	11	30	18.9	13.8 to 24.1
BRN Shear (m2/s2)	2	62	23	4.5 to 41.1
BRN	32	925	203	- 29.4 to 435
sfc-6km Mean Wind Dir.	173	288	215	185 to 255
sfc-6km Mean Speed (kts)	4	28	17	11 to 26
LFC-EL Mean Wind Dir.	187	273	230	201 to 251
LFC-EL Mean Speed (kts)	11	32	21	15 to 33
850-300 Mean Wind Dir.	183	272	232	202 to 250
850-300 Mean Speed (kts)	13	29	22	15 to 33

where U_{avg} is the mean wind speed between the surface and 6 km, average around 13.0 m^2 s^{-2}. Each feature suggests an atmosphere conducive to convective development, and whose towers are less sheared and more upright. The mean wind speeds also point to slow-moving convection. These are themes that will dominate the ensuing tabular analyses.

5.2.1.2 Extreme Mesohigh Events

Fourteen soundings contributed to the mean composite. Of course, precipitation values were much higher in this category and ranged from ~ 98.3 – 167.6 mm (3.87-6.60 inches) with an average of 119.4 mm (4.70 inches). The atmosphere was moderately unstable, although CAPE values were higher than with the unusual events (shown in Table 5.2). CINH was also non-zero, but as with CAPE that was likely a function of the larger sample size. Yet, while wind shear metrics were stronger in this category, they are still modest, with a mean BRN Shear of 23 m^2 s^{-2}. Amounts of precipitable water similar to the unusual mesohigh events were found here, while the mean equilibrium level was higher in these extreme events.

Table 5.2 Statistical analysis of stability parameters for extreme mesohigh events (N=14).

	Min	**Max**	**Mean**	**1 stdev.**
Precipitation (in)	2.8	3.04	2.92	2.75 to 3.09
LPL (mb)	1000	975	988	1005 to 970
LCL (mb)	879	842	861	887 to 834
LFC (mb)	879	832	861	889 to 822
EL (mb)	220	175	198	229 to 166
CAPE (J/kg)	1173	2812	1993	834 to 3151
CINH (J/kg)	0	0	0	0
Precipitable water (in)	1.3	1.4	1.35	1.28 to 1.42
Freezing Level (m)	12,484	13,271	12,878	12,321 to 13,434
700-500mb lapse rate (°C/km)	6.1	6.9	6.5	5.9 to 7.1
850-500mb lapse rate (°C/km)	6.4	7.1	6.8	6.3 to 7.2
NCAPE (J/kg-mb)	1.8	4.3	3.0	1.27 to 4.78
LI (°C)	-5	-8	-7	- 9 to - 4
TT	48	54	51	47 to 55
KI	29	31	30	29 to 31
ThetaE Diff	15	25	20	12.9 to 27.1
BRN Shear (m2/s2)	10	16	13	8.8 to 17.2
BRN				103 to 190
sfc-6km Mean Wind Dir.	206	217	212	204 to 219
sfc-6km Mean Speed (kts)	4	10	7	3 to 11
LFC-EL Mean Wind Dir.	240	244	242	239 to 245
LFC-EL Mean Speed (kts)	16	20	18	15 to 21
850-300 Mean Wind Dir.	242	242	242	242

5.2.1.3 Unusual Frontal Events

Seven soundings contributed to the mean composite. Table 5.3 shows the stability parameters of interest. With these events, values for precipitation varied between ~ 68.6 to 79.5 mm (2.70 and 3.13 inches) and had an average of 75.2 mm (2.96 inches). The indices suggest that the atmosphere was moderately unstable with enough wind shear to maintain forcing and moisture transport. With CAPE values in excess of 1700 J kg^{-1} and CINH values near -9 J kg^{-1}, and weak wind shear, this sounding suggests nearly upright convective towers maintained over a concentrated area.

5.2.1.4 Extreme Frontal Events

Fourteen soundings contributed to the mean composite Precipitation values ranged from ~ 103 to 229 mm (4.05-9.00 inches) and had an average of ~ 139 mm (5.46 inches) are shown in Table 5.4. Thunderstorm development was very likely, as the atmosphere was moderately unstable. Wind shear was

Table 5.3 Statistical analysis of stability parameters for unusual frontal events (N=7).

	Min	Max	Mean	1 stdev.
Precipitation (in)	2.7	3.13	2.96	2.80 to 3.12
LPL (mb)	1000	875	964	1005 to 924
LCL (mb)	929	860	890	922 to 858
LFC (mb)	910	795	842	888 to 797
EL (mb)	300	140	208	268 to 148
CAPE (J/kg)	410	3154	1735	621 to 2850
CINH (J/kg)	-45	0	-9	- 25.43 to 7.14
Precipitable water (in)	0.7	1.8	1.43	1.03 to 1.83
Freezing Level (m)	11,372	14,469	13,306	12,166 to 14,447
700-500mb LR (°C/km)	5.7	8	6.5	5.7 to 7.3
850-500mb LR (°C/km)	5.9	7.3	6.4	5.9 to 6.9
NCAPE	0.8	5	2.7	0.96 to 4.60
LI (°C)	-10	-3	-6	- 8 to - 4
TT	46	53	48	46 to 51
KI	30	35	33	31 to 35
ThetaE Diff	11	27	18	11.6 to 24.4
BRN Shear (m2/s2)	4	39	23	10.7 to 35.6
BRN	10	769	181	- 91 to 453
sfc-6km Mean Wind Dir.	183	265	198	162 to 234
sfc-6km Mean Speed (kts)	6	23	15	9 to 20
LFC-EL Mean Wind Dir.	192	264	210	183 to 237
LFC-EL Mean Speed (kts)	15	20	18	16 to 19
850-300 Mean Wind Dir.	189	258	213	188 to 238
850-300 Mean Speed (kts)	13	21	17	15 to 20

Table 5.4 Statistical analysis of stability parameters for extreme frontal events (N=14).

	Min	Max	Mean	1 stdev.
Precipitation (in)	4.05	9	5.47	3.85 to 7.08
LPL (mb)	1000	825	927	983 to 871
LCL (mb)	947	803	876	920 to 832
LFC (mb)	900	240	794	962 to 625
EL (mb)	450	140	232	329 to 135
CAPE (J/kg)	122	2308	1432	562 to 2301
CINH (J/kg)	-8	-1	-3	- 6.6 to 0.8
Precipitable water (in)	0.88	1.87	1.42	1.05 to 1.79
Freezing Level (m)	8,860	14,174	12018	9,996 to 14,039
700-500mb LR (°C/km)	5.7	7.9	6.4	5.8 to 7.0
850-500mb LR (°C/km)	5.9	7	6.4	6.0 to 6.7
NCAPE	0.4	8.8	2.6	1.15 to 3.63
LI (°C)	-8	-1	-5	- 7 to -3
TT	44	53	49	46 to 52
KI	28	36	33	31 to 35
ThetaE Diff	9	23	16.4	11.6 to 21.1
BRN Shear (m2/s2)	2	73	32	14 to 50
BRN	2	864	121	- 102 to 344
sfc-6km Mean Wind Dir.	179	270	206	177 to 234
sfc-6km Mean Speed (kts)	5	39	18	8 to 27
LFC-EL Mean Wind Dir.	201	303	220	190 to 249
LFC-EL Mean Speed (kts)	9	39	22	12to 33
850-300 Mean Wind Dir.	208	270	218	197 to 239
850-300 Mean Speed (kts)	7	39	21	11 to 31

strong in the lower 2 km, values larger than the unusual events, to maintain forcing and transporting moisture into the system. The depth of the convection was smaller than the unusual events, however the CAPE (~300 J kg^{-1} less) was distributed through a smaller layer. Normalized CAPE was larger as well. Values of precipitable water were nearly the same as the unusual events; however the extreme events produced almost 2.5 more inches of precipitation.

5.2.1.5 Unusual Synoptic Events

Fourteen soundings contributed to the mean composite Precipitation values ranged from ~ 68.6 to 110 mm (2.70 - 4.34 inches) and had an average of 76.5 mm (3.01 inches). The indices in Table 5.5 indicate that the atmosphere was moderately unstable. CAPE and normalized CAPE indicate that the convection occurred through a large depth of the atmosphere and the wind shear shows that the convective towers were slow moving and mostly vertical.

Table 5.5 Statistical analysis of stability parameters for unusual synoptic events (N=14).

	Min	Max	Mean	1 stdev.
Precipitation (in)	2.7	4.34	3.01	2.60 to 3.42
LPL (mb)	1000	825	945	1005 to 884
LCL (mb)	968	786	875	923 to 828
LFC (mb)	913	580	820	917 to 724
EL (mb)	530	120	224	349 to 100
CAPE (J/kg)	39	3755	1895	651 to 3139
CINH (J/kg)	-40	0	-6	- 17.6 to 5.1
Precipitable water (in)	1.08	2.17	1.56	1.26 to 1.86
Freezing Level (m)	9,296	15,072	12,684	10,847 to 14,520
700-500mb LR (°C/km)	5.7	7.6	6.3	5.7 to 6.9
850-500mb LR (°C/km)	5.7	7.4	6.4	5.9 to 6.9
NCAPE (J/kg-mb)	0.1	5.4	3.2	1.04 to 5.52
LI (°C)	-11	0	-6	- 9 to – 2
TT	42	56	49	44 to 53
KI	27	42	34	30 to 38
ThetaE Diff	4	31	17.6	9.9 to 25.4
BRN Shear (m2/s2)	1	63	24	3 to 45
BRN	2	1315	200	-144 to 528
sfc-6km Mean Wind Dir.	171	320	221	179 to 262
sfc-6km Mean Speed (kts)	0	31	16	6 to 25
LFC-EL Mean Wind Dir.	181	305	228	195 to 261
LFC-EL Mean Speed (kts)	2	41	18	7 to 28
850-300 Mean Wind Dir.	166	306	228	190 to 266
850-300 Mean Speed (kts)	5	40	19	9 to 29

5.2.1.6 Extreme Synoptic Events

Forty-one soundings contributed to the mean composite and indices in Table 5.6. Precipitation values ranged from ~ 101 to 232 mm (3.98 - 9.14 inches) with an average of 137 mm (5.39 inches). The atmosphere was moderately unstable. Although the depth of convection was nearly identical to the unusual events, the extreme cases had about 100 J kg^{-1} more CAPE, 3 J kg^{-1} less CINH, and less available precipitable water. Convection was likely to rise quickly in mid-levels. Wind shear was noticeably stronger (BRN Shear ~6 m^2 s^{-2} more) than the unusual events suggesting greater moisture transport into the system in low levels. Moreover, the height of the freezing level was higher so that more of the column was conducive for warm rain processes.

5.3 Mean Composites

Creating soundings of the mean parameters was pertinent for operational use. The mean values for the synoptic, frontal, and mesohigh cases at all intensity thresholds were entered into

Table 5.6 Statistical analysis of stability parameters for extreme synoptic events (N=41)

	min	**max**	**mean**	**1 stdev.**
Precipitation (in)	3.98	9.14	5.39	3.91 to 6.81
LPL (mb)	1000	775	945	993 to 898
LCL (mb)	965	769	890	936 to 843
LFC (mb)	950	375	823	928 to 717
EL (mb)	600	110	221	331 to 110
CAPE (J/kg)	57	5848	1924	413 to 3437
CINH (J/kg)	-83	0	-14	- 36.1 to 7.6
Precipitable water (in)	0.92	2.18	1.45	1.13 to 1.75
Freezing Level (m)	8,759	15,348	12,238	10,392 to 14,083
700-500mb LR (°C/km)	5	7.4	6.5	6.0 to 7.0
850-500mb LR (°C/km)	5.1	7.4	6.5	6.0 to 7.0
NCAPE (J/kg-mb)	0.2	16.7	3.2	0.68 to 5.8
LI (°C)	-13	2	-5	- 9 to – 2
TT	40	50	49	46 to 52
KI	20	42	32	27 to 37
ThetaE Diff	2	38	18.7	9.2 to 28.2
BRN Shear (m2/s2)	1	92	30	8 to 53
BRN	1	5522	266	- 605 to 1137
sfc-6km Mean Wind Dir.	167	318	220	185 to 255
sfc-6km Mean Speed (kts)	3	37	19	11 to 26
LFC-EL Mean Wind Dir.	180	284	226	201 to 251
LFC-EL Mean Speed (kts)	2	42	24	15 to 33
850-300 Mean Wind Dir.	179	283	226	201 to 251
850-300 Mean Speed (kts)	3	41	24	15 to 33

RAOB analysis software to generate composite soundings. The levels used were 1000 mb to 700 mb in increments of 25 mb, increments of 50 mb from 700 mb to 300 mb, and 25 mb increments from 300 mb to 200 mb. The most unstable parcel (MUCAPE) was used, as was the virtual temperature for CAPE values. Below are the composite soundings that are grouped by classification type.

5.3.1 Mean Mesohigh 2%

Figure 5.2 (composite of 2 events) shows a very shallow temperature inversion was present near the surface. MUCAPE was moderately narrow and if a parcel was lifted, convection would most likely be elevated. The freezing level was near 4060 m MSL.

The atmosphere was mostly dry except near 900 mb. Precipitable water available in that column of air was ~ 36.3 mm (1.43 inches). Weak veering and backing are both present from the surface to 700 mb. Speed shear was minimal from the surface to about 600 mb. Strong speed shear was present aloft

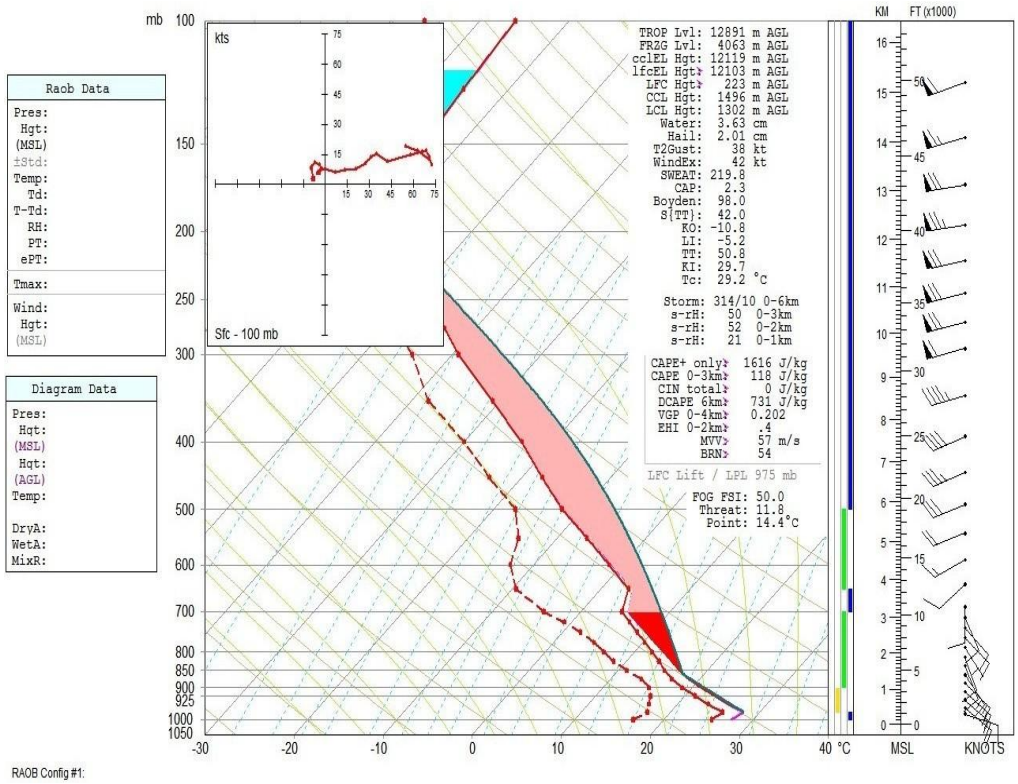

Figure 5.2 Skew-T log p diagram of the mean composite of the 2% Mesohigh events. Winds at right are in knots.

where a deep layer has winds greater than 70 knots. The presence of the upper-level jet was apparent in this sounding.

The values for TT, KI, LI, SWEAT, and CAPE indicate that the atmosphere was moderately unstable and development of thunderstorms was possible. The thunderstorms have better potential to yield heavy rain, but could become severe.

5.3.2 Mean Mesohigh 0.5%

In Fig. 5.3 (composite of 14 events) a temperature inversion can be seen near the surface. CAPE was moderately broad and CIN covers a depth of about 125 mb. Convection would most likely be elevated. The freezing level was near 4100 m MSL, providing adequate depth for warm cloud processes.

The atmosphere has ~ 41.7 mm (1.64 inches) of precipitable water. Strong directional shear was present in lower levels, but speed shear was minimal from the surface to about 700 mb. Mid-to-upper levels exhibit more pronounced speed shear; however, the increase was gradual. The strongest winds are 50 knots near 200 mb.

The values for TT, KI, LI, SWEAT, and CAPE indicate that the atmosphere was moderately unstable and development of thunderstorms, possibly severe, was likely.

Major differences from the 2% cases (Fig. 5.1) are the higher precipitable water with 0.5% cases, but that does not always happen. Additionally, the hodograph for extreme cases (Fig. 5.2) exhibits the shape of a letter 'M' indicating a mid-

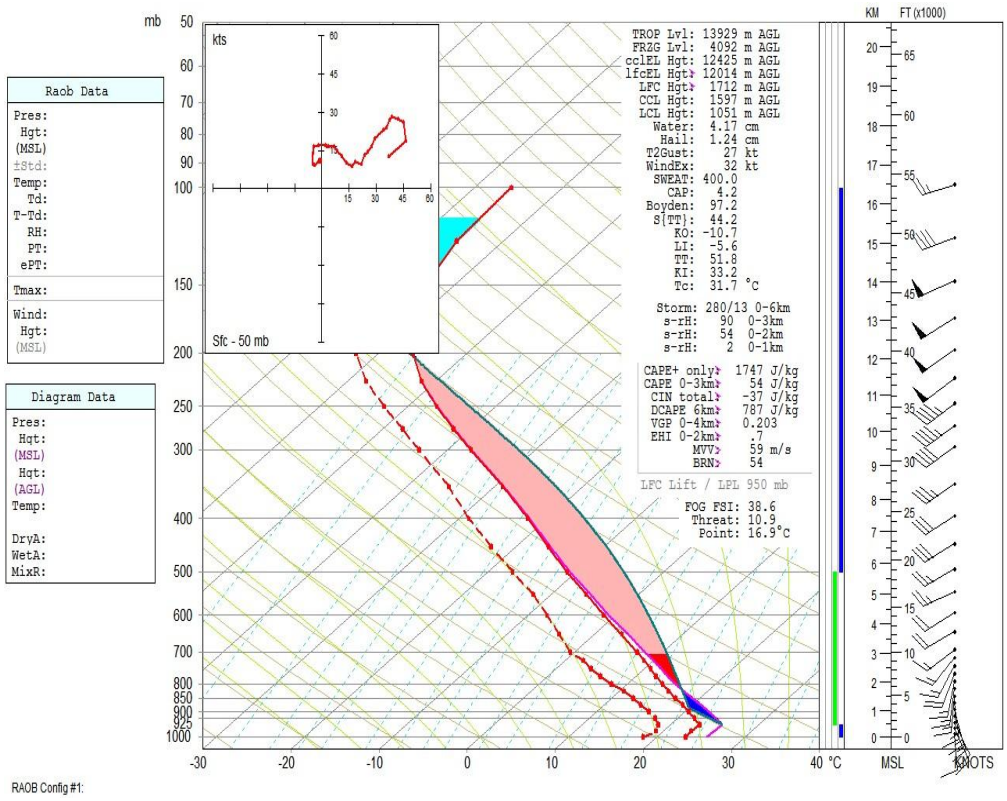

Figure 5.3 Skew-T log p diagram of the mean composite of the 0.5% Mesohigh events. Winds at right are in knots.

troposphere with little directional or speed shear, with veering wind direction below and a steady increase in speeds above, before dropping off above jet level. This stands in contrast to the 2% cases (Fig. 5.2) where there was a general increase in speeds above ~ 700 mb and a much stronger (75 knot) jet at 200 mb.

5.3.3 Mean Frontal 2%

One of the first noticeable features in Fig. 5.4 (composite of 7 events) was the shallow temperature inversion from the surface to 950 mb. The winds veer with height indicating warm air advection. Directional shear was stronger than speed shear at low levels. Speed shear was rather weak for the entire profile. The greatest wind speed was around 40 knots.

The atmosphere was rather moist with 44.1 mm (1.74 inches) of precipitable water. The freezing height occurs near 4300 m MSL. (LFC to the freezing level or 3-km or greater was an empirical threshold for collision/coalescence, Doswell et al. 1996). The values for TT, KI, LI, SWEAT, and CAPE indicate that the atmosphere was moderately unstable and conditions are favorable for thunderstorms to occur.

This is clearly a heavy rainfall sounding, with significant CAPE, a high precipitable water, and a high freezing level. Each of these factors promotes the collision and coalescence processes necessary for rain production in a warm cloud. Additionally, the deep veering signature allows warm, moist, southerly flow near the surface, and only weaker flow (~ 40

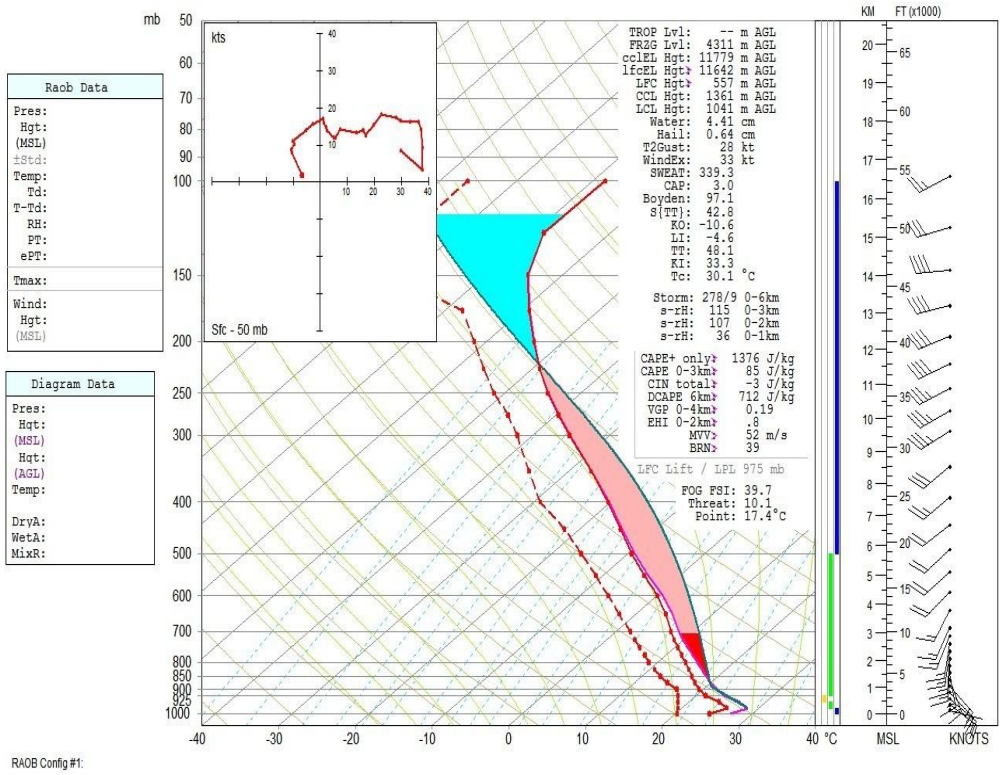

Figure 5.4 Skew-T log p diagram Representative of all the 2% Frontal events. Winds at right are in knots.

knots) as the maximum wind speed. Indeed storm motion is estimated to be only 9 knots.

5.3.4 Mean Frontal 0.5%

A shallow temperature inversion can be seen in Fig. 5.5 (composite of 14 events) from the surface to 925 mb. CIN was

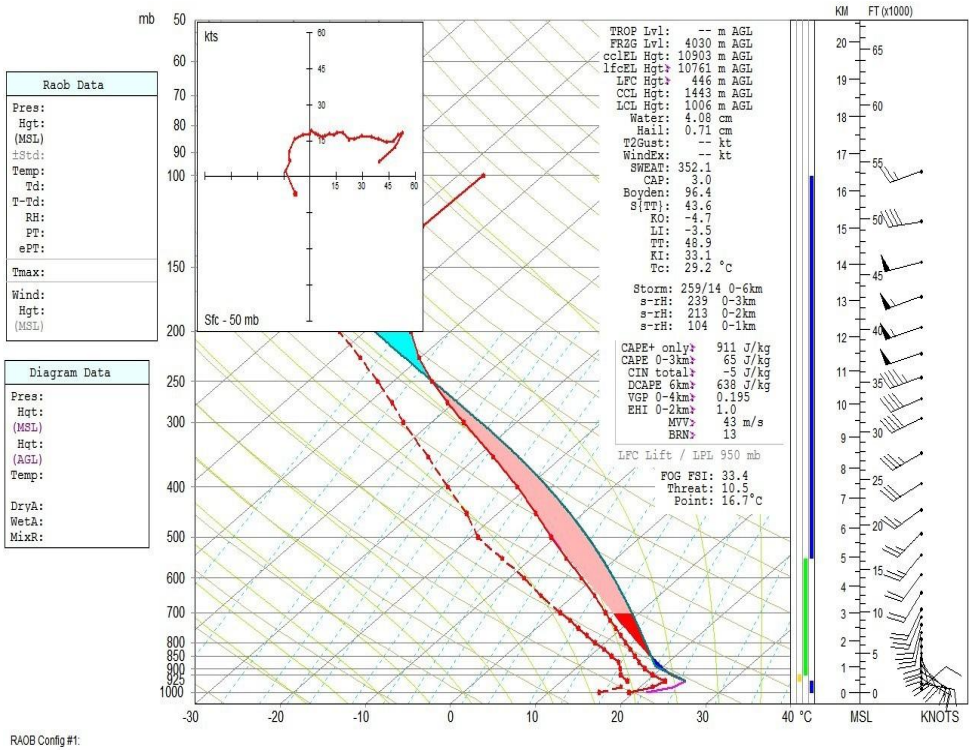

Figure 5.5 *Skew-T log p diagram of the mean composite of the 0.5% Frontal events. Winds at right are median direction with windspeed plotted in knots (short barb = 5kts, long barb = 10kts, and flag = 50 kts).*

present indicating that convection would likely to be elevated. CAPE values are lower resulting in a narrower CAPE. The freezing level was near 4030 m MSL.

There was about 40.9 mm (1.61 inches) of precipitable water; however, the column was relatively dry above 850 mb. Strong directional shear was present at low levels but the speed shear was weak. Aloft directional shear was very weak but with

significant speed shear. A deeper layer near 200 mb was experiencing winds near 55 knots. These are the strongest winds seen for the three composite soundings. The presence of a nearby upper-level jet appears likely.

However, it is interesting that many of the standard metrics for heavy rainfall with these 0.5% ('extreme') cases were *lower* than with the 2% cases (Fig. 5.4). Indeed, CAPE values are lower as is the precipitable water. Additionally, the warm cloud depth is ~300 m more shallow, and the wind profile suggests greater shear and faster moving cells. This is a reality of the composites for which no explanation can be offered. The values of TT, KI, LI, SWEAT, and CAPE indicate that the atmosphere was marginally-to-moderately unstable. Thunderstorms have the potential of becoming severe.

5.3.5 Mean Synoptic 2%

One noticeable feature in Fig. 5.6 (composite of 14 events) was the larger value of CAPE and that it was broad. The winds veer with height indicating that warm air advection was

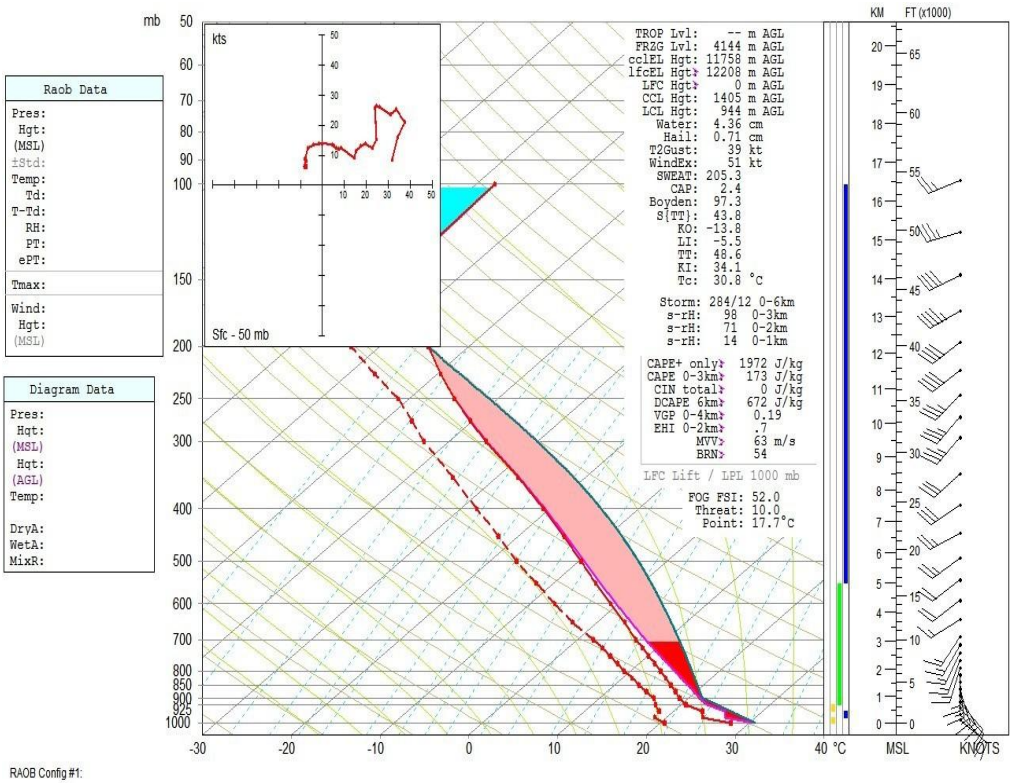

Figure 5.6 Skew-T log p diagram of the mean composite of the 2% Synoptic events. Winds at right are in knots.

occurring. Both directional shear and speed shear was weak near the surface. The maximum wind speed aloft was 45 knots.

The atmosphere was rather moist with ~43.7 mm (1.72 inches) of precipitable water. The freezing height occurs near 4150 m MSL. A higher freezing layer would decrease chances of hail development. The values for TT, KI, LI, SWEAT, and CAPE indicate that the atmosphere was moderately unstable and

development of thunderstorms was possible. The thunderstorms have better potential to yield heavy rain, but are not likely to become severe.

Yet, many of the same signatures appear as before. Of particular interest here is the pronounced letter 'M' signature in the hodograph. This backing with height suggests cold advection in the upper troposphere. Even so, there is no clear jet signature in this sounding.

5.3.6 Mean Synoptic 0.5%

A very shallow temperature inversion was present near the surface in Fig 5.7 (composite of 41 events). CAPE was very narrow and CIN covers a depth of about 175 mb. Convection would most likely be elevated. The freezing level was near 4020 m MSL.

The atmosphere was rather moist with ~40.1 mm (1.58 inches) of precipitable water. Strong directional shear was present in lower levels. Speed shear was minimal from the surface to about 600 mb. Mid-to-upper levels have stronger

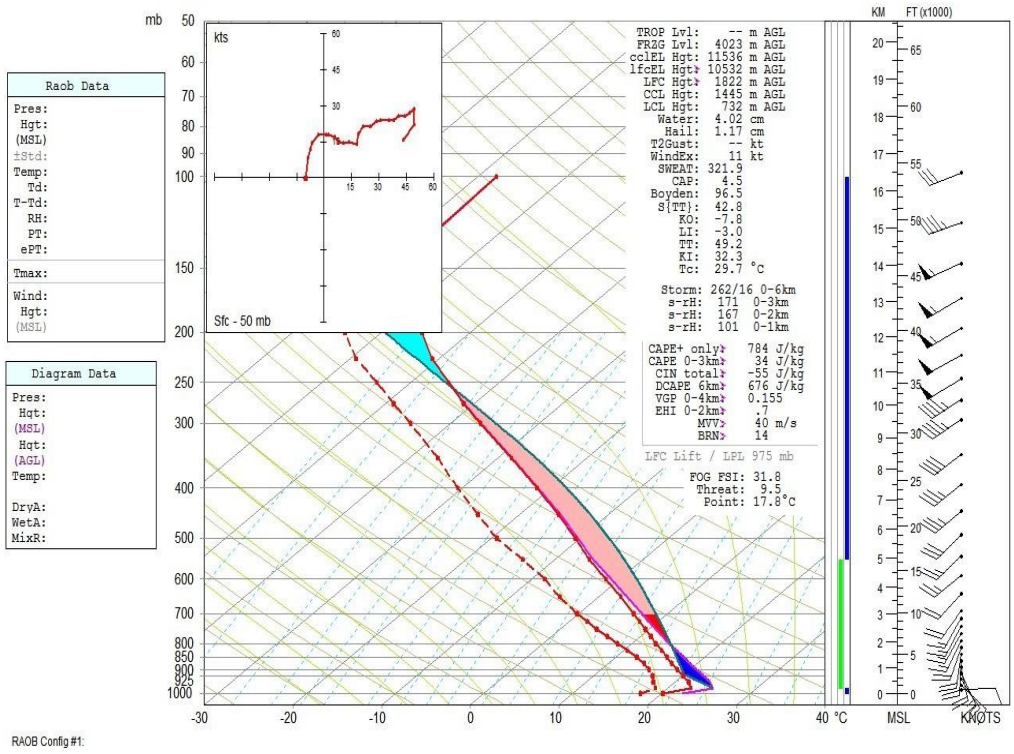

Figure 5.7 Skew-T log p diagram of the mean composite of the 0.5% Synoptic events. Winds at right are in knots.

speed shear. A deep layer has winds greater than 50 knots. An upper-level jet may be nearby.

The values for TT, KI, LI, SWEAT, and CAPE indicate that the atmosphere was marginally unstable and development of thunderstorms was possible. The thunderstorms have better potential to yield heavy rain, they may become severe.

As with the discussion of mean frontal 0.5% events, most metrics are lower for 0.5% synoptic events than for the 2% collection. Of chief interest here is the lower equilibrium level, by almost 2 km, in these cases as opposed to the 2% synoptic cases (Fig. 5.6), such that the convection should not be as deep. However, the heights of the freezing levels are comparable (within 200 m of one another), so the depths over which warm rain processes occur are nearly the same.

5.4 Seasonal Mean Composites

The mean soundings discussed in section 5.3 were only split by the thresholds. The events now have been divided by seasons. The months chosen in each season vary a little from the standard June, July, and August representing summer. To incorporate results from the histogram for mesohigh events and the Maddox et al. (1979) finding for the occurrence of mesohigh events, April-June will represent the season of Spring. July, August, and September will represent Summer. October,

November, and December will represent Fall which leaves January, February, and March representing the Winter season.

The 0.5% and 2% thresholds were used for this section. More events were classified by these two thresholds. Once again the most unstable parcel was used in all of the soundings.

5.4.1 Winter Mean Frontal 2%

A composite was not available for this threshold since a frontal event did not occur during the months of January, February, or March for this threshold.

5.4.2 Spring Mean Frontal 2%

Four events were compiled in the sounding representing a mean frontal Spring event was shown in Fig. 5.8. This composite sounding reveals a near-surface inversion, as would be expected from a frontal-type event. The bulk of the atmosphere is fairly moist below 500 mb, with dew point depressions generally < 7°C. One may quantify the moisture in the layer from the composite, which generates a precipitable

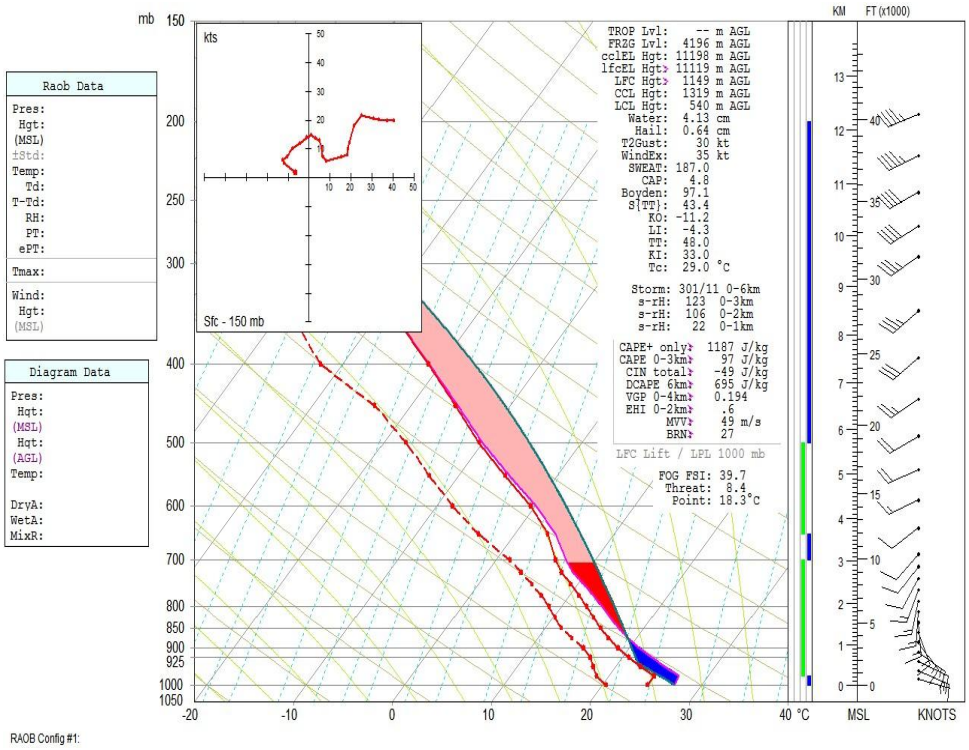

Figure 5.8 *Skew-T log p diagram of the mean composite of the Spring 2% Frontal events. Winds at right are median direction with windspeed plotted in knots (short barb = 5kts, long barb = 10kts, and flag = 50 kts).*

water value of 41.3 mm. Moderately weak CAPE was associated with these events, having a composite value of 1187 J kg^{-1}, while the CIN from the composite was -49.0 J kg^{-1}. So, the familiar pattern associated with heavy rainfall events emerges here.

The wind profile is of particular interest. The hodograph in Fig. 5.8 assumes the shape of a letter 'M' that allows for a deep

layer of veering, suggesting warm advection, up through 500 mb. Weak backing above that level suggests cold advection further aloft but the signature is weak. However, the surface-to-2km shear averaged 14.0 kts and ranged from 6.00 to 21.0 kts while the deeper surface-to-6km shear average was 28.3 kts. Additionally, the BRN Shear average was 23 $m^2 s^{-2}$ and ranged from 2.00 to 50.0 $m^2 s^{-2}$. Each of these figures suggests a weak wind profile as well as a weak shear profile. As before, the wind profile allows for slow-moving, upright convective towers that are thought to have greater precipitation efficiency.

5.4.3 Summer Mean Frontal 2%

This was the only sounding; however it was included for completeness. Figure 5.9 shows the most unstable parcel lifted from 975 mb. Moderately strong CAPE near 2200 J $kg^{-}1$ was associated with this event. Precipitable water was ~ 46.0 mm (~1.80 inches).

Directional shear of the winds was minimal at low levels. A moist layer was present near 900 mb and a pocket a drier just

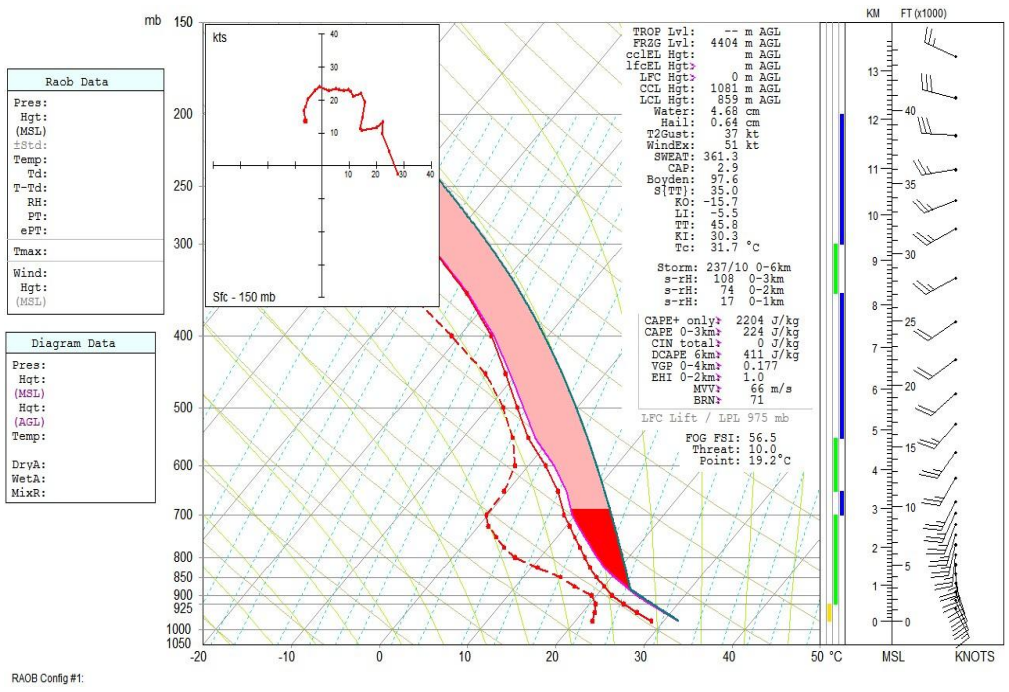

Figure 5.9 Skew-T log p diagram of the Summer 2% Frontal events is represented by one sounding. Winds at right are median direction with windspeed plotted in knots (short barb = 5kts, long barb = 10kts, and flag = 50 kts).

above spanning from 900 mb to 600 mb. A strong upper-level jet was not associated with this sounding.

5.4.4 Fall Mean Frontal 2%

Weak-to-moderately strong CAPE (Fig. 5.10) was associated with this sounding (composite consisted of 2 events) averaging

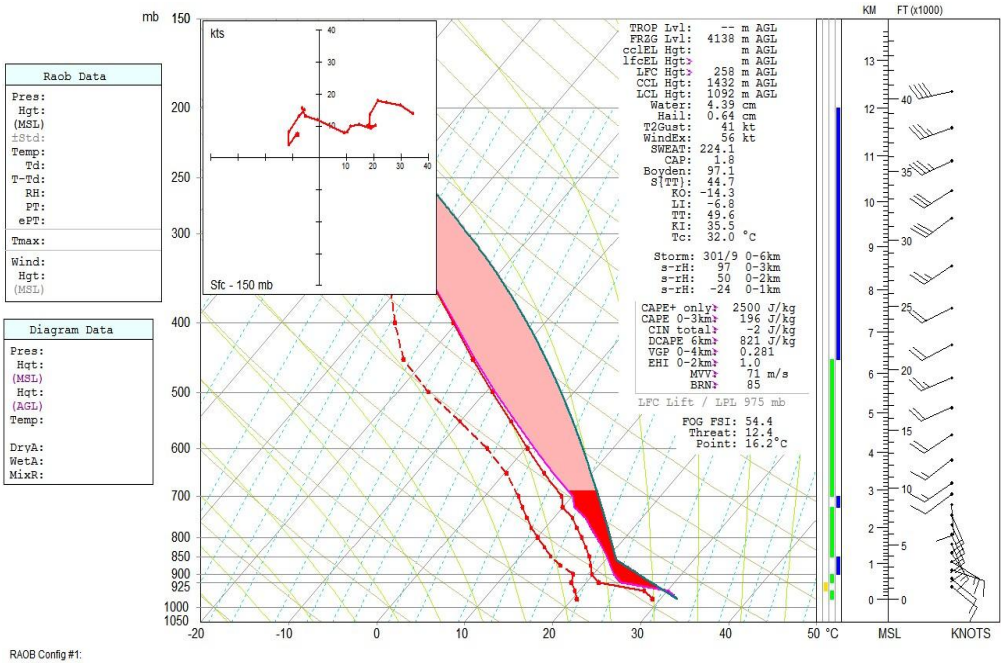

Figure 5.10 Skew-T log p diagram of the mean composite of the Fall 2% Frontal events. Winds at right are in knots.

around 1780 J kg^{-1}. Very abrupt changes in the wind direction occur near 700 mb, which is likely a vagary of the small sample size. Speed shear is weak aloft and the letter 'M' shaped hodograph confirms that both backing and veering of the winds were present in the vertical profile. The surface was relatively dry and the rest of the column from 925 mb was relatively moist. This is indeed a heavy rainfall sounding where the convective tower should have slow movement and remain mostly vertical. Precipitable water is ~ 43.9 mm (1.69 inches) and with

the moderately strong CAPE that is present, localized rainfall is very likely.

5.4.5 Winter Mean Frontal 0.5%

A temperature inversion is shown near the surface in Fig. 5.11. The majority of the column is very moist, minus a layer of dry air between 700 mb and 500 mb. Veering of lower level winds suggests strong warm air advection and associated aloft is a strong jet of 100 knots. Precipitable water values of 30.2 mm (1.19 inches) were lower than the previous soundings but were sufficient to produce greater rainfall amounts.

This sounding represents the only event that occurred for this threshold and was included for completeness. The inversion was larger than what you might see if more events were factored into the mean values. Convection would likely be elevated and maintained by low level wind shear.

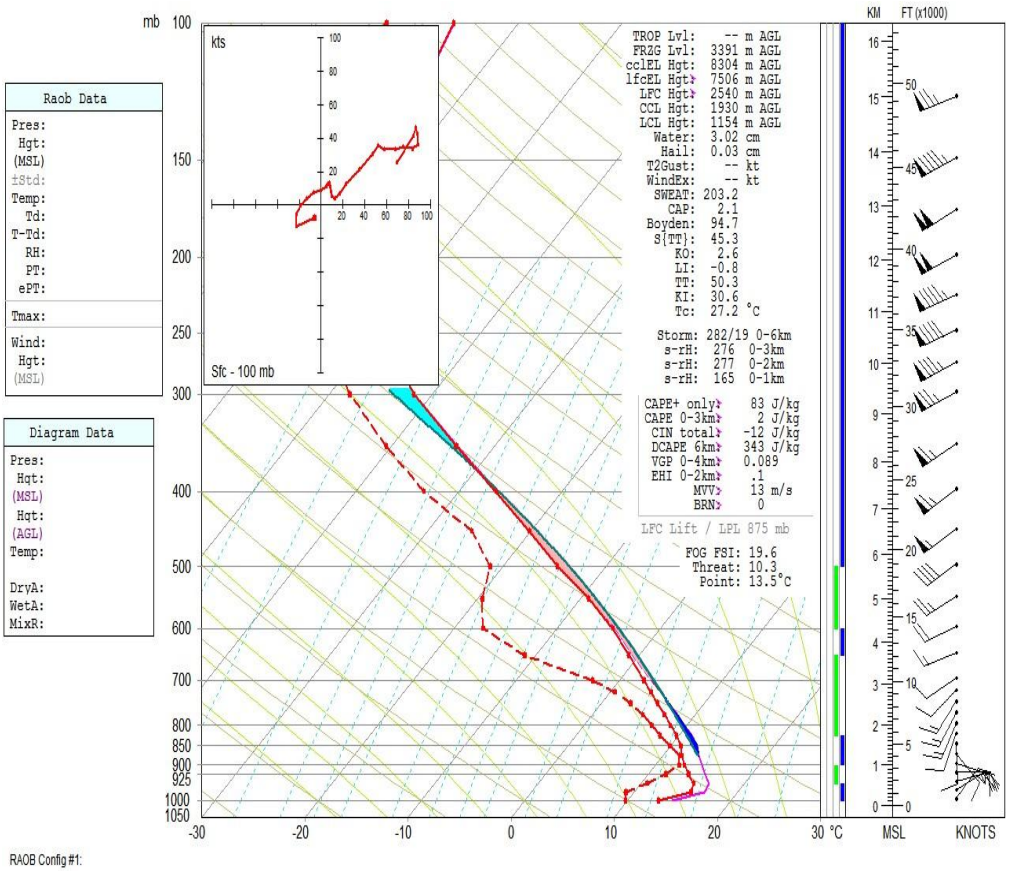

Figure 5.11 Skew-T log p diagram of the mean composite of the Winter 0.5% Frontal events. Winds at right are in knots.

5.4.6 Spring Mean Frontal 0.5%

Seven events were compiled into the composite sounding in Fig. 5.12. A solid profile of veering is seen in the winds on the sounding and the hodograph suggesting warm air advection. CAPE values associated with this sounding were very weak and

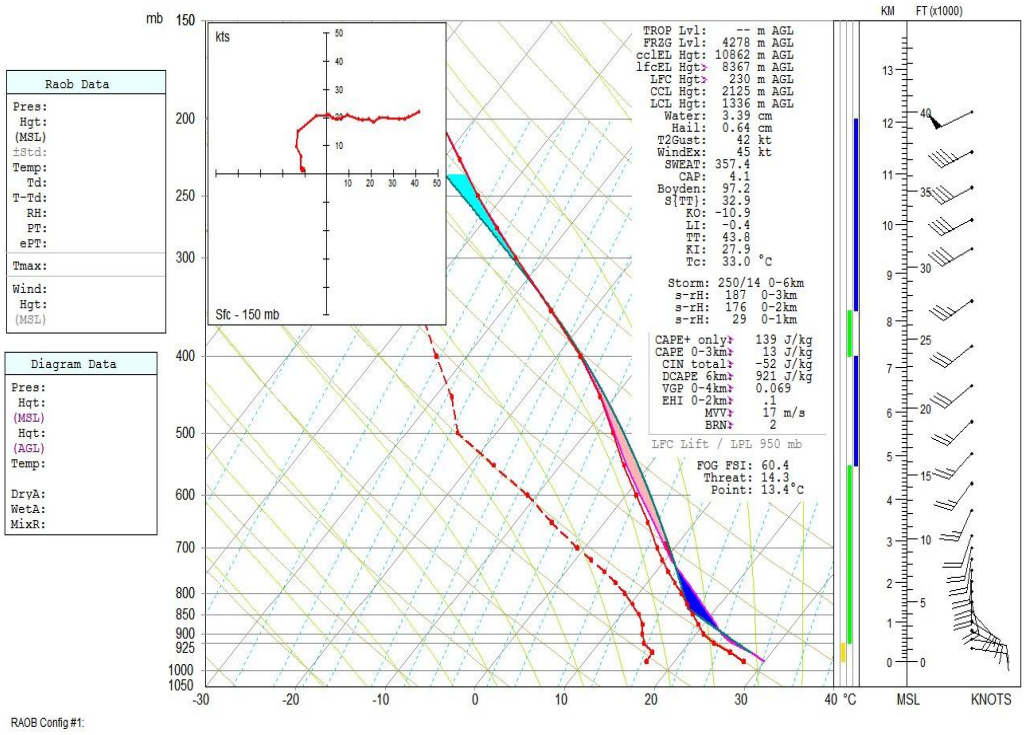

Figure 5.12 Skew-T log p diagram of the mean composite of the Spring 0.5% Frontal events. Winds at right are in knots.

the column appears to less moist than desired. The column appears to be dry for this sounding; however, slightly higher precipitable water values of 33.9 mm (1.33 inches) were present. The sounding lacked the presence of a strong upper-level jet. Speed shear was minimal so movement of the system was slow and resulted in localized rainfall.

5.4.7 Summer Mean Frontal 0.5%

Three events were used to make the composite sounding in Fig. 5.13. Two features are dominant in this sounding. The first being the moisture profile with precipitable water values of 44.9 mm (1.77 inches). The other being the presence of strong CAPE values of 3000 J kg^{-1} throughout the column.

Veering of the winds suggests warm air advection but it is not as strong as previous seasons. The hodograph takes on the shape of a question mark indicating that backing of the winds occur aloft. Speed shear is very minimal and the convective tower would remain mostly upright allowing the system to precipitate over a very localized area.

5.4.8 Fall Mean Frontal 0.5%

Figure 5.14 was the mean composite represented by 3 events. In general, the winds at low levels were nearly uniform from the southeast. The hodograph is mostly shaped like the letter 'M'. Directional shear occurred around 700 mb. Both warm air and cold air advection (although weak) appears to be

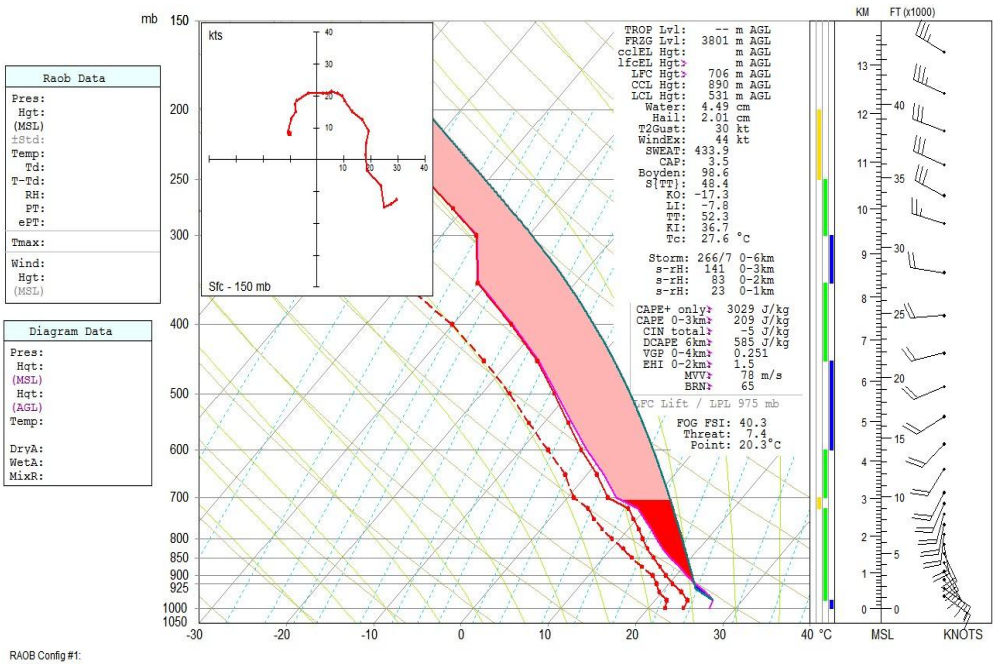

Figure 5.13 Skew-T log p diagram of the mean composite of the Summer 0.5% Frontal events. Winds at right are in knots.

present. An upper-level jet of 60 knots was associated with this sounding near 200 mb. A small temperature inversion creates a layer of CIN from the surface to about 900 mb, but CAPE was moderately strong (2000 J kg^{-1}) above 900 mb. Precipitable water values for this sounding were 46.1 mm (1.81 inches) and were higher than previous seasons. Heavy rainfall certainly seems likely to occur with this sounding.

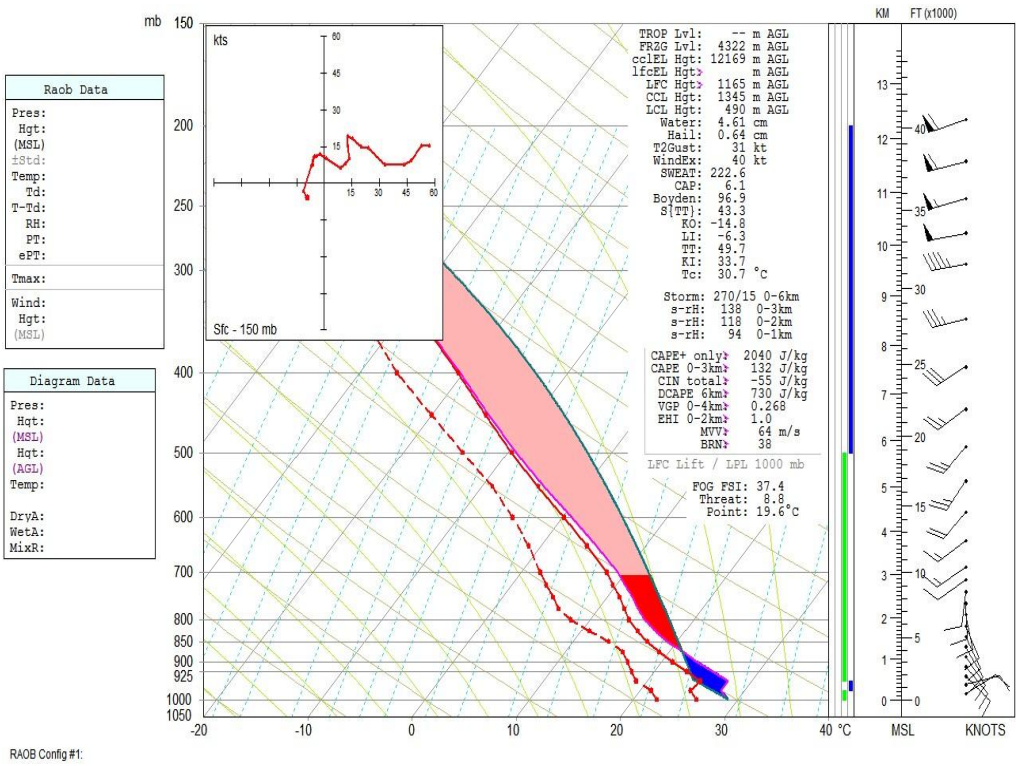

Figure 5.14 Skew-T log p diagram of the mean composite of the Fall 0.5% Frontal events. Winds at right are in knots.

5.4.9 Winter Mean Synoptic 2%

Two events are used in the mean composite shown in Fig. 5.15. The entire column of air was moist but lacks the association of CAPE. Precipitable water is 30.5 mm (1.20 inches). The winds veer and back in this sounding. The 'sigma' shaped hodograph confirms the wind profile having both warm

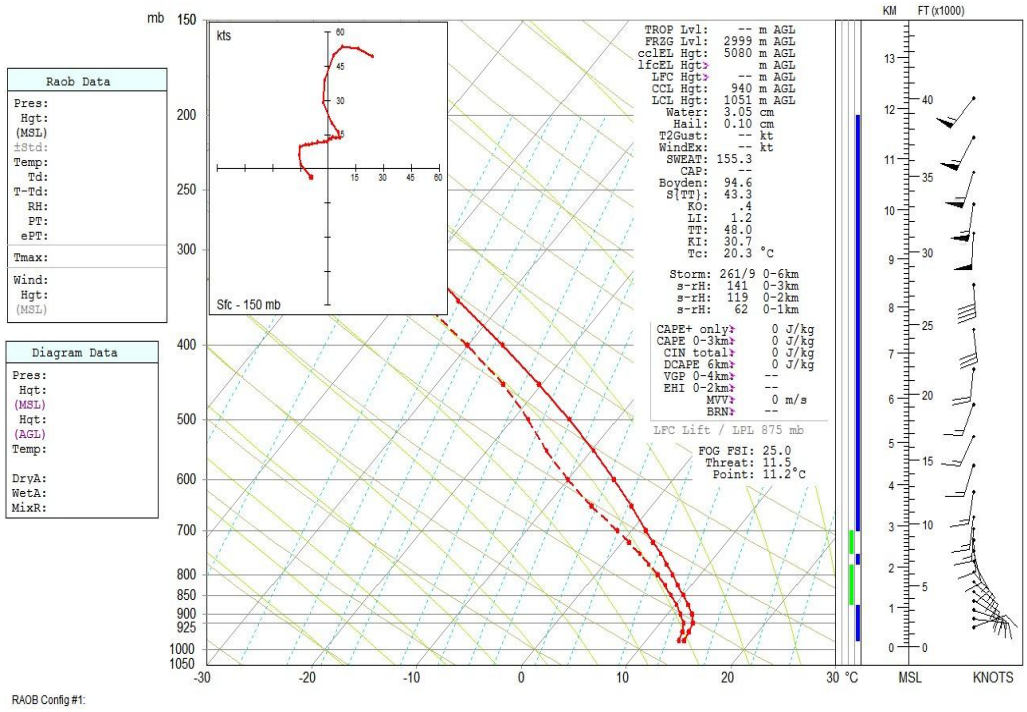

Figure 5.15 Skew-T log p diagram of the mean composite of the Winter 2% Synoptic events. Winds at right are in knots.

air advection and cold air advection present. Speed shear is very minimal from the surface to 500 mb. Thunderstorms are likely to occur and produce localized heavy rainfall.

5.4.10 Spring Mean Synoptic 2%

Five events were used in the composite sounding shown in Fig. 5.16. Moderately strong CAPE (~2600 J kg^{-1}) was

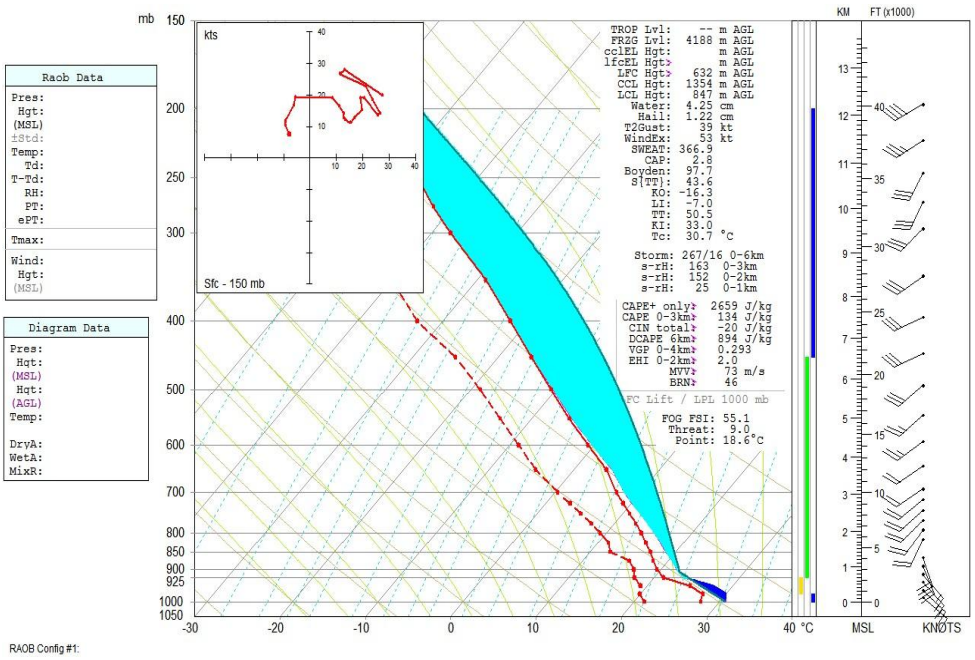

Figure 5.16 *Skew-T log p diagram of the mean composite of the Spring 2% Synoptic events. Winds at right are in knots.*

associated with these events. A temperature inversion was present at low levels and the air was dry from the surface to nearly 925 mb. Precipitable water was a little higher than the winter season at 42.5 mm (1.67 inches). CIN was present from the surface to nearly 925 mb. The freezing level was nearly 1000 m higher than the winter season.

Winds were southeasterly at low levels and had directional shear near 850 mb. The winds aloft were backing. This can also

be seen on the hodograph. An upper-level jet was not associated with this sounding. As has been the theme throughout, thunderstorms are likely to occur and produce localized heavy rainfall with such a sounding.

5.4.11 Summer Mean Synoptic 2%

Four events represent the mean composite shown in Fig. 5.17. Backing was present in lower levels indicating that cold air advection was occurring. Winds veer above 925 mb. Above this level wind speed and direction experience very minimal shear. The entire column of air was rather moist. Elevated convection was likely to occur and developing thunderstorms are likely produce localized heavy rainfall.

5.4.12 Fall Mean Synoptic 2%

Three events were used in the mean composite sounding shown in Fig. 5.18. Winds were nearly uniform at lower levels,

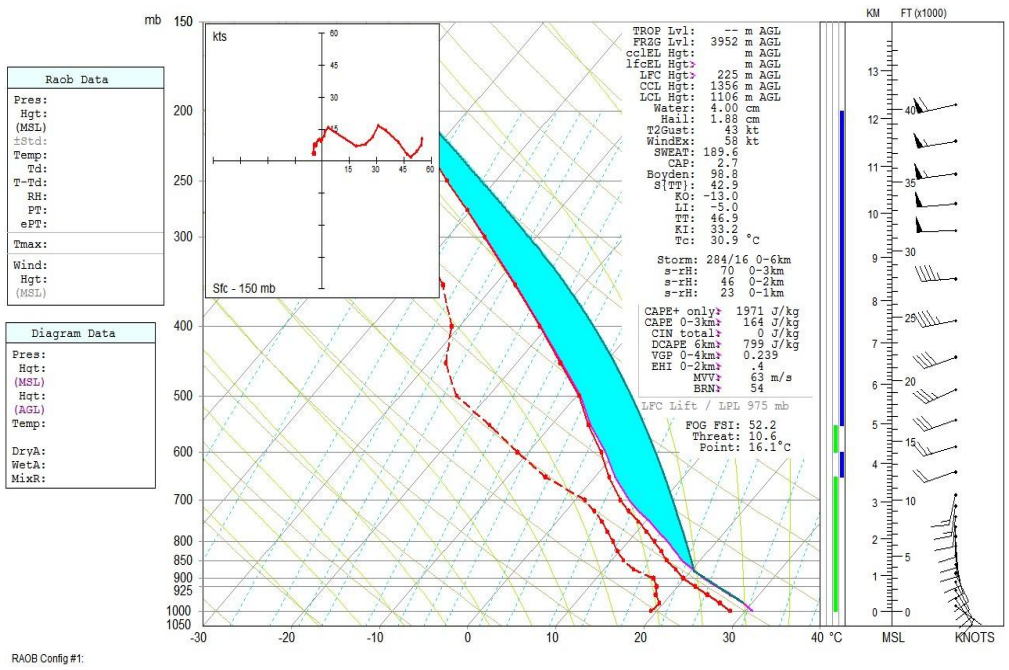

Figure 5.17 Skew-T log p diagram of the mean composite of the Summer 2% Synoptic events. Winds at right are in knots.

both speed and directional shear were nearly non-existent below 700 mb. An upper-level jet of 50 knots was present. The letter 'M' shaped hodograph shows that both, although weak, backing and veering of the winds. Precipitable water was 40.0 mm (1.57 inches), which is less than the summer season. Shear in the mid-levels and ample moisture in the atmosphere may help maintain the system and produce localized heavy rainfall.

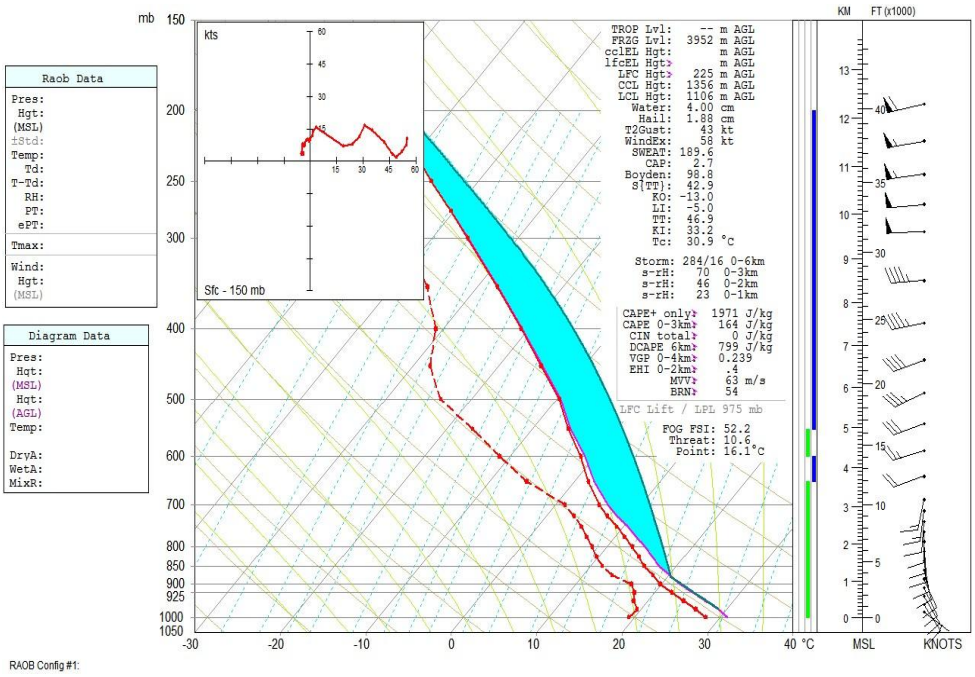

Figure 5.18 *Skew-T log p diagram of the mean composite of the Fall 2% Synoptic events. Winds at right are in knots.*

5.4.13 Winter Mean Synoptic 0.5%

Seven events were compiled to make the composite sounding shown in Fig. 5.19. Initially the winds are backing but quickly become veering at lower levels. Minor speed shear is present near the surface. There was an upper-level jet of 60 knots near 200 mb.

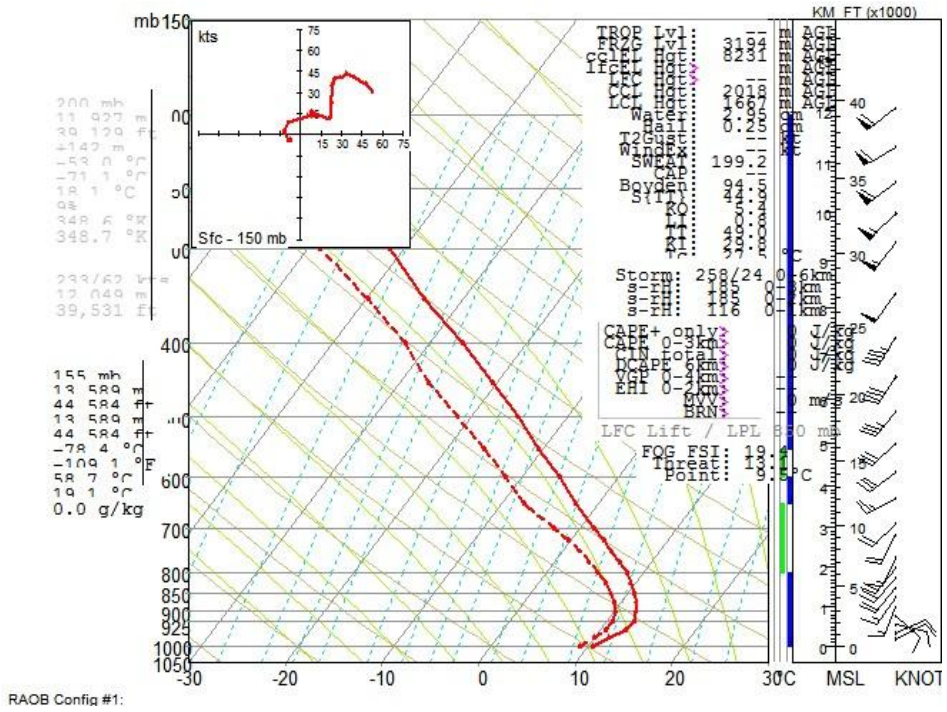

Figure 5.19 Skew-T log p diagram of the mean composite of the Winter 0.5% Synoptic events. Winds at right are in knots.

The hodograph is shaped liked a 'sigma' and shows that both backing and veering was present, although warm air advection was primarily occurring. A temperature is inversion lies near the surface and the sounding lacks CAPE. A weak upper-level jet was also present in this sounding. Even though the precipitable water less than the other seasons with a value 29.5 mm (1.16 inches), significant rainfall amounts occurred.

Shear at low levels was driving this system to produce localized heavy rain.

5.4.14 Spring Mean Synoptic 0.5%

Eleven events were compiled to make the composite sounding in Fig. 5.20. The entire column of air was fairly moist. Warm air advection was occurring in lower levels as shown in the hodograph. An upper-level jet of 50 knots occurred at 200 mb. Precipitable water was 38.1 mm (1.5 inches). Moderately strong CAPE (~1900 J kg^{-1}) and ~ 150 mb layer of CIN was present.

Thunderstorms that develop are likely to be maintained. The moderate CIN value of 46 J kg^{-1} corroborates this idea. In addition, the southerly flow suggests an influx of warm and moist air. In the typical synoptic setting of Maddox et al. (1979), these elements would almost certainly point to prolonged heavy rainfall.

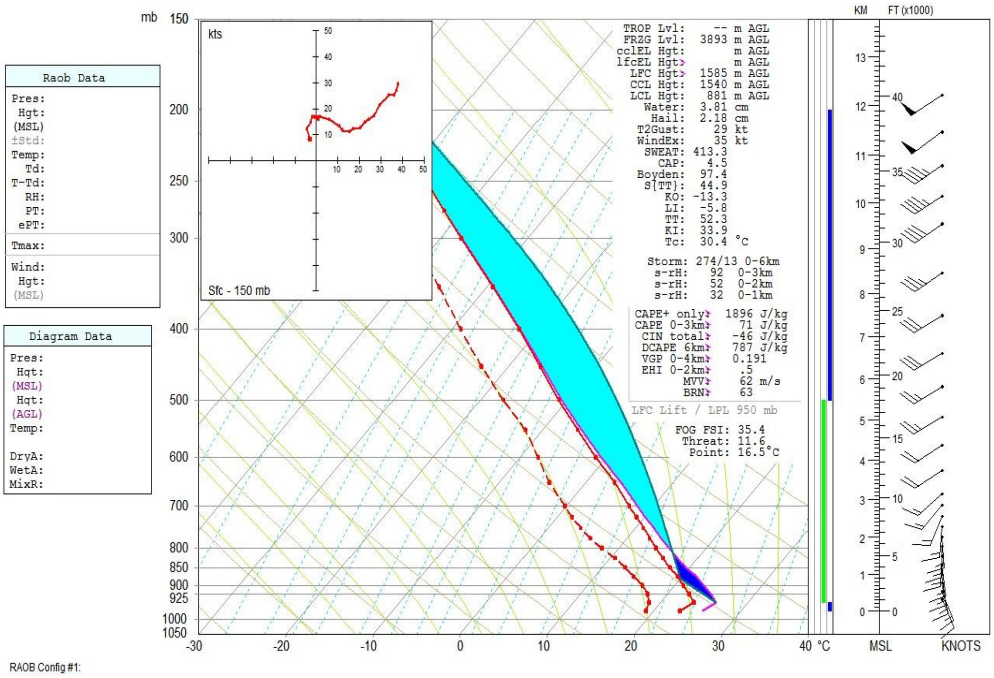

Figure 5.20 Skew-T log p diagram of the mean composite of the Spring 0.5% Synoptic events. Winds at right are in knots.

5.4.15 Summer Mean Synoptic 0.5%

Six events were compiled for this season (shown in Fig. 5.21). A temperature inversion was present near the surface which creates CIN. The CIN spans from the surface to around 925-mb. Moderately strong CAPE (~2500 J kg^{-1}) was associated with this sounding. The atmosphere was very moist throughout with precipitable water at 52.1 mm (2.05 inches). Weak, but present, veering can be seen at low levels indicating that warm

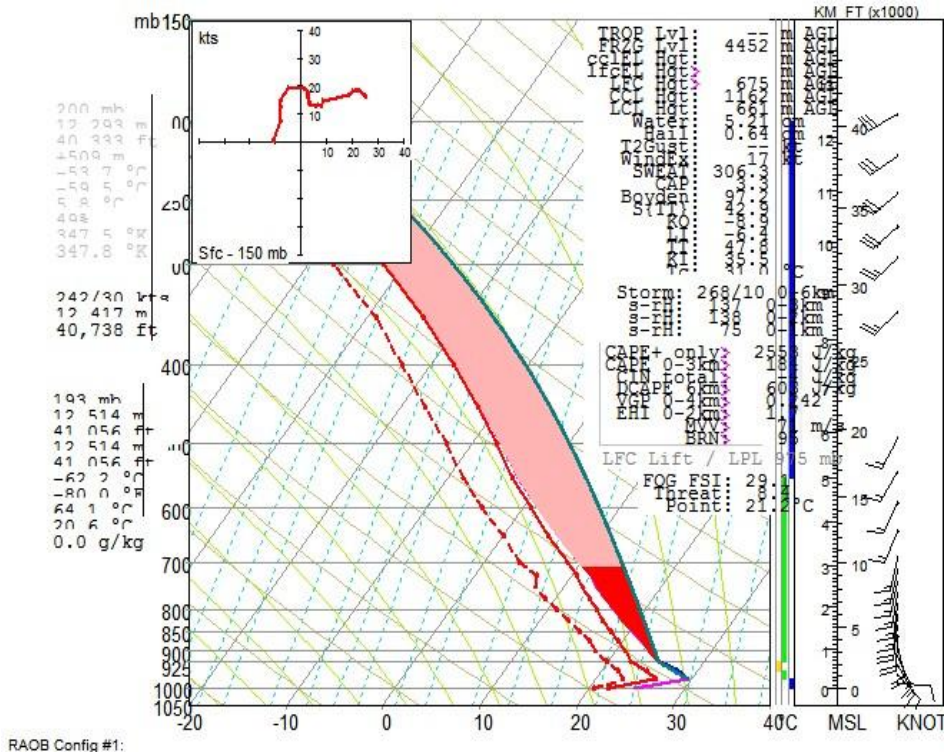

Figure 5.21 Skew-T log p diagram of the mean composite of the Summer 0.5% Synoptic events. Winds at right are in knots.

air advection was occurring. Thunderstorm development was eminent and most likely severe. The system should maintain itself due to forcing mechanisms and the vast amount of water available in the atmosphere. Heavy rainfall is likely with such a sounding.

5.4.16 Fall Mean Synoptic 0.5%

Seventeen events were used in this composite. Moderately strong CAPE values of ~ 1600 J kg^{-1} (shown in Fig. 5.22) were associated with this sounding. An upper-level jet of 60 knots occurred at 200 mb. A small temperature inversion was present near the surface which created a little CIN from 975 mb to around 900 mb.

The atmosphere was fairly moist below 800 mb and then becomes drier. Precipitable water was 42.8 mm (~1.69 inches). Weak, but present, veering can be seen at low levels indicating that warm air advection was occurring. The letter 'M' shaped hodograph confirms that veering and a little backing was present. Generally faster estimates of mean cell motion (~19 knots) suggest that prolonged forcing will be necessary to promote localized heavy rainfall. This behavior is no uncommon in the Fall season, when the jet stream takes on a more equatorward position and greater winds are found in the troposphere at this latitude.

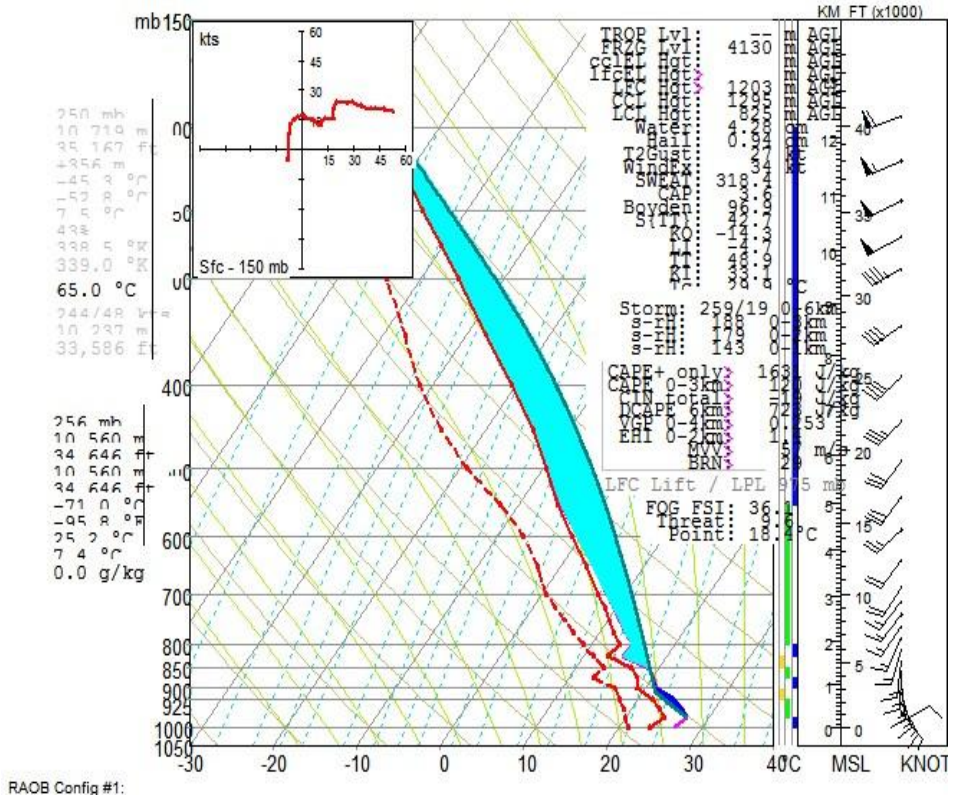

Figure 5.22 Skew-T log p diagram of the mean composite of the Fall 0.5% Synoptic events. Winds at right are in knots.

5.4.17 Winter Mean Mesohigh 2%

A composite was not available for this threshold since mesohigh events did not occur during the months of January, February, and March.

5.4.18 Spring Mean Mesohigh 2%

Two events were used in the composite sounding for this season shown in Fig. 5.23. From the surface to 900 mb the atmosphere was fairly dry. A small temperature inversion was present around 975 mb which created a small layer of CIN.

Winds at lower levels vacillated between veering and backing from the surface to 850 mb. The direction shifts above 700 mb from southeast to west-southwest. This is also reflected in the hodograph.

A strong upper-level jet of 75 knots was present at 200 mb. Precipitable water was 36.2 mm (1.43 inches), which was the lower of the seasons still produced significant rainfall amounts. This sounding indicates that shear was playing a large role in the development of thunderstorms.

5.4.19 Summer Mean Mesohigh 2%

A composite was not available for this threshold since mesohigh events did not occur during the months of July, August, and September.

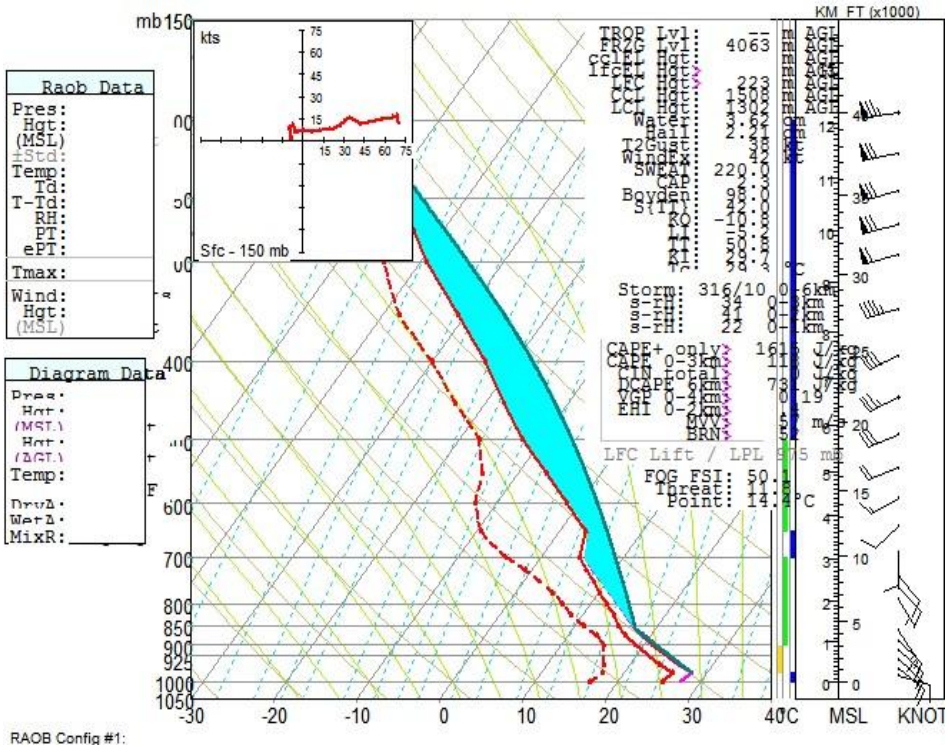

Figure 5.23 Skew-T log p diagram of the mean composite of the Spring 2% Mesohigh events. Winds at right are in knots.

5.4.20 Fall Mean Mesohigh 2%

A composite was not available for this threshold since mesohigh events did not occur during the months of October, November, and December.

5.4.21 Winter Mean Mesohigh 0.5%

Figure 5.24 (represented by 1 event) was included for completeness. The surface was moist and became drier aloft. CAPE was moderately strong with a value of ~1600 J kg^{-1}. A layer of CIN spans from 925 mb to 825 mb making convection more of an elevated nature. Speed and directional wind shear was minimal at lower levels, although it weakened in mid-levels. Stronger, low level winds were driving and maintaining thunderstorm development.

5.4.22 Spring Mean Mesohigh 0.5%

Twelve events were used to make this seasonal composite. Moderately strong CAPE of ~ 1900 J kg^{-1} (shown in Fig. 5.25) was associated with this sounding. An upper-level jet of 50 knots was present at 200 mb. A small temperature inversion was present around 950 mb which created a small layer of CIN from 935 mb to 825 mb.

Winds at lower levels were veering very slightly from the surface to 750 mb and can be seen in the hodograph. Warm air

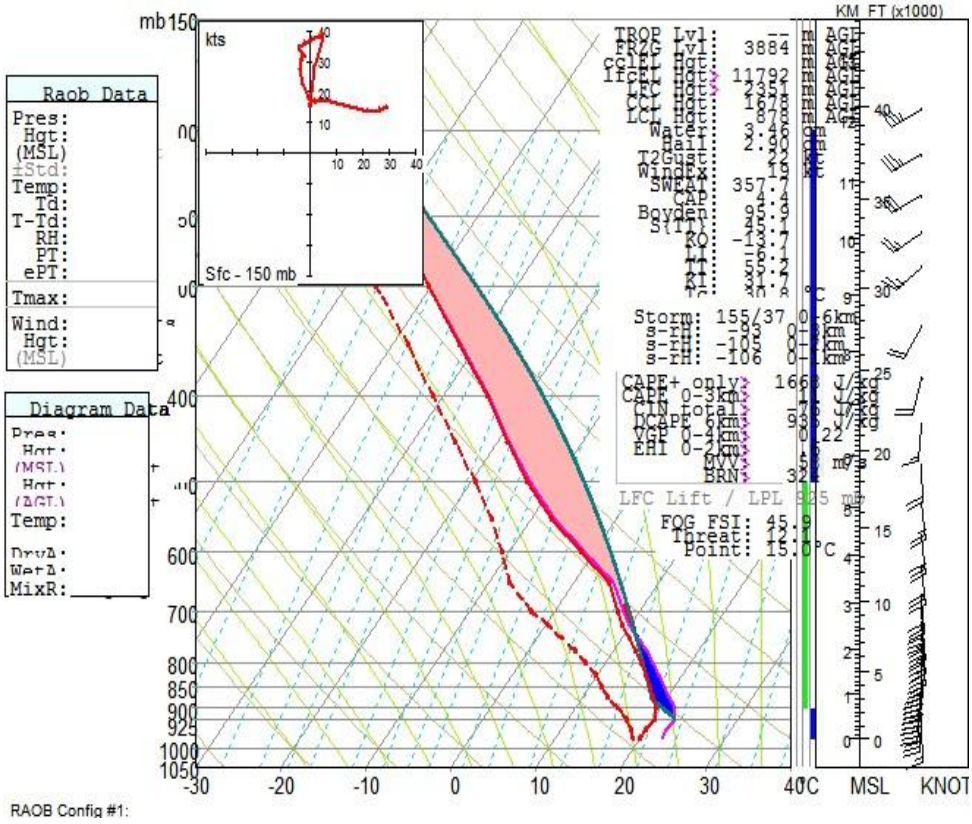

Figure 5.24 Skew-T log p diagram of the mean composite of the Winter 0.5% Mesohigh events. Winds at right are in knots.

advection was likely to be occurring. The convection was slightly elevated and upon initiation, ascended fairly quickly. Thunderstorm motion is likely to be slow with such a sounding, enhancing heavy rainfall over a localized area.

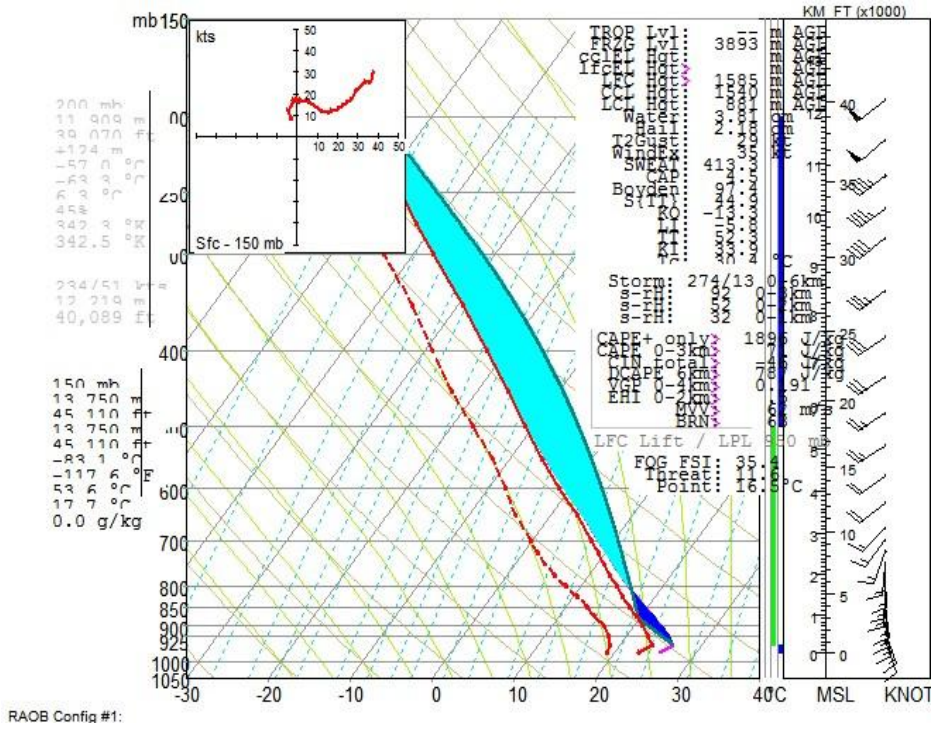

Figure 5.25 Skew-T log p diagram of the mean composite of the Spring 0.5% Mesohigh events. Winds at right are in knots.

5.4.23 Summer Mean Mesohigh 0.5%

Figure 5.26 (1 event) was included for completeness. The atmosphere was relatively moist throughout the whole column. Veering of low levels winds was more apparent above 925 mb. The winds are backing slightly from the surface to 925 mb. Continual decay of surrounding thunderstorms help maintain the heavy rainfall.

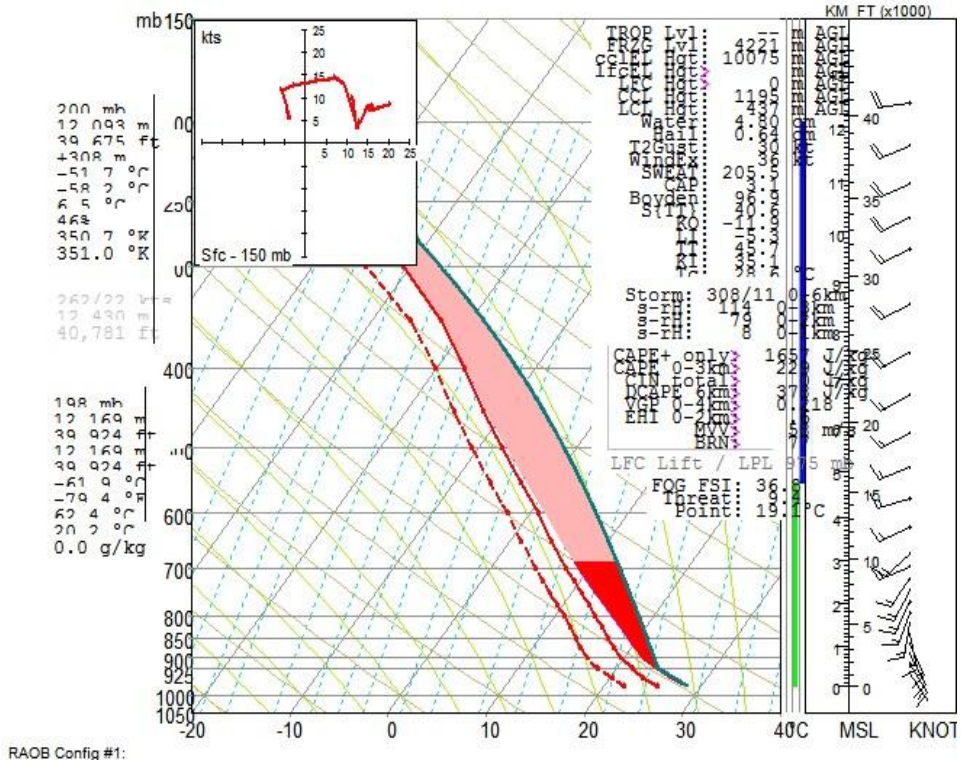

Figure 5.26 Skew-T log p diagram of the mean composite of the Summer 0.5% Mesohigh events. Winds at right are in knots.

5.4.24 Fall Mean Mesohigh 0.5%

A composite was not available for this threshold since mesohigh events did not occur during the months of October, November, and December.

5.5 Summary

The heaviest rainfall for the 24-hr time period was assumed to occur immediately after the time of the sounding with the largest CAPE value. In theory this would represent the time period that the atmosphere was the most unstable. This assumption was made so that the time period of where the rain rate was the heaviest could be identified, however the total rainfall amount for the event could also have fallen over a time period of three hours.

Mean values of stability parameters, along with median wind directional values, were calculated and given in Tables 5.7-5.12. Tables 5.7 and 5.8 are for the 0.5% and 2.0% thresholds for Mesohigh events, respectively. Tables 5.9 and 5.10 are for Frontal events and Tables 5.11 to 5.12 are given for Synoptic events. Maximum and minimum values were given from the composited data. The mean values along with a one standard deviation range given for each parameter. The tables are meant to be used strictly as guidance. At this point in time, it stands as a list of values that may occur during such an event. The

Table 5.7 Maximum value, minimum value, mean value, and range of one standard deviation of stability indices and parameters given for the 0.5% threshold Mesohigh events.

	Min	Max	Mean	1 std. dev. Range	
Precipitation (in)	2.8	3.04	2.92	2.75	3.09
LPL (mb)	1000	975	988	1005	970
LCL (mb)	879	842	861	887	834
LFC (mb)	879	832	856	889	822
EL (mb)	220	175	198	229	166
CAPE (J/kg)	1170	2810	1990	834	3150
CINH (J/kg)	0	0	0	0	0
Precipitable water (in)	1.3	1.4	1.35	1.28	1.42
Freezing Level (m)	12,500	13,300	12,900	12,320	13,430
700-500 mb LR (°C/km)	6.1	6.9	6.5	5.9	7.1
850-500 mb LR (°C/km)	6.4	7.1	6.8	6.3	7.2
NCAPE (J /kg-mb)	1.8	4.3	3.0	1.3	4.8
LI (°C)	-8	-5	-7	-9	-4
TT	48	54	51	47	55
KI	29	31	30	29	31
ThetaE Difference	15	25	20	12.9	27.1
BRN Shear	10	16	13	9	17
BRN	116	177	147	103	190
sfc-6km Mean Wind (°)	206	217	212	204	219
sfc-6km Mean Wind (kts)	4	10	7	3	11
LFC-EL Mean Wind (°)	240	244	242	239	245
LFC-EL Mean Wind (kts)	16	20	18	15	21
850-300 Mean Wind (°)	242	242	242	242	242
850-300 Mean Wind (kts)	18	19	18.5	18	19

Table 5.8 Maximum value, minimum value, mean value, and range of one standard deviation of stability indices and parameters given for the 2.0% threshold Mesohigh events.

	Min	Max	Mean	1 std. dev. Range	
Precipitation (in)	3.87	6.6	4.71	3.96	5.46
LPL (mb)	1000	900	954	981	926
LCL (mb)	955	804	881	837	926
LFC (mb)	933	720	831	910	752
EL (mb)	225	145	182	208	156
CAPE (J/kg)	1310	4180	2330	1470	3190
CINH (J/kg)	-148	0	-28	-78	22
Precipitable water (in)	0.88	1.86	1.44	1.14	1.73
Freezing Level (m)	10,200	14,100	12,400	11,200	13,600
700-500 mb LR (°C/km)	5.9	8	7	6.4	7.6
850-500 mb LR (°C/km)	6	7.9	7	6.4	7.5
NCAPE (J /kg-mb)	1.8	5.9	3.6	2.5	4.6
LI (°C)	-9	-5	-7	-9	-6
TT	45	56	52	49	55
KI	25	41	32.9	28	38
ThetaE Difference	11	30	18.9	13.8	24.1
BRN Shear	2	62	23	4	41
BRN	32	925	203	-29	435
sfc-6km Mean Wind (°)	179	288	215	179	251
sfc-6km Mean Wind (kts)	4	28	17	9	25
LFC-EL Mean Wind (°)	187	262	230	204	255
LFC-EL Mean Wind (kts)	11	29	21	15	28
850-300 Mean Wind (°)	187	272	232	205	258
850-300 Mean Wind (kts)	13	29	22	17	27

Table 5.9 Maximum value, minimum value, mean value, and range of one standard deviation of stability indices and parameters given for the 2.0% threshold Frontal events.

	Min	Max	Mean	1 std. dev. Range	
Precipitation (in)	2.7	3.13	2.96	2.8	3.12
LPL (mb)	1000	875	964	1000	924
LCL (mb)	940	860	890	922	858
LFC (mb)	910	795	842	888	797
EL (mb)	300	140	208	268	148
CAPE (J/kg)	410	3150	1735	621	2850
CINH (J/kg)	-45	0	-9	-25	7
Precipitable water (in)	0.7	1.8	1.43	1.03	1.823
Freezing Level (m)	11,370	14,460	13,300	12,200	14,400
700-500 mb LR (°C/km)	5.7	8	6.5	5.7	7.3
850-500 mb LR (°C/km)	5.9	7.3	6.4	5.9	6.9
NCAPE (J /kg-mb)	0.8	5.0	2.7	1.0	4.6
LI (°C)	-10	-3	-6	-8	-4
TT	46	53	48	46	51
KI	30	35	33	31	35
ThetaE Difference	11	27	18	11.6	24.4
BRN Shear	4	39	23	11	36
BRN	10	769	181	-91	453
sfc-6km Mean Wind (°)	183	265	198	162	234
sfc-6km Mean Wind (kts)	6	23	15	9	20
LFC-EL Mean Wind (°)	192	264	210	183	237
LFC-EL Mean Wind (kts)	15	20	18	16	19
850-300 Mean Wind (°)	189	258	213	188	238
850-300 Mean Wind (kts)	13	21	17	15	20

Table 5.10 Maximum value, minimum value, mean value, and range of one standard deviation of stability indices and parameters given for the 0.5%threshold Frontal events.

	Min	Max	Mean	1 std. dev. Range	
Precipitation (in)	4.05	9	5.47	3.85	7.08
LPL (mb)	1000	825	927	983	871
LCL (mb)	947	803	876	920	832
LFC (mb)	240	900	794	962	625
EL (mb)	140	450	232	329	135
CAPE (J/kg)	122	2930	1430	562	2300
CINH (J/kg)	-12	0	-3	-7	1
Precipitable water (in)	0.79	1.87	1.42	1.05	1.79
Freezing Level (m)	8,860	14,850	12,020	10,920	12,340
700-500 mb LR (°C/km)	5.6	7.9	6.4	5.8	7
850-500 mb LR (°C/km)	5.8	7	6.4	6	6.7
NCAPE (J /kg-mb)	0.4	8.8	2.6	1.2	3.6
LI (°C)	-8	-1	-5	-7	-3
TT	44	53	49	46	52
KI	28	36	33.2	31	35
ThetaE Difference	6	23	16.4	11.6	21.1
BRN Shear	2	73	32	14	51
BRN	2	84	121	-102	344
sfc-6km Mean Wind (°)	179	270	206	177	234
sfc-6km Mean Wind (kts)	5	39	18	8	28
LFC-EL Mean Wind (°)	201	303	220	190	249
LFC-EL Mean Wind (kts)	7	39	22	12	33
850-300 Mean Wind (°)	205	270	218	196	239
850-300 Mean Wind (kts)	7	39	21	11	31

Table 5.11 Maximum value, minimum value, mean value, and range of one standard deviation of stability indices and parameters given for the 2.0 % threshold Synoptic events.

	Min	Max	Mean	1 std. dev. Range	
Precipitation (in)	2.7	4.34	3.01	2.6	3.42
LPL (mb)	1000	825	945	1005	884
LCL (mb)	968	786	875	923	827
LFC (mb)	913	580	820	917	724
EL (mb)	530	120	225	349	100
CAPE (J/kg)	39	3755	1895	651	3139
CINH (J/kg)	-40	0	-6	-18	5
Precipitable water (in)	1.08	2.17	1.56	1.26	1.86
Freezing Level (m)	9,296	15,072	12,684	10,847	14,520
700-500 mb LR (°C/km)	5.7	7.6	6.3	5.7	6.9
850-500 mb LR (°C/km)	5.9	7.4	6.4	5.9	6.9
NCAPE (J /kg-mb)	0.2	5.8	3.2	1.0	5.5
LI (°C)	-11	0	-6	-9	-2
TT	43	56	49	44	53
KI	27	42	34	30	38
ThetaE Difference	4	31	17.6	9.9	25.4
BRN Shear	1	63	24	3	45
BRN	2	1315	200	-144	544
sfc-6km Mean Wind (°)	171	320	221	179	262
sfc-6km Mean Wind (kts)	0	31	16	6	25
LFC-EL Mean Wind (°)	181	305	228	195	261
LFC-EL Mean Wind (kts)	2	41	18	7	28
850-300 Mean Wind (°)	166	306	228	190	266
850-300 Mean Wind (kts)	5	40	19	9	29

Table 5.12 Maximum value, minimum value, mean value, and range of one standard deviation of stability indices and parameters given for the 0.5% threshold Synoptic events.

	Min	Max	Mean	1 std. dev. Range	
Precipitation (in)	3.18	9.14	5.39	3.97	6.8
LPL (mb)	1000	775	946	993	898
LCL (mb)	965	769	890	936	843
LFC (mb)	950	375	823	928	717
EL (mb)	600	110	221	331	110
CAPE (J/kg)	57	5848	1925	413	3437
CINH (J/kg)	-83	0	-14	-36	-8
Precipitable water (in)	0.92	2.18	1.45	1.13	1.77
Freezing Level (m)	8,759	15,348	12,238	10,393	14,084
700-500 mb LR (°C/km)	5	7.4	6.5	6	7
850-500 mb LR (°C/km)	5	7.4	6.5	6	7
NCAPE (J /kg-mb)	0.3	7.4	3.2	0.7	5.8
LI (°C)	-13	2	-5	-9	-2
TT	40	54	49	46	52
KI	20	42	32	27	37
ThetaE Difference	2	38	18.7	9.2	28.2
BRN Shear	1	92	30	8	53
BRN	1	5522	266	-605	1137
sfc-6km Mean Wind (°)	167	318	220	185	255
sfc-6km Mean Wind (kts)	3	37	19	11	28
LFC-EL Mean Wind (°)	180	284	226	201	251
LFC-EL Mean Wind (kts)	2	42	24	15	33
850-300 Mean Wind (°)	179	283	226	202	250
850-300 Mean Wind (kts)	3	41	24	15	33

importance of using one parameter over the other could not be established via statistical testing.

Mean values of temperature, dewpoint, wind speed, along with median wind directions were then used in RAOB to create a mean composite sounding. Using the Grice and Maddox (1982) classifications and the three calculated thresholds, nine composite soundings were created. These composite soundings depicted atmospheres that may result in heavy rain events. Most of the soundings had wind shear at low levels and usually associated with moderately strong values of CAPE. In some cases the wind profile suggested shear sufficient to provide sustained forcing to maintain thunderstorms. The movement of cells was generally slow, which would lead to local areas to repeatedly receive large amounts of heavy rainfall.

The soundings varied only slightly from each threshold and from each type. All the same, the events were then broken down into seasonal components. From these twenty-four potential categories (using the 'unusual' 2% and 'extreme' 0.5% cases), nineteen new soundings emerged producing soundings differing by more than just the mean soundings.

Comparing the 0.5% soundings for each classification resulted as follows. Frontal seasons did see larger precipitable water values and veering of the winds at lower levels. Summer and Fall had much larger values of CAPE than the Winter and Spring soundings.

The Mesohigh 0.5% soundings had very little veering of the winds while still having larger precipitable water values. All three soundings had moderately strong CAPE values associated with them.

The Synoptic seasonal soundings had little to moderate veering present at lower levels, winter having moderately strong directional shear. Precipitable water values were much lower in the Spring and Winter season. The Summer season had the highest value of all the seasonal soundings. Summer and Fall had moderately-strong to strong CAPE values. Spring had weak CAPE values and Winter had no CAPE present.

Chapter 6: Conclusions

Twenty-five years of daily (24-hour) rainfall data were examined for the Texas Hill Country using observations from 86 cooperative climate stations in the region; the period examined for this study was 1982-2006. Days with measurable precipitation were treated as a gamma distribution in order to determine the top 2%, 1%, and 0.5% to define events as unusual, rare, and extreme, respectively. This approach was applied to each station as well as to the aggregate data for all 86 stations, resulting in an analysis of 130,986 observations of 24-hour precipitation. From this sample, rainfall amounts were also calculated for each station that represent 25-, 50-, 100-, and 200-year return frequencies. For the aggregate gamma distribution, the parameters values of α=0.4678 and β=1.0082 were obtained.

While individual stations varied greatly, the aggregate data yielded a 24-hour rainfall threshold of 67 mm (2.64 in) for an observation to be in the upper 2%, 82.6 mm (3.25 in) to be in the upper 1%, and 98.30 mm (3.87 in) to be in the upper 0.5% of the distribution (which corresponds well to the 4.00” threshold

in cases studied by Grice and Maddox [1982]). Three-hourly soundings were reconstructed using North American Regional Reanalysis grids via NSHARP for all each cases of heavy rainfall. For all cases, the sounding with the highest CAPE in the 24-hours prior to the time of the daily rainfall total was chosen for compositing the classic Mesohigh, Frontal, and Synoptic classifications.

Unfortunately, great distinctions were not discovered between the soundings having unusual, rare, or extreme rainfall totals within the three classic classifications. Even when comparing the extreme soundings from the Mesohigh, Frontal, and Synoptic classifications, similar patterns emerged. Each composite environment was moist (all three >4.0 cm of precipitable water), unstable (all three with values of MUCAPE > 700 J kg^{-1}) and had only weak shear values (winds below 400 mb typically less than 35 knots). These conditions suggest an atmosphere with higher precipitation efficiency, with more upright convective towers and slower cell motion. Indeed, storm motions based upon the 0-6 km wind never exceeded 16 knots.

Moreover, each composite featured a jet of 50-55 knots which maximized at the ~200-mb level.

However, some differences were noted. While the extreme rain event soundings for the Mesohigh, Frontal, and Synoptic classifications each had a near-surface inversion, the most pronounced was with the Frontal type, less so with the Synoptic type, and least with the Mesohigh collection. The Frontal and Synoptic composites had a smaller NCAPE (~0.1 J kg^{-1} mb^{-1}) than the Mesohigh events. Another distinction of the Frontal and Synoptic composites from the Mesohigh composite type was the enhanced veering in the wind profile in the former types. Both the Frontal and Synoptic types had substantial easterly flow through the lowest ~50 mb, while the near surface flow with the Mesohigh type composite events was southerly with only a weak easterly component. As a quantitative check on this conclusion, the 0-1-km storm relative helicity for the Frontal (Synoptic) type was 104 (101) m^2 s^{-2}, while the same metric was only 2 m^2 s^{-2} for the Mesohigh events.

A great deal of additional work is possible on these events. First, I focused here only on those events that lasted a single

day. There were a great many events that spanned from two to as many as six days, and went unstudied in this work. Secondly, these sounding-centric results, while a helpful departure from classical plan view analyses, do point out the need for more than just one type of analysis in the forecasting of such events. In that vein, detailed case studies of individual events is strongly recommended for future investigators. Finally, the thresholds that were set in this work to separate 'unusual' from 'extreme' rainfall events were likely too close to one another. Any future work should define clearly subsets of events for which rain occurred, but where one subset involves flash flooding (and in excess of the 4.00 in day^{-1} criterion, advanced by Grice and Maddox [1982] and corroborated here) and the second subset does not.

BIBLIOGRAPHY

Ashley, S.T. and W.S. Ashley, 2008: Flood Fatalities in the United States. *J. Appl. Meteor. Climatol.*, 47, 805-818.

Blaha, R., and B. Thoren, 1997: The heavy rain and flood event of June 21-22, 1997 in South Central Texas and the Texas Hill Country. NOAA/NWS Tech. Attach. SR/SSD 97-55, National Weather Service Southern Region, Ft Worth, TX, 7 pp.

Blanchard, D.O., 1998: Assessing the Vertical Distribution of Convective Available Potential Energy. Weather and Forecasting, 13, 870-877.

Collier, C. G. and N. I. Fox, 2003: Assessing the flooding susceptibility of river catchments to extreme rainfall. *Int*. *J. of River Basin Management*, 1 (3).

Collier,C.G. and P.J. Hardaker, 1997: Estimating probable maximum precipitation using a storm model approach., Journ. Hydrol. 183, 277-306.

Department of Commerce, 2008. NOAA Central Library. [Online]

http://docs.lib.noaa.gov/rescue/dwm/data_rescue_daily_weather_maps.html.

Doswell, C.A., H.E. Brooks, and R.A. Maddox, 1996: Flash flood forecasting: An ingredients-based methodology. *Weather and Forecasting*, 11, 560-581.

Grice, G.K., and R.A. Maddox, 1982: Synoptic aspects of heavy rain events in South Texas associated with the westerlies. NOAA Tech. Memo. NWS SR-106, National Weather Service Southern Region, Ft. Worth, TX, 21 pp.

Guinan, P.E., 2005: A Seasonally Adjusted Index for Projecting Agricultural Drought. University of Missouri Doctoral Dissertation. 108.

Huff, F. A., and J.R. Angel, 1992: *Rainfall Frequency Analysis of the Midwest*. Bulletin 71, Midwest Climate Center, Research Report 92-03 pp.

Jennings, A.H., 1963: *Maximum Recorded United States Point Rainfall*. Weather Bureau Technical Paper No. 2. U.S. Dept. of Commerce/U.S. Weather Bureau, Washington, DC, 56 pp.

Locatelli, J.D. and P.V. Hobbs, 1995: A World Record Rainfall Rate at Holt, Missouri: Was it Due to Cold Frontogenesis Aloft? *Weather and Forecasting*, VOL 10, 779-785.

Maddox, R.A., C.F. Chappell, and L.R. Hoxit, 1979: Synoptic and meso-α scale aspects of flash flood events. *Bull. Amer. Meteor. Soc.*, 60, 115-123.

Maddox, R.A., and G.K. Grice, 1986: The Austin, Texas, flash flood: an examination from two perspectives—forecasting and research. *Wea. Forecasting*, 1, 66-76.

Nielsen-Gammon, J.W., F. Zhang, A.M. Odins, and B. Myoung, 2005: Extreme rainfall in Texas: Patterns and predictability. *Phys. Geog*., 26(5)**,** 340-364.

Panofsky, H.A., and G.W. Brier, 1968: *Some Applications of Statistics in Meteorology.* Pennsylvania State University Press, State College, PA, 224 pp.

Storm Prediction Center, 2008: Hourly Mesoscale Analysis.

[Online] www.spc.noaa.gov/exper/mesoanalysis/help/begin.html

University Corporation of Atmospheric Research, 2008: Unidata.

[Online] http://www.unidata.ucar.edu/software/gempak/ .

VITA

Amy Schnetzler was born in Columbia, Missouri and grew up in Boonville, Missouri. She attended the University of Missouri for her undergraduate degree and majored in Soils, Environmental, and Atmospheric Sciences. In her last semester, she volunteered 130 hours at the National Weather Service in Pleasant Hill, Missouri.

After graduation she moved to Juneau, Alaska where she was a summer intern at the National Weather Service through the Student Temporary Employment Program. Along with forecaster duties, she conducted research on the correlation between precipitation and temperature for south Alaska. After completion of the internship, she attended the University of Missouri's graduate program in Soils, Environmental, and Atmospheric Sciences.